



# LUND UNIVERSITY

## **Biophysical and Human Controls of Land Productivity under Global Change Development and Demonstration of Parsimonious Modelling Techniques** Sallaba, Florian

2016

*Document Version:*  
Publisher's PDF, also known as Version of record

[Link to publication](#)

*Citation for published version (APA):*  
Sallaba, F. (2016). *Biophysical and Human Controls of Land Productivity under Global Change: Development and Demonstration of Parsimonious Modelling Techniques*. [Doctoral Thesis (compilation), Faculty of Science, Dept of Physical Geography and Ecosystem Science]. Lund University, Faculty of Science, Department of Physical Geography and Ecosystem Science.

*Total number of authors:*  
1

### **General rights**

Unless other specific re-use rights are stated the following general rights apply:  
Copyright and moral rights for the publications made accessible in the public portal are retained by the authors and/or other copyright owners and it is a condition of accessing publications that users recognise and abide by the legal requirements associated with these rights.

- Users may download and print one copy of any publication from the public portal for the purpose of private study or research.
- You may not further distribute the material or use it for any profit-making activity or commercial gain
- You may freely distribute the URL identifying the publication in the public portal

Read more about Creative commons licenses: <https://creativecommons.org/licenses/>

### **Take down policy**

If you believe that this document breaches copyright please contact us providing details, and we will remove access to the work immediately and investigate your claim.

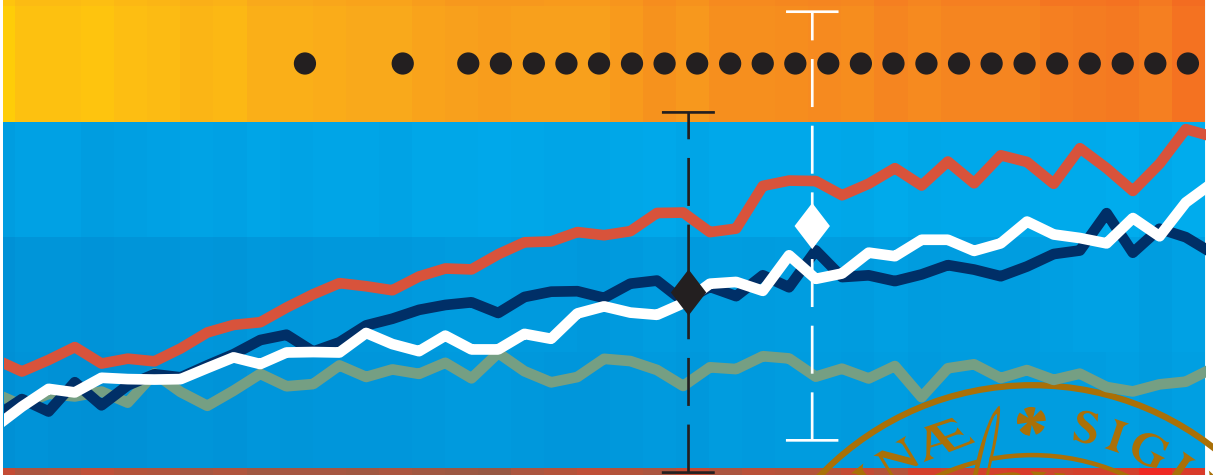
LUND UNIVERSITY

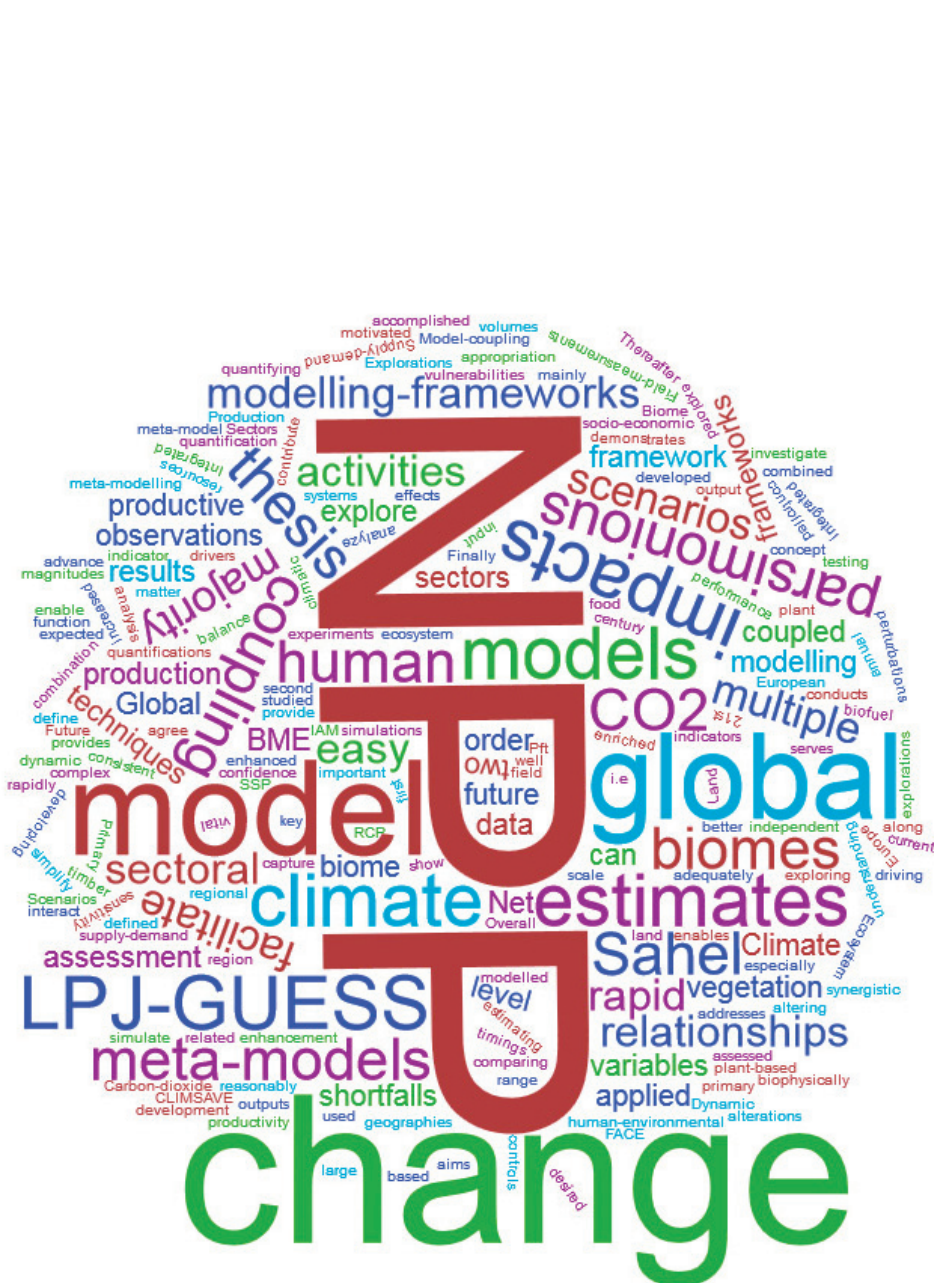
PO Box 117  
221 00 Lund  
+46 46-222 00 00

# Biophysical and Human Controls of Land Productivity under Global Change

Development and Demonstration of Parsimonious Modelling Techniques

FLORIAN SALLABA | FACULTY OF SCIENCE | LUND UNIVERSITY





# Biophysical and Human Controls of Land Productivity under Global Change

Development and Demonstration of Parsimonious Modelling  
Techniques



# Biophysical and Human Controls of Land Productivity under Global Change

Development and Demonstration of  
Parsimonious Modelling Techniques

Florian Sallaba



**LUND**  
UNIVERSITY

DOCTORAL DISSERTATION

by due permission of the Faculty of Science, Lund University, Sweden.  
To be publicly defended at Världen auditorium (room 111), Geocentrum I,  
Sölvegatan 12, Lund. Tuesday the 20<sup>th</sup> of December 2016, at 10.00 AM.

*Faculty opponent*

Marc J. Metzger, University of Edinburgh

Organization: LUND UNIVERSITY	Document name: DOCTORAL DISSERTATION	
Department of Physical Geography and Ecosystem Science, Sölvegatan 12, SE- 22362 Lund, Sweden	Date of issue: 2016-11-10	
Author: Florian Sallaba	Sponsoring organization: European Commission	
Title: Biophysical and Human Controls of Land Productivity under Global Change Subtitle: Development and Demonstration of Parsimonious Modelling Techniques		
<p>Abstract: Net primary production (NPP) serves as an indicator for plant-based resources such as food, timber and biofuel for human appropriation. It is defined by the annual production of plant matter and is mainly controlled by climate and human activities. Climate change in combination with human activities is altering NPP. As the controls of NPP are expected to further change in the future, it is vital to investigate alterations in NPP and their magnitudes. The impacts of climate change and human activities on NPP can be explored in integrated assessment (IA) frameworks, where sectoral models are coupled and interact rapidly. For such frameworks, parsimonious models are desired because they enable rapid estimates and facilitate easy model coupling for explorations of multiple global change scenarios (i.e. large volumes of data).</p> <p>This thesis aims to advance parsimonious modelling techniques for quantifying current and future NPP on land. This is accomplished by developing and testing rapid models that facilitate easy model coupling to explore the impacts of multiple global change scenarios on NPP. The model development is based on the meta-modelling concept, which can be applied to simplify the dynamic vegetation model LPJ-GUESS in a parsimonious model. For this, multiple climate change and [CO<sub>2</sub>] perturbations are applied to LPJ-GUESS to simulate NPP. The NPP data are then used to define biophysically motivated relationships between NPP and the driving climate variables along with [CO<sub>2</sub>]. The relationships are then combined in a synergistic function – the meta-model. Thereafter, the meta-models are assessed for their performance in estimating NPP by comparing them to LPJ-GUESS NPP simulations, to independent field observations and to NPP experiments under enriched [CO<sub>2</sub>] on biome level. The results provide confidence in the modelled NPP estimates for the most productive biomes, which are important for global quantifications of NPP. The meta-models capture NPP enhancement under enhanced [CO<sub>2</sub>] adequately in the majority of the studied biomes. Finally, the NPP meta-models are coupled with other sectoral models in two IA modelling-frameworks in order to explore the impacts of global change on ecosystem indicators. The first framework enables an IA of climate change impacts and vulnerabilities for a range of sectors on the European level. This thesis conducts a sensitivity analysis on the effects of climatic and socio-economic change drivers on model outputs related to key sectors. This provides better quantification and increased understanding of the complex relationships between input and output variables in IA modelling-frameworks. The second framework addresses the NPP supply-demand balance in the Sahel region by coupling two sectoral models in order to analyze the timings and geographies of NPP shortfalls in the 21<sup>st</sup> century Sahel under global change. The results show consistent regional NPP shortfalls in the Sahel for the majority of global change scenarios.</p> <p>Overall, the parsimonious modelling techniques developed in this thesis contribute with rapid NPP estimates on the biome and global scale. BME NPP estimates agree reasonably well with NPP observations in the majority of biomes (especially in the most productive biomes). This thesis demonstrates that NPP meta-models facilitate easy model coupling for exploring the impacts of global change on human-environmental systems in IA modelling-frameworks.</p>		
Key words: Ecosystem model, Meta-modelling, Net Primary Production, Global Change, Model coupling		
Classification system and/or index terms (if any)		
Supplementary bibliographical information		Language: English
ISSN and key title		ISBN (print): 978-91-85793-69-3 ISBN (PDF): 978-91-85793-70-9
Recipient's notes	Number of pages 234	Price
	Security classification	

I, the undersigned, being the copyright owner of the abstract of the above-mentioned dissertation, hereby grant to all reference sources permission to publish and disseminate the abstract of the above-mentioned dissertation.

Signature:



Date: 2016-11-10

# Biophysical and Human Controls of Land Productivity under Global Change

Development and Demonstration of  
Parsimonious Modelling Techniques

Florian Sallaba



**LUND**  
UNIVERSITY



A doctoral thesis at a university in Sweden is produced either as a monograph or as a collection of papers. In the latter case the introductory part constitutes the formal thesis, which summarizes the accompanying papers already published or manuscripts at various stages (in press, submitted, or in preparation).

Copyright © Florian Sallaba

Cover by Florian Sallaba.

Faculty of Science  
Department of Physical Geography and  
Ecosystem Science

ISBN (print): 978-91-85793-69-3

ISBN (PDF): 978-91-85793-70-9

Printed in Sweden by Media-Tryck, Lund University  
Lund 2016



*To my beloved parents Eva-Maria and Helmut, and  
to my brother Marcus whom I dearly miss.*



# Content

List of papers	11
List of Contribution	11
Abstract	13
Sammanfattning	15
1. Introduction	17
1.1. Global change	17
1.2. Net primary production	19
1.3. Integrated assessment modelling-frameworks	21
1.4. Thesis aim and objectives	22
2. Methods and materials	23
2.1. Dynamic vegetation model	23
2.2. Parsimonious modelling techniques	24
2.2.1. European NPP meta-model (Paper I)	24
2.2.2. Global Biome-based NPP Meta-model Ensemble (Paper III)	26
2.2.3. Model evaluation (Paper I and III)	27
2.3. Model coupling and application	29
2.3.1. Sensitivity analysis of an integrated assessment modelling-framework (Paper II)	29
2.3.2. NPP supply-demand balance in the Sahel	30
2.4. Scenarios	33
3. Results and discussion	35
3.1. Evaluation of the NPP meta-models (Paper I)	35
3.2. Validation of global Biome-based Meta-model Ensemble (Paper III)	36
3.3. Sensitivity analysis of an integrated assessment modelling-framework (Paper II)	38
3.4. NPP supply-demand balance in the Sahel (Paper IV)	38
4. Conclusions and outlook	41
Acknowledgements	43
References	45

## Papers I-IV



## List of papers

- I. Sallaba, F., Lehsten, D., Seaquist, J., Sykes, M.T., 2015. A rapid NPP meta-model for current and future climate and CO<sub>2</sub> scenarios in Europe. *Ecological Modelling* 302, 29-41.
- II. Kebede, A.S., Dunford, R., Mokrech, M., Audsley, E., Harrison, P.A., Holman, I.P., Nicholls, R.J., Rickebusch, S., Rounsevell, M.D.A., Sabaté, S., Sallaba, F., Sanchez, A., Savin, C., Trnka, M., Wimmer, F., 2015. Direct and indirect impacts of climate and socio-economic change in Europe: a sensitivity analysis for key land- and water-based sectors. *Climatic Change* 128, 261-277.
- III. Sallaba, F., Olin, S., Lehsten, V., Seaquist, J. W. Development and validation of a parsimonious terrestrial productivity model with an exploration of future global trends. *Manuscript*.
- IV. Sallaba, F., Olin, S., Engström, K., Abdi, A. M., Boke-Olén, N., Lehsten, V., Ardö, J., Seaquist, J. W. Future supply and demand of net primary production in the Sahel. *Manuscript*

## List of Contribution

- I. FS co-developed the study design, performed the simulations and analysis, interpreted the results in discussion with co-authors and led the writing of the paper.
- II. FS participated in the study design, performed parts of the simulations, and commented on the draft paper.
- III. FS developed the study design, performed the simulations and analysis, interpreted the results in discussion with co-authors and led the writing of the paper.
- IV. FS contributed to the study design, performed the meta-model simulations and analysis, interpreted the results in discussion with co-authors and led the writing of the paper.



# Abstract

Net primary production (NPP) serves as an indicator for plant-based resources such as food, timber and biofuel for human appropriation. It is defined by the annual production of plant matter and is mainly controlled by climate and human activities. Climate change in combination with human activities is altering NPP. As the controls of NPP are expected to further change in the future, it is vital to investigate alterations in NPP and their magnitudes. The impacts of climate change and human activities on NPP can be explored in integrated assessment (IA) frameworks, where sectoral models are coupled and interact rapidly. For such frameworks, parsimonious models are desired because they enable rapid estimates and facilitate easy model coupling for explorations of multiple global change scenarios (i.e. large volumes of data).

This thesis aims to advance parsimonious modelling techniques for quantifying current and future NPP on land. This is accomplished by developing and testing rapid models that facilitate easy model coupling to explore the impacts of multiple global change scenarios on NPP. The model development is based on the meta-modelling concept, which can be applied to simplify the dynamic vegetation model LPJ-GUESS in a parsimonious model. For this, multiple climate change and [CO<sub>2</sub>] perturbations are applied to LPJ-GUESS to simulate NPP. The NPP data are then used to define biophysically motivated relationships between NPP and the driving climate variables along with [CO<sub>2</sub>]. The relationships are then combined in a synergistic function – the meta-model. Thereafter, the meta-models are assessed for their performance in estimating NPP by comparing them to LPJ-GUESS NPP simulations, to independent field observations and to NPP experiments under enriched [CO<sub>2</sub>] on biome level. The results provide confidence in the modelled NPP estimates for the most productive biomes, which are important for global quantifications of NPP. The meta-models capture NPP enhancement under enhanced [CO<sub>2</sub>] adequately in the majority of the studied biomes. Finally, the NPP meta-models are coupled with other sectoral models in two IA modelling-frameworks in order to explore the impacts of global change on ecosystem indicators. The first framework enables an IA of climate change impacts and vulnerabilities for a range of sectors on the European level. This thesis conducts a sensitivity analysis on the effects of climatic and socio-economic change drivers on model outputs related to key sectors. This provides better quantification and increased understanding of the complex relationships between input and output variables in IA modelling-frameworks. The second framework addresses the NPP supply-demand balance in the Sahel region by coupling two sectoral models in order to analyze the timings and geographies of NPP shortfalls in the 21<sup>st</sup> century Sahel under global change. The results show consistent regional NPP shortfalls in the Sahel for the majority of global change scenarios.



Overall, the parsimonious modelling techniques developed in this thesis contribute with rapid NPP estimates on the biome and global scale. BME NPP estimates agree reasonably well with NPP observations in the majority of biomes (especially in the most productive biomes). This thesis demonstrates that NPP meta-models facilitate easy model coupling for exploring the impacts of global change on human-environmental systems in IA modelling-frameworks.

# Sammanfattning

Nettoprimärproduktionen (NPP), är källan till den mat vi äter, virket vi bygger hus av och veden vi eldar med. NPP spelar också en stor roll i den globala kolcykeln, genom fotosyntesen så binder växterna koldioxid från luften och producerar blad och stammar. Hur mycket växterna producerar styrs till stor utsträckning av klimatet samt hur mycket koldioxid som finns i atmosfären. Detta gör att de förändringar som vi står inför, klimatförändringarna, som till stor del kan härledas till en ökad koldioxidhalt i atmosfären är intressanta att studera. Mänskliga aktiviteter så som jord- och skogsbruk, har också en stor inverkan på NPP. Då den globala befolkningen spås öka till 9 miljarder fram till 2050, så kommer också trycket på Jordens ekosystem att öka genom större uttag av NPP från skogar och jordbruk. Det är av stor vikt för mänskligheten att vi kan studera hur samspelet mellan hur vi sköter de ekosystem som vi är så beroende av och klimatförändringarna för att kunna ta adekvata beslut inför framtiden. För att studera detta samspel så krävs Integrerade Modeller (IM), modeller som binder samman ekosystemen och de mänskliga systemen.

För att kunna modellera detta kopplade system så krävs det förenklingar, och då framtiden är osäker, så krävs det att man utforskar många olika scenarier. För att kunna göra det, är det viktigt att dessa modeller är så snabba att man kan utföra en stor mängd simuleringar.

I den här avhandlingen så kommer jag att presentera förenklade metoder för att uppskatta NPP i naturlig vegetation baserat på en begränsad mängd klimatvariabler (t.ex. årlig medelnederbörd eller årligt temperaturmaximum) och jämföra det med mer komplexa modeller som i större utsträckning förlitar sig på detaljerad klimatdata.

Dessa förenklade modeller bygger på det så kallade metamodelleringskonceptet, där man genom att fånga hur de mest elementära processerna påverkas av en liten mängd yttre variabler kan skapa snabba responsmodeller. Jag utvärderar här, både hur de komplexa och förenklade modellerna lyckas simulera observationer från fältförsök utförda i olika ekosystemtyper runt om Jorden samt hur väl dessa modeller fångar ökningen i NPP på grund av den ökade koldioxidhalten från så kallade FACE-experiment (Free-Air Carbon Experiment).

Jag kommer också att visa hur dessa förenklade ekosystemproduktionsmodeller kan kopplas till modeller som simulerar mänskliga system. I två fallstudier, en i Europa och en i Sahelregionen i Afrika, så studeras dessa integrerade system. I studien för Sahel, så studeras de kombinerade effekterna av klimatförändringar och populationsökningar på tillgången till NPP för mänsklig konsumtion.



# 1. Introduction

Terrestrial ecosystems are the engines of the Earth's ice-free land, fueled by solar energy and maintained by water, carbon-dioxide and nutrients. They provide many important services for humanity such as food, timber and biofuel resources, pollination, storage of carbon in soils and recreational aspects (Tao et al. 2005, Baisden 2006, Metzger et al. 2006, Field et al. 2008, Abdi et al. 2014). At the same time, humanity is exerting growing pressure on terrestrial ecosystems by increasing the appropriation of natural resources to meet the increasing demand in human appropriation. Changes in land productivity are driven by many processes that can be combined under the term global change. The multi-dimensional impacts of global change on land productivity can be explored in integrated assessment (IA) frameworks. For such frameworks, parsimonious models are desired because they enable rapid estimates and facilitate easy model coupling for explorations of multiple global change scenarios.

In this thesis, parsimonious modelling techniques for quantifying current and future land productivity are developed. They are based on the principle of parsimony: *"with all things being equal, the simplest explanation tends to be the right one"* (William of Ockham). This enables the exploration of biophysical and human controls on current land productivity but also future land productivity under global change. Biophysical controls are climate variables that limit vegetation growth on land while human controls are land use and land cover changes (LULCC) aiming to increase land productivity.

## 1.1. Global change

Global change encompasses many processes that are altering human-environmental systems from the local to the global scale. Global change induced impacts on these systems have become a strategic, economic and political concern for decision-makers and stakeholders (e.g. Harrison et al. (2013)) because these effects have the potential to affect society, cause high capital costs and to irreversibly damage ecosystems. One challenge for future human-environmental systems is the impact of global change on vegetation growth, since plant biomass supports the global food chain (Haberl et al. 2007, Running 2012). Three

examples of global change processes are climate change, societal developments (population growth) and LULCC.

Climate change affects vegetation growth through increasing temperatures, changing precipitation patterns (e.g. more intense rainfall events and extended periods of droughts in some regions) and increasing carbon-dioxide concentrations ( $[\text{CO}_2]$ ). Possible developments of mean terrestrial temperature and future global  $[\text{CO}_2]$  are shown in Figure 1.

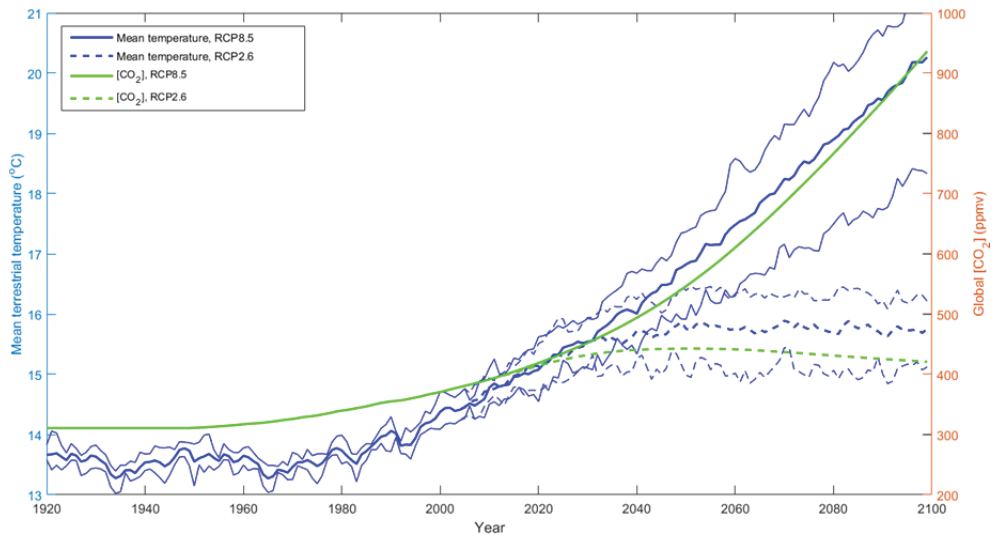


**Figure 1 Predicted developments of mean terrestrial temperature and global  $[\text{CO}_2]$ .**

The shown mean terrestrial temperature (excluding oceans) and  $[\text{CO}_2]$  developments are used in this thesis and are based on two representative concentration pathways (RCPs – see Table 1) (Moss et al. 2010, van Vuuren et al. 2011). The thick blue lines (solid and dashed) are the mean values of the five General Circulation models used in Paper IV while the smaller lines indicates the standard deviations.

Societal developments can accelerate climate change mainly by increasing the emission of greenhouse gases to the atmosphere due to fossil fuel combustion and LULCC. In general, societal developments are interrelated and combine among others changes in population development, economic growth, consumption and diets, policy orientation and technological change.

LULCC is the conversion from natural land to other land cover and land use, and this thesis targets the conversion to agricultural land in order to increase the production of food commodities. LULCC is mainly driven by population growth (see Figure 2) but also by dietary changes (towards animal products), in particular over the last two decades (Alexander et al. 2015). At present, about 35% of the total ice-free land surface is used for agriculture (Ramankutty et al. 2008). Agricultural land (grassland and cropland) expanded by 3% between 1985 and

2005 and is expected to further increase, especially in the tropics (Foley et al. 2011).

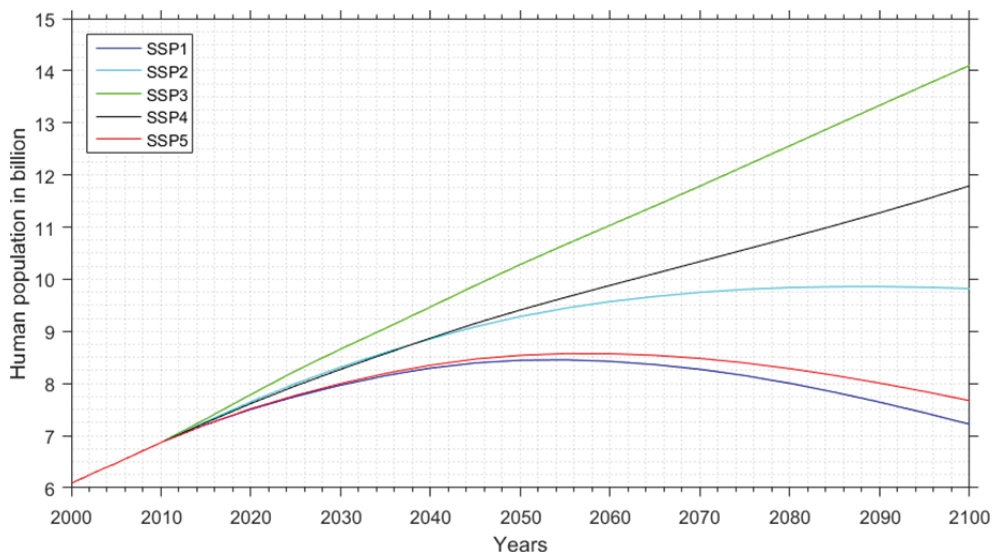


**Figure 2 Population growth developments based on shared socio-economic pathways (SSPs).**  
Based on socio-economic developments of the SSPs that are summarized in Table 2.

Global change has already led to high rates of biodiversity loss, which is one of several planetary boundaries defining a safe operating space for humanity with regard to the Earth's biophysical limits. The planetary boundary of biodiversity loss has already been overstepped due to high extinction rates but humanity may soon approach more planetary boundaries (Rockström et al. 2009). Running (2012) suggests the application of annual plant growth of terrestrial ecosystems as an alternative planetary boundary since it combines several of the boundaries suggested by Rockström et al. (2009), and the monitoring of current NPP can be facilitated consistently with satellite systems (Running et al. 2004).

## 1.2. Net primary production

In general, vegetation growth, the annual increase in plant matter including leaves, can be measured by net primary production (NPP). NPP describes the annual net fixation of carbon by plants, estimated as the difference in gross photosynthetic assimilation of carbon and carbon loss due to autotrophic respiration, per area per unit time (Foley 1994). NPP serves as a quantification of how much energy is available to sustain the global food web. It is also a measure for other plant-based

resources such as timber and biofuel for human consumption, and it plays an important role in the global carbon cycle (Cleveland et al. 2015).

Several methods exist for quantifying NPP. It can be measured in field, which is referred to as NPP observations but the accuracy of these measurements is limited since errors and inconsistencies occur when assessing below-ground and short-lived above-ground plant matter (e.g. fine roots, leaves and fruits) (Geider et al. 2001). For a complete description of measuring NPP in field see Norby et al. (2001).

At larger scales, past and current NPP can be monitored with satellite-based observations (Running et al. 2004, Ito 2011). However, these methods incorporate uncertainties because they are also location-specific, particularly in the case of purely empirical approaches (Seaquist et al. 2003). Satellite-based measurements are however limited to past (ca. 40 years) and current observations of NPP and cannot facilitate future predictions of vegetation growth.

The modelling of annual plant growth has an over 40 year history. The first widely known NPP model was the MIAMI model, developed by Lieth and Whittaker (1975) in the 1970s. The MIAMI model employs empirical relationships between climate variables (i.e. temperature and precipitation) and NPP observations. It applies Liebig's 'Law of the Minimum', choosing the climate variable yielding lowest NPP (Lieth and Whittaker 1975). Empirical NPP models are simple and rapid but are based on NPP observation under current climate, and thus cannot be forced with future global change scenarios without extrapolation concerns (Adams et al. 2004, Shoo and Valdez Ramirez 2010).

However, these extrapolation concerns can be overcome with dynamic vegetation models (DVMs) because they are formulated on a mechanistic representation of bio-geophysical and biogeochemical processes describing plant growth and maintenance at various temporal resolutions. DVMs are forced with time-series of various climate variables,  $[\text{CO}_2]$  and nutrient inputs (Smith et al. 2001, Sitch et al. 2003, Prentice I.C. 2007, Sitch et al. 2008, Friedlingstein et al. 2014, Friend et al. 2014, Smith et al. 2014). The process-based nature of DVMs allows NPP simulations under future global warming and  $[\text{CO}_2]$  scenarios but also for historical climate of the Holocene (Giesecke et al. 2007, Bradshaw 2008, Miller et al. 2008) since they can be driven by historical climate records and future climate change scenarios.

### 1.3. Integrated assessment modelling-frameworks

IA modelling-frameworks can be applied to holistically investigate possible impacts of global change on human-environmental systems. IA has been defined by the Intergovernmental Panel on Climate Change as “an interdisciplinary process that combines, interprets, and communicates knowledge from diverse scientific disciplines from the natural and social sciences to investigate and understand causal relationships within and between complicated systems” (IPCC 2001). IA modelling-frameworks can address cross-sectoral questions (e.g. impact of LULCC and increasing temperatures on land productivity) since they combine several sectoral models, and thus can consider interactions between sectors (Harrison et al. 2016). By contrast, individual models can only assess questions that are linked to the individual model purpose. For instance, DVMs can only investigate ecosystem parameters (e.g. NPP).

IA facilitates investigations of combined socio-economic and climate change scenarios. For explorations of multiple global change scenarios, the sectoral models must provide rapid estimates for cross sectoral model interactions, and thus must enable easy model coupling. Process-based models can become unhandy in IA modelling-frameworks due to their time-consuming simulations. For instance, process-based DVMs makes global and regional explorations of NPP under multiple climate scenarios time-consuming, and thus inhibits their feasibility in IA frameworks where rapid interactions between models are desired e.g. CLIMSAVE (Harrison et al. 2013).

This limitation can be overcome by developing parsimonious NPP models that are able to capture the main processes driving plant growth in DVMs, and can be applied to predict future NPP.



## 1.4. Thesis aim and objectives

The overall aim of this thesis is to develop parsimonious modelling techniques for quantifying terrestrial productivity under global change.

The objectives are to:

- i. Develop and test biophysically based meta-modelling techniques of NPP under future global change (Paper I & III).
- ii. Couple NPP meta-models with other sectoral models (Paper II & IV).
- iii. Explore and analyze the impacts of global change on indicators in IA modelling-frameworks (Paper II & IV).

In order to address the specific thesis objectives, four papers are presented, each paper targets one (or more) thesis aims. The overall conceptual flow and the structure of this thesis are visualized in Figure 3.

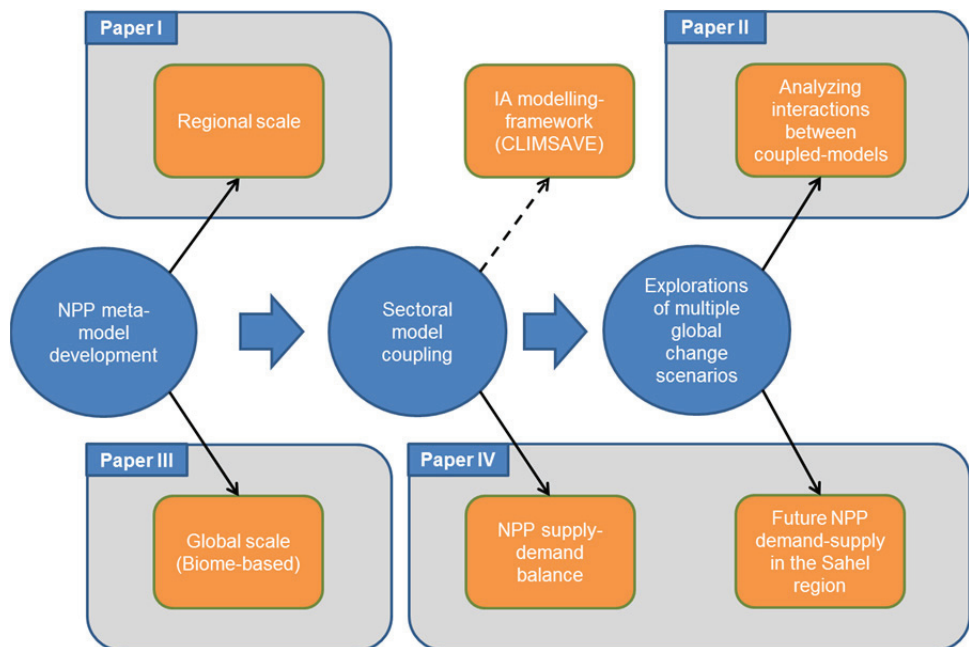


**Figure 3 The conceptual flow of this thesis.**

The blue circles bind the overall aims while the blue arrows indicate the direction of accomplishing the aims, starting with NPP meta-model development and then the coupling of meta-models with other models in order to explore the impact of multiple future climate and socio-economic scenarios on NPP. The orange boxes represent parts of the main aims (black solid arrows), and projects connected to this thesis (black dashed arrows) while the grey boxes indicate the papers covering the parts.

## 2. Methods and materials

This section is organized into four parts. In the first part I briefly outline the dynamic vegetation model (DVM) that was used to develop parsimonious models. Thereafter I describe the techniques used to develop these models and assess their performance. I then explain the coupling of the developed models to other sectoral models in integrated assessment modelling-frameworks. Finally I demonstrate two applications of these frameworks and outline the climate and socio-economic scenarios used in this work.

### 2.1. Dynamic vegetation model

The Lund-Potsdam-Jena (LPJ) General Ecosystem Simulator (GUESS) DVM was used to develop the parsimonious NPP models. LPJ-GUESS is a mechanistic framework for describing plant physiological and biogeochemical processes including plant-atmosphere interactions such as carbon and nitrogen cycles and water fluxes. In Paper I, the carbon-only LPJ-GUESS (Smith et al. 2001) version was applied while in Paper III an updated version of LPJ-GUESS (Smith et al. 2014) was used including the nitrogen cycle and carbon-nitrogen interactions. In general, the applied model includes a detailed individual- and patch-based representation of vegetation structure. In this structure the individual plants differ in growth form, phenology, photosynthetic pathway, demography, and resource competition.

LPJ-GUESS was forced with solar radiation, temperature, precipitation, atmospheric  $[\text{CO}_2]$ , nitrogen inputs and soil characteristics. It simulates vegetation as plant functional types (PFTs) which can range in level of detail from generalized global PFTs (Paper III) to specific species-specific PFTs (Paper I). Each PFT is represented with different age cohorts interacting on the patch level.

The patches are applied in parallel within a grid cell that incorporates establishment of vegetation, fire impacts, random disturbance and mortality (Smith et al. 2001, Sitch et al. 2003, Smith et al. 2014). In Paper I and III, LPJ-GUESS was applied in cohort mode that represents individual PFTs (or species) in different age classes competing for resources (light, water and space) within each

patch. The vegetation can be disturbed by several kinds of events. For example, wildfires can kill individuals, or parts of it, based on a pre-defined fire occurrence rate that is influenced by the availability of fire fuels (amount of litter and moisture regimes). Stochastic disturbance, i.e. insect attacks or wind fells, remove all vegetation based on a priori probability. LPJ-GUESS exhibits an overall good skill in predicting NPP at regional and global scale (Hickler et al. 2006, Hickler et al. 2008, Tang et al. 2010, Smith et al. 2014).

## 2.2. Parsimonious modelling techniques

In this thesis, the meta-modelling concept is used, which aims to simplify complex models with straightforward but efficient techniques (Ratto et al. 2012, Razavi et al. 2012). These techniques, however, can range in complexity from traditional statistical methods (i.e. linear regression) to advanced statistical machine learning theory (e.g. support vector machines - SVM). The latter usually yield better accuracy in mimicking model behavior (Villa-Vialaneix et al. 2012) but do not allow deeper analysis of model drivers, especially in terms of biophysical interpretation. I therefore employed biophysically motivated relationships to mimic the behavior of LPJ-GUESS.

### 2.2.1. European NPP meta-model (Paper I)

The European NPP meta-model was developed to emulate LPJ-GUESS (Smith et al. 2001) NPP simulations for European potential natural vegetation (PNV). The conceptual logic of the meta-model is shown in Figure 4. The meta-model development was based on LPJ-GUESS NPP simulations for selected sample points along two cross European transects, covering most of the European environmental zones. The historical climate of the sample points, taken from CRU TS 3.0 climate database (Mitchell and Jones 2005, Harris et al. 2014), were changed in order to mimic the IPCC scenario families (IPCC 2007), resulting in 500 climate change and increasing  $[\text{CO}_2]$  perturbations. LPJ-GUESS was forced with baseline climate and the perturbations in order to simulate NPP under climate change conditions. This enabled the development of a NPP meta-model that can be employed for future NPP predictions under climate and  $[\text{CO}_2]$  scenarios.

In general, the meta-model development was based on the assumption that maximum NPP at  $[\text{CO}_2]$  baseline can only be reached when the most limiting climate variables of the ecosystems are at their optimum. These climate variables are annual maximum and minimum temperature as well as total summer and winter precipitation. In the first step (see Figure 4), the relationships between each

climate variable and maximum NPP were described with mathematical functions. The variables (or functions) constantly interact when limiting plant growth. For instance, optimum maximum and minimum temperature and winter precipitation cannot yield maximum NPP when summer precipitation is not at its optimum. In the second step (see Figure 4), the interactions were captured by combining the functions of the limiting variables in a synergistic function.

In the last step, the CO<sub>2</sub> fertilization effect on NPP was implemented. In general, [CO<sub>2</sub>]-dependent plant growth can be described as a saturation function but is also dependent on climate (Haxeltine and Prentice 1996). This concept was implemented by applying a linear relationship between the ratio of NPP yields at enriched [CO<sub>2</sub>] and baseline [CO<sub>2</sub>] (350ppm) and the reciprocal ratio of the [CO<sub>2</sub>] at baseline and enriched levels. The model was developed for European PNV species and their total NPP.

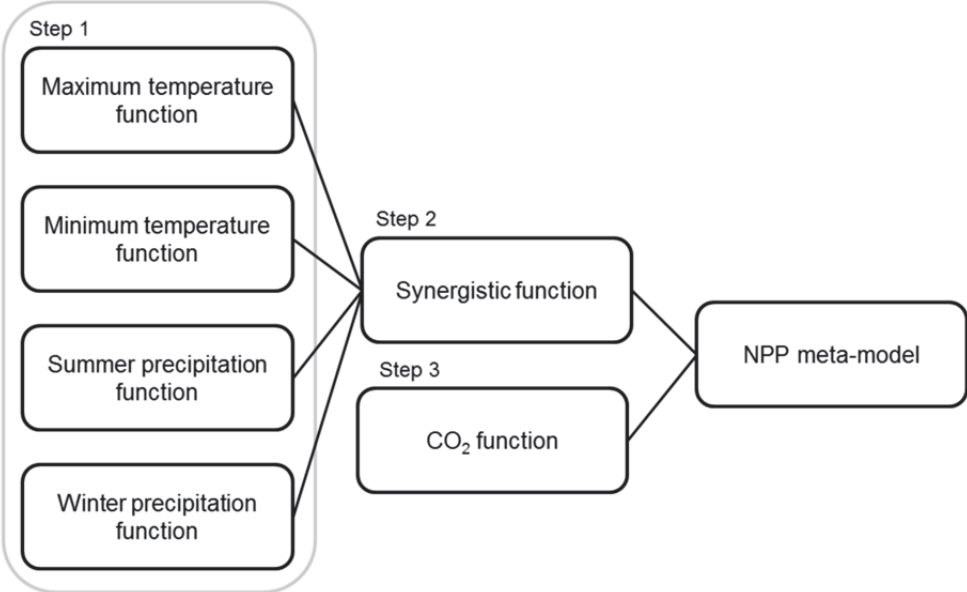


Figure 4 Conceptual logic of European NPP meta-model.

### 2.2.2. Global Biome-based NPP Meta-model Ensemble (Paper III)

In Paper III, the meta-modelling approach was extended to the global scale while considering regional climate regimes and vegetation types. The regional NPP meta-models were assembled in a NPP Biome-based Meta-model ensemble (BME) that can be easily coupled to other sectoral models into a range of studies from the regional to the global scale. BME was developed to mimic the behavior of LPJ-GUESS (Smith et al. 2014) which incorporates the global nitrogen cycle. The conceptual logic of BME is similar to the European NPP meta-model as can be seen in Figure 5.

In the first step (see Figure 5), the Earth's ice-free land was stratified into thirteen biomes using the major biome classification (Reich and Eswaran 2002), which groups biomes according to soil temperature and soil moisture. This stratification enables NPP meta-models to be tailored to the vegetation and climate characteristics for each biome (see Figure 6). In contrast to the European NPP meta-model, sample points were randomly chosen using the biome stratification but the climate of the sample points were changed using the same methodology as described in Section 2.2.1. LPJ-GUESS was forced with the 500 perturbations (including baseline) to simulate NPP, enabling the constructions of NPP meta-models that can estimate NPP under potential future climate change conditions.

In line with the European meta-model, BME development is based on the assumption that maximum NPP at  $[\text{CO}_2]$  baseline can only be given when the most limiting climate variables of the respective biomes are at their optimum. In Paper III, the climate variables are total annual precipitation, maximum and minimum temperature. In the second step (see Figure 5), the relationships between NPP at baseline  $[\text{CO}_2]$  and the climate variables were described with mathematical functions.

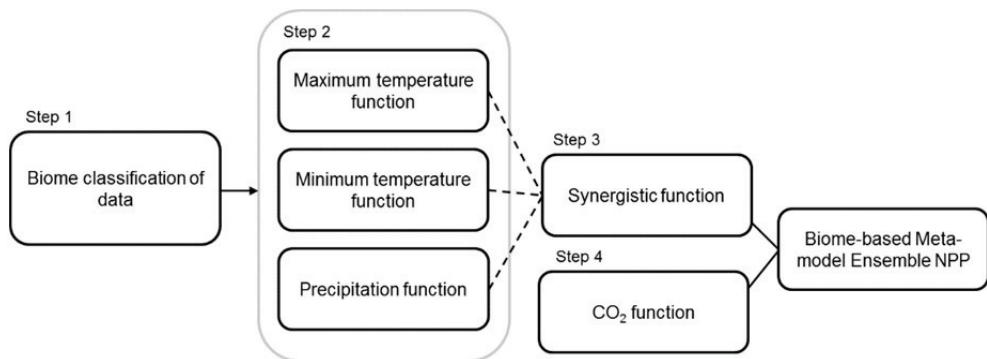


Figure 5 Conceptual logic of Biome-based Meta-model Ensemble

In the third step, the climate variable functions were combined into several groupings in order to carry out model selection using Bayesian information criterion (BIC) (Schwarz 1978, Burnham and Anderson 2002). In all biomes the best results were obtained by combining annual precipitation with maximum or minimum temperature in the synergistic function.

In the final step, the fertilization effect of  $[\text{CO}_2]$  on NPP was tailored to the climate conditions of each biome following the methodology described in Paper I (see Section 2.2.1).

### **2.2.3. Model evaluation (Paper I and III)**

In this section the NPP meta-models were evaluated for their performance in estimating current and future NPP in order to determine their applicability for modelling experiments. In general, model performance was evaluated with the coefficient of determination ( $R^2$  value) and the root mean square error (RMSE). The first specifies the strength of linear association between modelled and observed data in relative values ranging from 0 to 1 (where 1 indicates perfect association while 0 no association) while RMSE determines the total difference between two datasets (in their unit) (Smith et al. 1997, Smith and Smith 2007). Furthermore, the performance of the models were investigated with performance ratios (hereafter referred to as 'Q' while in Paper I as  $NPP_{ratio}$ ) by dividing the modelled NPP value by the independent NPP estimate or measurement. Model overestimation was indicated by  $Q > 1$  and underestimation by  $Q < 1$ . By assessing model performance, it is important to keep in mind that the model is only a simplification of an observed system and thus must by definition involve some degree of inaccuracy. It was therefore necessary to define an acceptable performance error range, which is dependent on the given assessment exercise and the applied data (see further details below).

In Paper I, the performance of the European meta-model in estimating NPP was gauged by comparing it with randomly chosen NPP predictions originating from LPJ-GUESS, and with a transect analysis of LPJ-GUESS NPP simulations on the European scale. In the latter, large parts of Europe were covered using baseline climate time-series (Mitchell and Jones 2005, Harris et al. 2014) and observed  $[\text{CO}_2]$ . Given the comparison between "meta-modelled" and "modelled" NPP data, acceptable model performance was defined to be within a stringent error range of  $Q = 0.9-1.1$ .

In Paper III, BME performance was examined by validating BME NPP estimates with a novel combination of more than 1200 NPP field-observations (Luyssaert et al. 2009, Michaletz et al. 2016). The temporal distribution of the NPP observations ranges from 1959 to 2006 while the geographical distribution is biased because

most are located in the northern hemisphere (particularly China) as can be seen in Figure 6. BME was forced with CRU climate “observations”<sup>1</sup> of the sites and global [CO<sub>2</sub>] in order to estimate NPP. BME NPP estimates were validated with NPP observations using a biome-by-biome comparison. For this NPP estimates and observations located in the same biome were averaged. Acceptable BME performance was defined by relaxing the Q error range to Q = 0.8 – 1.25, given the application of independent NPP observations and interpolated climate data, and the parsimony of BME.

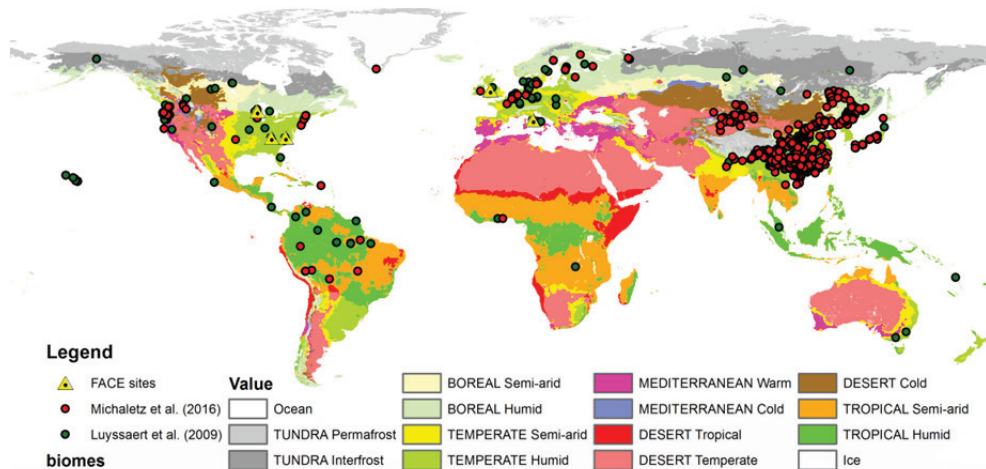


**Figure 6 Biome map and validation sites.**

Spatial distribution of the validation sites and major biome classification scheme (Reich and Eswaran 2002) used to stratify global ecosystems.

The ability of BME to reproduce NPP response to enriched [CO<sub>2</sub>] was evaluated with Free-Air CO<sub>2</sub> Enrichment (FACE) experiments (King et al. 2005, Norby et al. 2005, Norby et al. 2010, Hoosbeek et al. 2011, Zak et al. 2011, Smith et al. 2013). In a FACE site, ecosystems are subjected to ambient and enriched [CO<sub>2</sub>]. In total, six FACE sites covering four biomes were used, where all have an enriched [CO<sub>2</sub>] of 550 ppm, except one with [CO<sub>2</sub>] of 580ppm. Their geographical location and biome membership is shown in Figure 6. For the evaluation of the FACE experiments, CRU climate and [CO<sub>2</sub>] of the sites were applied to BME. Finally, the relative differences between NPP estimates using ambient and enriched [CO<sub>2</sub>] were calculated in order to determine NPP enhancement under enriched [CO<sub>2</sub>]. The results were evaluated by a biome-by-biome comparison, calculating average values for each biome analyzed.

<sup>1</sup> CRU climate data are interpolations and thus cannot represent the micro-climate of the sites (i.e. influence of relief).

## 2.3. Model coupling and application

This section deals with the coupling of parsimonious models to other sectoral models in integrated assessment (IA) modelling-frameworks. For each framework, I provide applications which are generally driven under future global change scenarios.

### **2.3.1. Sensitivity analysis of an integrated assessment modelling-framework (Paper II)**

The European meta-model was embedded in the CLIMSAVE (climate change integrated methodology for cross-sectoral adaption and vulnerability in Europe) framework. CLIMSAVE is a pan-European project that has developed an integrated assessment platform (IAP) enabling the investigation of cross-sectoral impacts of climate and socio-economic drivers while allowing explorations of possible adaptation to reduce potential vulnerabilities for a range of sectors on the European scale. The sectors are represented by meta-models covering agriculture, forests, biodiversity, coasts, water resources and urban development (Harrison et al. 2013). A simplified schematic workflow of the CLIMSAVE IAP is given in Figure 7.

Paper II explores the implications of multiple climate change scenarios and socio-economic scenarios for a range of ecosystem indicators in the CLIMSAVE IAP. This study aims to investigate the direct and indirect impacts of multiple climate and socio-economic drivers to identify:

- the sectors and regions most sensitive to future changes
- the mechanisms and directions of sensitivity (direct/indirect and positive/negative)
- the form and magnitudes of sensitivity (linear/non-linear and strong/weak/insignificant)
- the relative importance of the key drivers across sectors and regions

Paper II demonstrated the ability of parsimonious models to be easily coupled and to rapidly interact with other sectoral models in an IA modelling-framework.



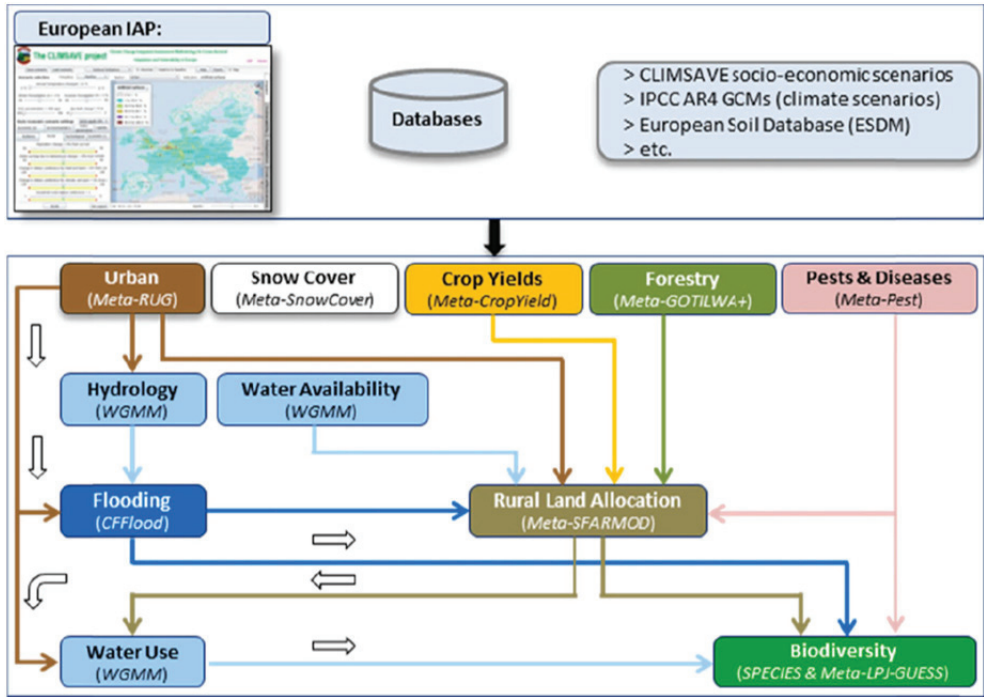
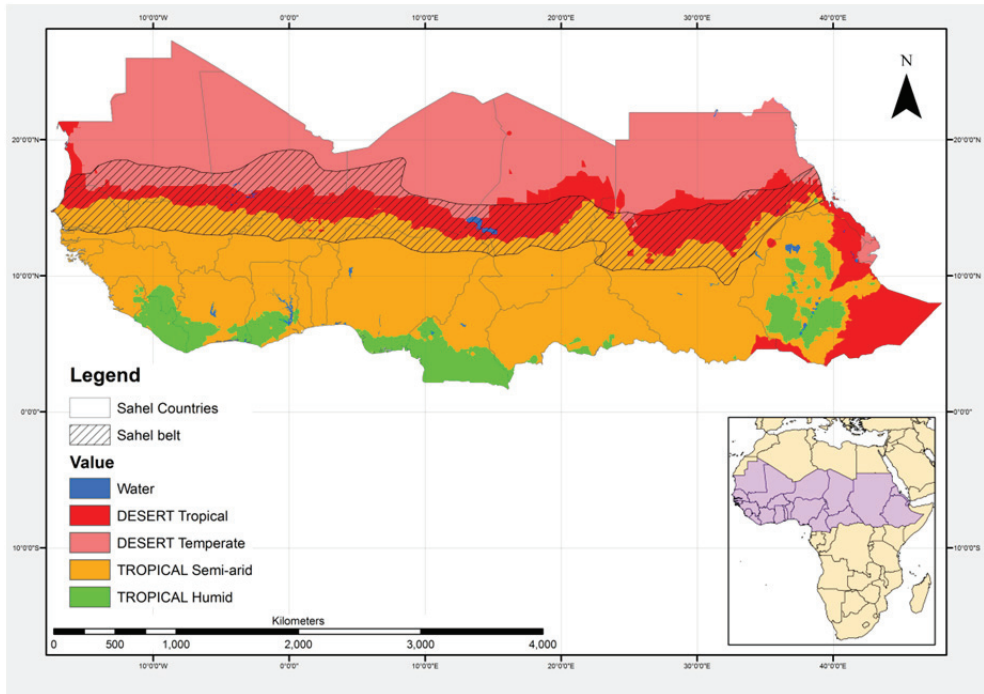


Figure 7 Simplified schematic workflow of the CLIMSAVE integrated assessment platform taken from Kebede et al. (2015)

### 2.3.2. NPP supply-demand balance in the Sahel

The balance between NPP supply and demand is a useful indicator of the biomass required for human consumption over broad regions (Abdi et al. 2014). This indicator is used in order to explore future NPP supply-demand balances under global change in the Sahel region, Africa (Paper IV).

The Sahel region is located between roughly 5° and 25° northern latitude and stretches from the Red Sea to the Atlantic Ocean, hereafter referred to as the greater Sahel (see Figure 8), which also includes the neighboring countries of the Sahel belt following Abdi et al. (2014). The Sahel is one of the most technologically underdeveloped regions in the world where the population largely relies on rain-fed farming practices. The region has a high reliance on their own land where 95% of food produce is for domestic consumption, (Abdi et al. 2014, Running 2014). The poor transportation infrastructure constrains the distribution of food resources (Olsson 1993). The vulnerability of the population to climatic induced variations in agricultural supply has led to several food shortages between late-1960s to the early 1990s.



**Figure 8** Map of the greater Sahel region as in 2000<sup>2</sup> and the respective Major Biomes of the region. Republic of South-Sudan is not shown on the map since it became an independent state in 2011. The Major Biome Map is taken from Reich and Eswaran (2002).

The investigation of NPP supply-demand balance in the Sahel was organized in three steps (see Figure 9). In the first step, BME (i.e. NPP model) was driven by climate data from several General Circulation Models for four representative concentration pathways (RCPs) ranging from 2.6 to 8.5 W m<sup>-2</sup> (van Vuuren et al. 2011) and LULC information (Hurtt et al. 2011). In the second step, country-level NPP demand and LULCC were modelled by PLUM (Parsimonious Land Use Model) (Engström et al. 2016b), which was driven by shared socio-economic pathways (SSPs) (van Vuuren et al. 2013, O'Neill et al. *in press*) and coupled to BME (providing annual country-level NPP based on cropland fractions taken from Hurtt et al. (2011)). In the last step, PLUM LULCC for cropland and grassland were applied to NPP supply in order to achieve consistency with the SSP narratives. NPP demand was disaggregated to the grid cell-level using SSP- and RCP based gridded population density data and subtracted from the gridded supply. The NPP supply-demand balances enabled the detection of NPP shortages

<sup>2</sup> Note that this study uses the African country definition for the year 2000 where South Sudan was a part of Sudan.

and surplus on regional-, country- and local-level. For a more detailed description see Paper IV.

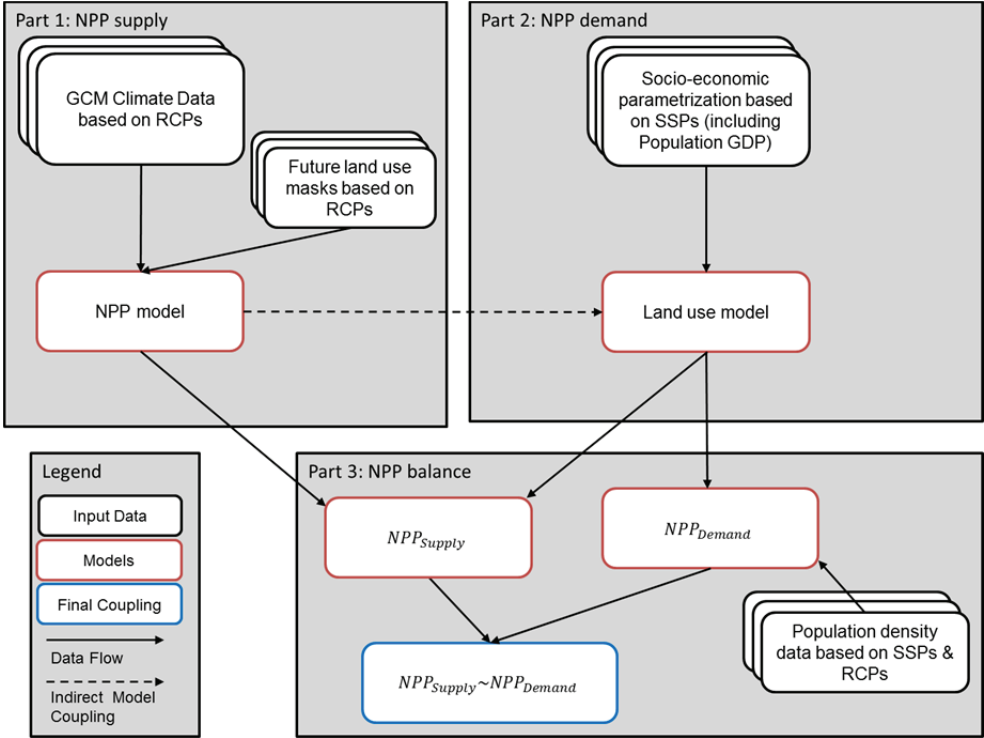


**Figure 9 Conceptual logic behind the NPP supply-demand balance framework.** The framework is based on three components enclosed by three grey boxes: (1) NPP supply (2) NPP demand and (3) NPP balance. The white boxes indicate data inputs originating from modelling studies (as referenced in section 2.2). The main models and equations developed and used in the current study are specified given in the white boxes outlined in red, which are connected with solid arrows to visualize the data flow. The dashed arrow between NPP model (section 2.1.1) and the land use model (section 2.1.2) presents an indirect model coupling by the land use model with NPP estimates for cropland and pasture. The box with the blue outline indicates the final coupling of the results, allowing the assessment of NPP supply and NPP demand relationships.

## 2.4. Scenarios

The future is unknown but possible future climate and socio-economic developments can be framed in different pathways (Moss et al. 2010, van Vuuren et al. 2011, O'Neill et al. *in press*). Future changes in climate (i.e. stable or increase in temperature) are represented with representative concentration pathways (RCPs). The pathways are underpinned by certain assumption about the future. For instance, a high consumption of fossil fuel will lead to high atmospheric [CO<sub>2</sub>], and thus increase in global mean temperature. At present, four RCPs are available with different cumulative pathways of future human greenhouse gases (GHG) emissions specified by their radiative forcing targets for the year 2100, ranging from 2.6 to 8.5 W m<sup>-2</sup> (van Vuuren et al. 2011). The pathways of mean global temperature and atmospheric [CO<sub>2</sub>] for the 21<sup>st</sup> century are shown in Figure 1 (based on RCP2.6 and RCP8.5), and are briefly summarized in Table 1.

**Table 1** Summary of the representative concentration pathways (RCPs) based on van Vuuren et al. (2011) and Moss et al. (2010).

Pathway	Key characteristics
<b>RCP 2.6</b>	Lowest scenario severity Before 2100: peak in radiative forcing of ~3 W m <sup>-2</sup> and in [CO <sub>2</sub> ] of ~490 ppm By 2100: decline in radiative forcing to 2.6 W m <sup>-2</sup> and [CO <sub>2</sub> ]
<b>RCP 4.5</b>	Medium-low severity By 2100: stabilization in radiative forcing at 4.5 W m <sup>-2</sup> and at [CO <sub>2</sub> ] of ~650 After 2100 stabilization
<b>RCP 6.0</b>	Medium-high severity By 2100: stabilization in radiative forcing at 6 W m <sup>-2</sup> and at [CO <sub>2</sub> ] of ~850 After 2100: stabilization
<b>RCP 8.5</b>	Highest severity By 2100: radiative forcing leading to 8.5 W m <sup>-2</sup> and to [CO <sub>2</sub> ] of ~1370 After 2100 continued rising

Future societal developments can be narrated using shared socio-economic pathways (SSPs) (O'Neill et al. *in press*), which are also based on certain assumptions about future developments. Five SSPs are applied, which are summarized by their key characteristics in Table 2. An important part of societal developments is human population growth, which steers the demand for food resources. Depending on the SSP, total human population predictions range from 8 to 10 billion humans for the year 2050, as shown in Figure 2. These numbers exert strong pressure on agricultural land which needs to be expanded in order to meet the demand for natural resources.

**Table 2** Summary of the Shared Socio-economic Pathway key characteristics (population development, economic growth, consumption & diet, policy orientation and technological change) based on (Engström et al. 2016a, O'Neill et al. *in press*).

<b>Pathway</b>	<b>Key characteristics</b>
<b>SSP1: Sustainability - Taking the green road</b>	Relatively low population development Medium to high economic growth Low growth in material consumption, low-meat diets Towards sustainable development Rapid technology development and transfer
<b>SSP2: Middle of the road</b>	Medium population development Medium (but uneven) economic growth Material-intensive consumption, medium meat consumption Weak focus on sustainability Medium technology development and slow transfer
<b>SSP3: Regional rivalry - A rocky road</b>	High population development Slow economic growth Material-intensive consumption Oriented toward security Slow technology development and transfer
<b>SSP4: Inequality - A road divided</b>	Relatively high population development Low to medium economic growth Elites: high consumption, rest: low consumption Toward the benefit of the political and business elite Rapid technology transfer in high-tech sectors, but slow in other, little transfer within countries to poorer people
<b>SSP5: Fossil-fuel development - Taking the highway</b>	Relatively low population development High economic growth Materialisms, status consumption, meat-rich diets Toward development, free markets, human capital Rapid technology change and transfer

# 3. Results and discussion

## 3.1. Evaluation of the NPP meta-models (Paper I)

The main aim of Paper I was to develop a rapid European meta-model of LPJ-GUESS that rapidly estimates NPP for potential natural vegetation (PNV) under current and future climate change scenario. The meta-model combines biophysical relationships between NPP and driving climate variables (maximum temperature, minimum temperature, summer precipitation, winter precipitation) along with the NPP response to enriched  $[\text{CO}_2]$ .

Overall the meta-model performed reasonably well in estimating total NPP by yielding an agreement of  $R^2 = 0.68$  and  $\text{RMSE} = 0.06 \text{ kg C m}^{-2} \text{ yr}^{-1}$  at baseline  $[\text{CO}_2] = 350 \text{ ppm}$  in comparison to LPJ-GUESS simulations. At enhanced  $[\text{CO}_2]$  the model agreement slightly decreased to  $R^2 = 0.62$  and  $\text{RMSE} = 0.08 \text{ kg C m}^{-2} \text{ yr}^{-1}$ . On the European scale, the meta-model yielded a good model performance in 65% (i.e.  $Q = 0.9-1.1$ ) of the grid cells in comparison to LPJ-GUESS NPP simulations at baseline  $[\text{CO}_2] = 350 \text{ ppm}$  (see Figure 10). Furthermore, the meta-model estimated NPP substantially faster than LPJ-GUESS.

The chosen synergistic approach is in line with other studies (e.g. Zaks et al. (2007)) by enabling co-limiting interactions between climate variables and their intra-annual variability to estimate NPP. The European meta-model is a useful alternative to traditional empirical models that control NPP with the most limiting climate variable (e.g. (Lieth and Whittaker 1975, Del Grosso et al. 2008)).

A main finding, which was important for the further development of thesis, was that parsimonious modelling techniques can be applied to estimate NPP for global change scenarios while capturing the general increase in NPP under enriched  $[\text{CO}_2]$ .

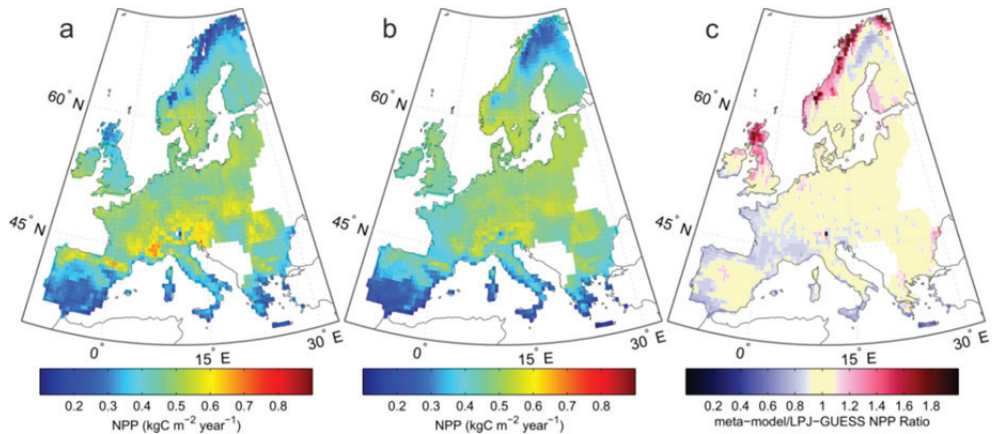


**Figure 10 Meta-model performance in estimating NPP compared to LPJ-GUESS NPP simulations.** The meta-model and LPJ-GUESS were driven by observed European climate and global  $[\text{CO}_2]$ . The left panel (a) shows LPJ-GUESS NPP simulations, the middle panel (b) visualizes meta-model NPP estimates and the right panel (c) illustrates the performance ratio (Q) between the model estimates.  $Q > 1$  indicates that the meta-model overestimates NPP while  $Q < 1$  shows that the meta-model underestimates NPP in comparison to LPJ-GUESS. Satisfactory model performance ( $Q$  between 0.9 - 1.1) is illustrated with yellow colored areas.

## 3.2. Validation of global Biome-based Meta-model Ensemble (Paper III)

In Paper III, the main aim was to extend the parsimonious modelling techniques developed in Paper I to the global level by developing a Biome-based Meta-model Ensemble (BME). Furthermore, Paper III aimed to validate BME with about 1500 independent NPP observations using a biome-by-biome comparison, and to evaluate BME's ability for capturing NPP enhancement under enhanced  $[\text{CO}_2]$  with FACE experiments.

As can be seen in Figure 11, BME yields acceptable model agreement ( $R^2 = 0.57$  and  $\text{RMSE} = 0.26 \text{ kg C m}^{-2} \text{ yr}^{-1}$ ) at the overall average biome level. However, BME's performance varies notably across the biomes; yielding good performance in the temperate humid biome ( $Q = 0.95$ ) and weak performance in the desert temperate biome ( $Q = 0.28$ ). BME captures the NPP enhancement due to enriched  $[\text{CO}_2]$  in three out of a total of four biomes. Furthermore, BME exhibits good skill in emulating LPJ-GUESS behavior in the majority of biomes. On the global scale, NPP estimates by BME agree well with other methods quantifying global NPP.

The results in Paper III, give confidence in BME NPP estimates for the majority of biomes. For the further development of this thesis, Paper III demonstrated that BME can be applied on biome-to-global levels in order to rapidly estimate current and future NPP for human consumption. Furthermore, Paper III extended the work

presented in Paper I to the global level by considering differences in plant growth on biome level instead of using administrative boundaries.

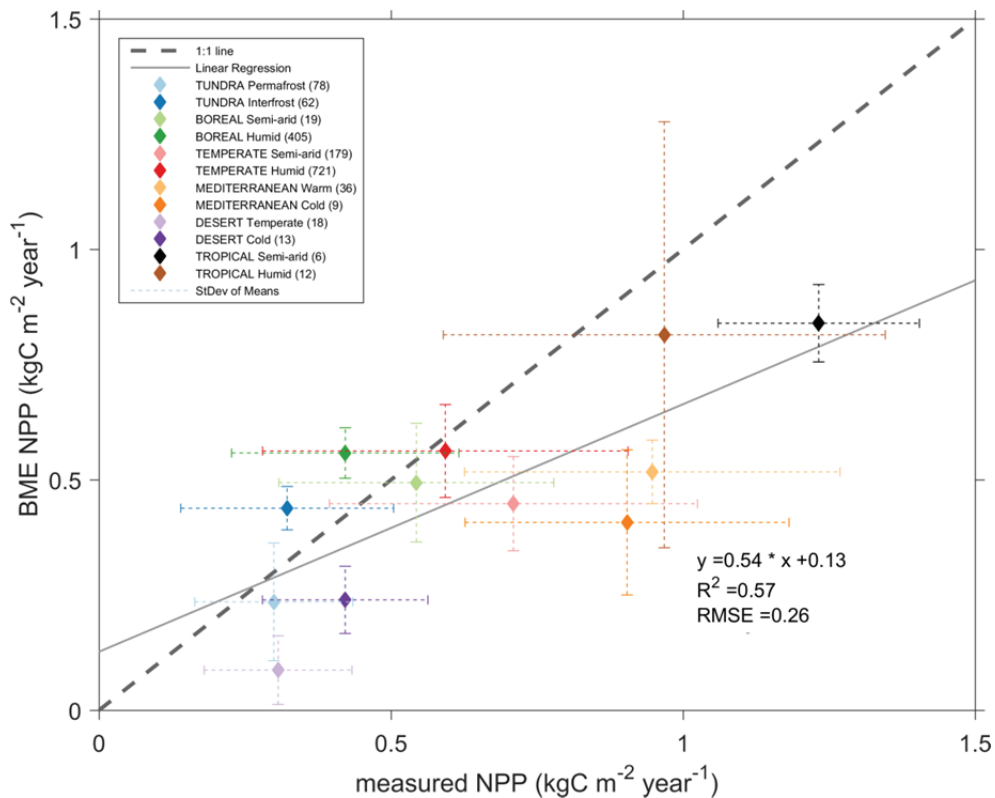


**Figure 11 Validation of Biome-based Meta-model Ensemble (BME).**

Biome-by-biome comparison between mean biome BME NPP estimates and mean biome in situ NPP measurements. Diamonds illustrate the mean values, horizontal dotted lines are the standard deviations of the mean observed data while the vertical dotted lines illustrate the standard deviation of the mean estimated BME NPP. The perfect agreement line is dashed.



### 3.3. Sensitivity analysis of an integrated assessment modelling-framework (Paper II)

Paper II aimed to conduct a sensitivity analysis of the European IA model developed within the CLIMSAVE project. Furthermore, Paper II explored the effects of wide ranges of climatic and socio-economic change drivers on model outputs related to key land- and water-based sectors in Europe. Such analysis provides better quantification and increased understanding of the complex relationships between input and output variables in an integrated model.

The results show that most sectors are either directly or indirectly sensitive to a large number of drivers. Over twelve of these drivers have indirect impacts on biodiversity, forests, land use diversity and water. Indirect effects on flooding were observed for four drivers. For the urban sector, by contrast, all the drivers are direct. Most of the driver–indicator relationships are non-linear, resulting in unpredictable behavior. This highlights the importance of considering cross-sectoral interactions in impact assessments. Such systematic analysis provides improved information for decision-makers to formulate appropriate adaptation policies to maximize benefits and minimize unintended consequences.

### 3.4. NPP supply-demand balance in the Sahel (Paper IV)

The main aim of Paper IV was to develop a simple IA modelling-framework that facilitates the NPP supply-demand balance. With regard to this thesis, an important aim was to couple BME (estimates NPP supply) with a LULC model (predicting NPP demand) to explore variations in the timing and geography of NPP supply and demand under several global change scenarios for the 21<sup>st</sup> century Sahel.

Paper IV reports that for the majority of the scenarios, per capita NPP demand outstrips the supply of NPP in the Sahel region. For instance, the scenario that deviates least from current socio-economic and climate trends (i.e. scenario: SSP2-RCP6.0) shows robust NPP shortages starting in the 2070s (see dots in Figure 12a) where per capita NPP demand outstrips its supply. For twelve out of fifteen scenarios the timing of the onset of NPP shortfalls varies and the demand cannot consistently be met as shown in Figure 12b (blue delineates NPP surplus while red and yellow indicate NPP shortage). For all scenarios, total per capita NPP supply doubles by 2050 in comparison to 2000. The demand increases due to

a combination of population growth and adoption of diets rich in animal products as narrated by the SSPs.

In three scenarios, per capita NPP demand can be met by the supply but the demand decreases also substantially in these scenarios. Variations in the timing of onset and end of per capita supply shortfalls stem from the shared socio-economic pathways than the representative concentration pathways.

An important finding is that this IA modelling-framework can be conducted with parsimonious models to explore the balance of NPP supply and demand on the regional scale.

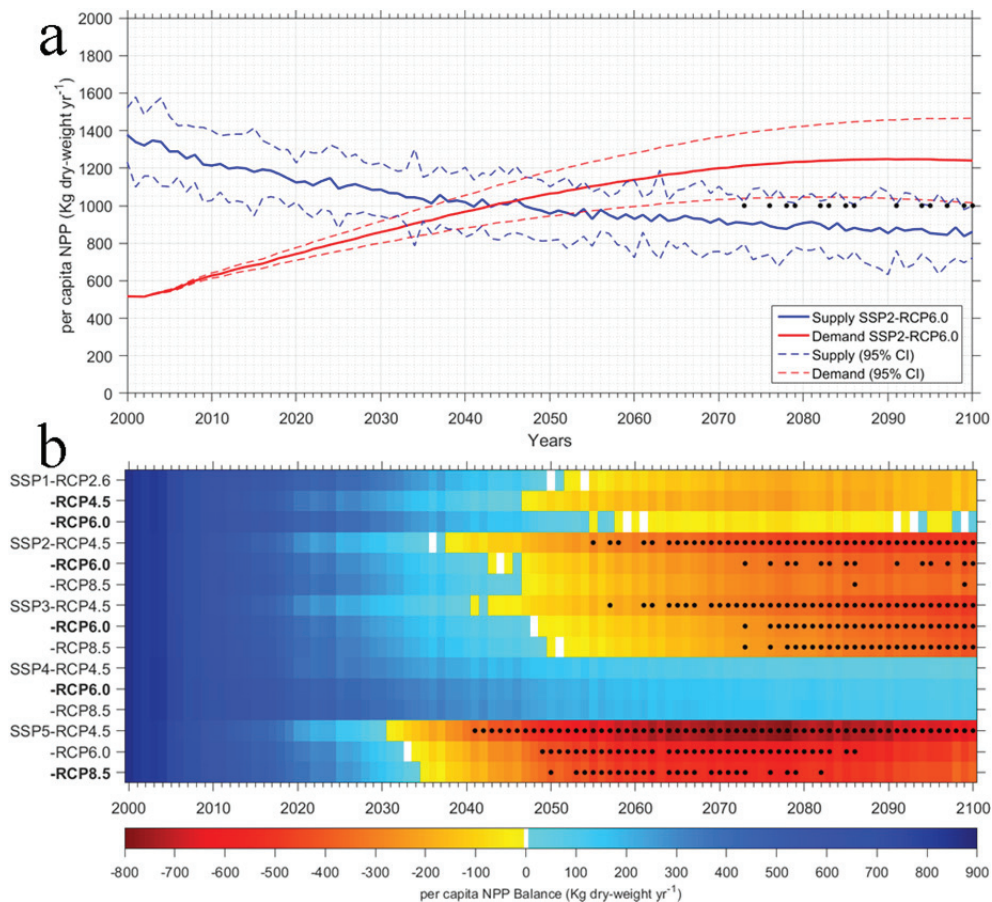


**Figure 12** The per capita NPP supply, demand and balance for the entire Sahel region over the simulated time period.

**a)** shows NPP supply (red) and demand (blue). The solid curves illustrate the mean of the SSP2-RCP6.0 combination. The dashed blue curves show supply uncertainty (95% confidence interval around the mean) based on the five GCMs NPP results. The dashed red curves show demand uncertainty (95% confidence interval around the mean) based on the uncertainty related to the interpretation and quantification of SSP2. **b)** shows the different magnitudes of the NPP balance and the varying onsets of shortage across all SSP-RCP combinations. Black dots illustrate years with a shortage outside of the 95% confidence intervals. The combinations are grouped according to the socio-economic scenarios (y-axis). The RCPs are ordered from low to high radiative forcing in each SSP group. The temporal trajectory is shown along the x-axis and the colouring indicates the sign of the annual NPP balance. Blues show a surplus of the NPP supply while yellow to red represent small to very large NPP shortages (i.e. the gap between supply and demand). SSP-RCP combinations in bold indicate the most likely SSP-RCP pairs based on Engström et al. (2016a).

## 4. Conclusions and outlook

The main objectives of this thesis were to develop and test parsimonious modelling techniques for quantifying terrestrial productivity under global change. The work of Paper I and Paper III resulted in NPP meta-models that are developed for applications ranging from the biome/regional to the global scale. It can be concluded that NPP parsimonious modelling techniques (i.e. NPP meta-models) are useful because they enable rapid NPP estimates. Furthermore, it can be concluded, that the European NPP meta-model emulates reasonably well LPJ-GUESS NPP simulations under current and future climate scenarios. However, it is suggested to apply BME since it is validated with NPP observation (and covers Europe), which allows drawing more robust conclusion about BME performance. BME can be applied with confidence to estimate current and future NPP for the most productive biomes of the planet, which are important for quantifying global NPP.

The coupling of the NPP meta-models with other sectoral models in IA modelling frameworks was the second thesis objective. This was accomplished in Paper II and Paper IV, demonstrating that the meta-models fulfil their purpose and are useful for future model coupling experiments, qualified by their parsimony, rapidness and reasonable model performance. Paper IV, has demonstrated that BME can provide valuable exploration of future land productivity under global change when coupled to other models. The NPP supply-demand balance advances previous research by exploring the impact of changing socio-economic and climate assumptions in the Sahel to support policy.

Overall, this thesis contributed with the development of parsimonious modelling techniques that are able to emulate complex process-based DVM NPP simulations under global change. This thesis demonstrates that NPP meta-models enable rapid NPP estimates and facilitate IA model coupling for exploring the impacts of global change on human-environmental systems.

For future work, it is suggest that BME could be improved by considering different environmental variables expressing intra- and inter-annual variability of plant growth. However, it is important to remember that an increase of driving variables potentially results in greater model complexity. With regard to the NPP supply-demand balance, the NPP supply represents PNV which cannot entirely represent agricultural productivity. This suggests the development of a

biophysically motivated meta-model that emulates DVM simulations of agricultural yields. Furthermore, the Sahel region framework should involve stakeholders and decision-maker participation (as conducted in the CLIMSAVE project). This could facilitate a better knowledge transfer on how the impacts of chosen policy interventions could affect the availability of natural resources.

# Acknowledgements

First of all, I'm very grateful to Jonathan Seaquist, my main supervisor, and Stefan Olin and Veiko Lehsten, my co-supervisors, for their excellent scientific guidance, encouragement, and great support throughout my PhD studies. I would also like to express my gratitude to Martin Sykes and Dörte Lehsten for guidance in the beginning of my PhD studies.

I would like to thank all co-authors for valuable discussions, shared data-sets and comments on manuscripts. My warmest thanks to my colleagues at the Department of Physical Geography and Ecosystem Science, Lund University. Furthermore, I would like to thank all collaborators in the European CLIMSAVE project, especially Paula Harrison, Ian Holman, George Cojocaru and Abyi Kebede for sharing their knowledge and support. I would also like to thank to my friends and colleagues at Lund Doctoral Student Union, especially Aleksandra Popovic, that do a great job in guarding the education and interests of the doctoral students at Lund University.

Many individuals have been great inspiration to this work and have become good friends. Niklas, you are a great friend and an unbeatable tennis partner, thank you for always believing in that I can do it. Kerstin, thank you for sitting in the same boat and the good collaboration on the Sahel paper. Stefan, you are a great guy and an excellent scientist, thank you for supporting me in solving many problems (= 42). Cecilia, you are a great friend and quizmaster, thanks for good advices and support. Ylva, thank you for sharing so much positive energy on a daily basis. I would also like to thank, Jan, Hakim, Lina, Bakhtiyor, David, Thomas, Bala and all the remaining fellow PhD students.

Johanna, thank you for your support and that you never stop believing in me, without you I would have never come so far. I'm thankful for your patience especially in the end of my dissertation work. I would like to thank Gunilla and Göran Eckerwall for knowing how it is to write a doctoral dissertation and providing useful advice.

I would like express my warmest thanks to my family in Gussow, my relatives and my great friends. Einen ganz besonderen Dank an meine Eltern Eva-Maria und Helmut und meinen Bruder Marcus Sallaba. Ich bin sehr dankbar für euer Vertrauen und eure Unterstützung, besonders in den letzten Jahren. Ohne euch, und vor allem ohne dich, liebe Mutti, hätte ich die eine oder andere Krise nicht so schnell überstanden. Ihr seid immer für mich da, dafür bin ich sehr dankbar.

My work was supported by the CLIMSAVE Project (Climate change integrated assessment methodology for cross-sectoral adaptation and vulnerability in Europe) funded under the Seventh Framework Programme of the European Commission, and by the Helge Ax:son Johnsons Stiftelse.

## References

- Abdi, A. M., J. Seaquist, D. E. Tenenbaum, L. Eklundh, and J. Ardo. 2014. The supply and demand of net primary production in the Sahel. *Environmental Research Letters* **9**:094003.
- Adams, B., A. White, and T. M. Lenton. 2004. An analysis of some diverse approaches to modelling terrestrial net primary productivity. *Ecological Modelling* **177**:353-391.
- Alexander, P., M. D. A. Rounsevell, C. Dislich, J. R. Dodson, K. Engström, and D. Moran. 2015. Drivers for global agricultural land use change: The nexus of diet, population, yield and bioenergy. *Global Environmental Change* **35**:138-147.
- Baisden, W. T. 2006. Agricultural and forest productivity for modelling policy scenarios: Evaluating approaches for New Zealand greenhouse gas mitigation. *Journal of the Royal Society of New Zealand* **36**:1-15.
- Bradshaw, R. H. W. 2008. Detecting human impact in the pollen record using data-model comparison. *Vegetation History and Archaeobotany* **17**:597-603.
- Burnham, K. P., and D. R. Anderson. 2002. *Model Selection and Multimodal Inference. A Practical Information-Theoretic Approach*. Second Edition edition. Springer, New York.
- Cleveland, C. C., P. Taylor, K. D. Chadwick, K. Dahlin, C. E. Doughty, Y. Malhi, W. K. Smith, B. W. Sullivan, W. R. Wieder, and A. R. Townsend. 2015. A comparison of plot-based satellite and Earth system model estimates of tropical forest net primary production. *Global Biogeochemical Cycles* **29**:626-644.
- Del Grosso, S., W. Parton, T. Stohlgren, D. Zheng, D. Bachelet, S. Prince, K. Hibbard, and R. Olson. 2008. Global potential net primary production predicted from vegetation class, precipitation, and temperature. *Ecology* **89**:2117-2126.
- Engström, K., S. Olin, M. D. A. Rounsevell, S. Brogaard, D. P. van Vuuren, P. Alexander, D. Murray-Rust, and A. Arneth. 2016a. Assessing uncertainties in global cropland futures using a conditional probabilistic modelling framework. *Earth System Dynamics Discussions* **2016**:1-33.
- Engström, K., M. D. A. Rounsevell, D. Murray-Rust, C. Hardacre, P. Alexander, X. F. Cui, P. I. Palmer, and A. Arneth. 2016b. Applying Occam's razor to global agricultural land use change. *Environmental Modelling & Software* **75**:212-229.
- Field, C. B., J. E. Campbell, and D. B. Lobell. 2008. Biomass energy: the scale of the potential resource. *Trends Ecol Evol* **23**:65-72.
- Foley, J. A. 1994. Net Primary Productivity in the Terrestrial Biosphere - the Application of a Global-Model. *Journal of Geophysical Research-Atmospheres* **99**:20773-20783.
- Foley, J. A., N. Ramankutty, K. A. Brauman, E. S. Cassidy, J. S. Gerber, M. Johnston, N. D. Mueller, C. O'Connell, D. K. Ray, P. C. West, C. Balzer, E. M. Bennett, S. R. Carpenter, J. Hill, C. Monfreda, S. Polasky, J. Rockstrom, J. Sheehan, S. Siebert, D. Tilman, and D. P. Zaks. 2011. Solutions for a cultivated planet. *Nature* **478**:337-342.



- Friedlingstein, P., M. Meinshausen, V. K. Arora, C. D. Jones, A. Anav, S. K. Liddicoat, and R. Knutti. 2014. Uncertainties in CMIP5 Climate Projections due to Carbon Cycle Feedbacks. *Journal of Climate* **27**:511-526.
- Friend, A. D., W. Lucht, T. T. Rademacher, R. Keribin, R. Betts, P. Cadule, P. Ciais, D. B. Clark, R. Dankers, P. D. Falloon, A. Ito, R. Kahana, A. Kleidon, M. R. Lomas, K. Nishina, S. Ostberg, R. Pavlick, P. Peylin, S. Schaphoff, N. Vuichard, L. Warszawski, A. Wiltshire, and F. I. Woodward. 2014. Carbon residence time dominates uncertainty in terrestrial vegetation responses to future climate and atmospheric CO<sub>2</sub>. *Proceedings of the National Academy of Sciences* **111**:3280-3285.
- Geider, R. J., E. H. Delucia, P. G. Falkowski, A. C. Finzi, J. P. Grime, J. Grace, T. M. Kana, J. La Roche, S. P. Long, B. A. Osborne, T. Platt, I. C. Prentice, J. A. Raven, W. H. Schlesinger, V. Smetacek, V. Stuart, S. Sathyendranath, R. B. Thomas, T. C. Vogelmann, P. Williams, and F. I. Woodward. 2001. Primary productivity of planet earth: biological determinants and physical constraints in terrestrial and aquatic habitats. *Global Change Biology* **7**:849-882.
- Giesecke, T., T. Hickler, T. Kunkel, M. T. Sykes, and R. H. W. Bradshaw. 2007. ORIGINAL ARTICLE: Towards an understanding of the Holocene distribution of *Fagus sylvatica* L. *Journal of Biogeography* **34**:118-131.
- Haberl, H., K. H. Erb, F. Krausmann, V. Gaube, A. Bondeau, C. Plutzar, S. Gingrich, W. Lucht, and M. Fischer-Kowalski. 2007. Quantifying and mapping the human appropriation of net primary production in earth's terrestrial ecosystems. *Proc Natl Acad Sci U S A* **104**:12942-12947.
- Harris, I., P. D. Jones, T. J. Osborn, and D. H. Lister. 2014. Updated high-resolution grids of monthly climatic observations – the CRU TS3.10 Dataset. *International Journal of Climatology* **34**:623-642.
- Harrison, P. A., R. W. Dunford, I. P. Holman, and M. D. A. Rounsevell. 2016. Climate change impact modelling needs to include cross-sectoral interactions. *Nature Clim. Change*.
- Harrison, P. A., I. P. Holman, G. Cojocaru, K. Kok, A. Kontogianni, M. J. Metzger, and M. Gramberger. 2013. Combining qualitative and quantitative understanding for exploring cross-sectoral climate change impacts, adaptation and vulnerability in Europe. *Regional Environmental Change* **13**:761-780.
- Haxeltine, A., and I. C. Prentice. 1996. A general model for the light-use efficiency of primary production. *Functional Ecology* **10**:551-561.
- Hickler, T., I. C. Prentice, B. Smith, M. T. Sykes, and S. Zaehle. 2006. Implementing plant hydraulic architecture within the LPJ Dynamic Global Vegetation Model. *Global Ecology and Biogeography* **15**:567-577.
- Hickler, T., B. Smith, I. C. Prentice, K. Mjöfors, P. Miller, A. Arneth, and M. T. Sykes. 2008. CO<sub>2</sub> fertilization in temperate FACE experiments not representative of boreal and tropical forests. *Global Change Biology* **14**:1531-1542.
- Hoosbeek, M. R., M. Lukac, E. Velthorst, A. R. Smith, and D. L. Godbold. 2011. Free atmospheric CO<sub>2</sub> enrichment increased above ground biomass but did not affect symbiotic N<sub>2</sub>-fixation and soil carbon dynamics in a mixed deciduous stand in Wales. *Biogeosciences* **8**:353-364.

- Hurttt, G. C., L. P. Chini, S. Frolking, R. A. Betts, J. Feddema, G. Fischer, J. P. Fisk, K. Hibbard, R. A. Houghton, A. Janetos, C. D. Jones, G. Kindermann, T. Kinoshita, K. K. Goldewijk, K. Riahi, E. Shevliakova, S. Smith, E. Stehfest, A. Thomson, P. Thornton, D. P. van Vuuren, and Y. P. Wang. 2011. Harmonization of land-use scenarios for the period 1500-2100: 600 years of global gridded annual land-use transitions, wood harvest, and resulting secondary lands. *Climatic Change* **109**:117-161.
- IPCC. 2001. Technical Summary. *Climate change 2001: Impacts, Adaptation, and Vulnerability. A Report of Working Group II of Intergovernmental Panel on Climate Change*, Cambridge University Press, New York, p. 1000.
- IPCC, editor. 2007. *Climate change 2007: Impacts, adaptation and vulnerability. Contribution of Working Group II to the Fourth Assessment Report of the Intergovernmental Panel on Climate Change*. Cambridge University Press., Cambridge, UK.
- Ito, A. 2011. A historical meta-analysis of global terrestrial net primary productivity: are estimates converging? *Global Change Biology* **17**:3161-3175.
- Kebede, A. S., R. Dunford, M. Mokrech, E. Audsley, P. A. Harrison, I. P. Holman, R. J. Nicholls, S. Rickebusch, M. D. A. Rounsevell, S. Sabaté, F. Sallaba, A. Sanchez, C. Savin, M. Trnka, and F. Wimmer. 2015. Direct and indirect impacts of climate and socio-economic change in Europe: a sensitivity analysis for key land- and water-based sectors. *Climatic Change* **128**:261-277.
- King, J. S., M. E. Kubiske, K. S. Pregitzer, G. R. Hendrey, E. P. McDonald, C. P. Giardina, V. S. Quinn, and D. F. Karnosky. 2005. Tropospheric O<sub>3</sub> compromises net primary production in young stands of trembling aspen, paper birch and sugar maple in response to elevated atmospheric CO<sub>2</sub>. *New Phytologist* **168**:623-636.
- Lieth, H., and R. H. Whittaker. 1975. *Primary productivity of the biosphere*. Springer-Verlag, New York.
- Luyssaert, S., I. Inglima, and M. Jung. 2009. Global Forest Ecosystem Structure and Function Data for Carbon Balance Research. *Global Forest Ecosystem Structure and Function Data for Carbon Balance Research*. Data set. Available on-line [<http://daac.ornl.gov/>] from Oak Ridge National Laboratory Distributed Active Archive Center, Oak Ridge, Tennessee, U.S.A. doi:10.3334/ORNLDAAC/949.
- Metzger, M. J., M. D. A. Rounsevell, L. Acosta-Michlik, R. Leemans, and D. Schröter. 2006. The vulnerability of ecosystem services to land use change. *Agriculture, Ecosystems & Environment* **114**:69-85.
- Michaletz, S. T., D. Cheng, A. J. Kerkhoff, and B. J. Enquist. 2016. Corrigendum: Convergence of terrestrial plant production across global climate gradients. *Nature* **537**:432-432.
- Miller, P. A., T. Giesecke, T. Hickler, R. H. W. Bradshaw, B. Smith, H. Seppä, P. J. Valdes, and M. T. Sykes. 2008. Exploring climatic and biotic controls on Holocene vegetation change in Fennoscandia. *Journal of Ecology* **96**:247-259.
- Mitchell, T. D., and P. D. Jones. 2005. An improved method of constructing a database of monthly climate observations and associated high-resolution grids. *International Journal of Climatology* **25**:693-712.

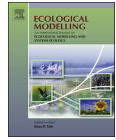
- Moss, R. H., J. A. Edmonds, K. A. Hibbard, M. R. Manning, S. K. Rose, D. P. van Vuuren, T. R. Carter, S. Emori, M. Kainuma, T. Kram, G. A. Meehl, J. F. B. Mitchell, N. Nakicenovic, K. Riahi, S. J. Smith, R. J. Stouffer, A. M. Thomson, J. P. Weyant, and T. J. Wilbanks. 2010. The next generation of scenarios for climate change research and assessment. *Nature* **463**:747-756.
- Norby, R. J., E. H. DeLucia, B. Gielen, C. Calfapietra, C. P. Giardina, J. S. King, J. Ledford, H. R. McCarthy, D. J. P. Moore, R. Ceulemans, P. De Angelis, A. C. Finzi, D. F. Karnosky, M. E. Kubiske, M. Lukac, K. S. Pregitzer, G. E. Scarascia-Mugnozza, W. H. Schlesinger, and R. Oren. 2005. Forest response to elevated CO<sub>2</sub> is conserved across a broad range of productivity. *Proceedings of the National Academy of Sciences of the United States of America* **102**:18052-18056.
- Norby, R. J., C. M. Iversen, J. Childs, and M. L. Tharp. 2010. ORNL Net Primary Productivity Data. Carbon Dioxide Information Analysis Center (<http://cdiac.ornl.gov>), U.S. Department of Energy, Oak Ridge National Laboratory, Oak Ridge, TN.
- Norby, R. J., D. E. Todd, J. Fufts, and D. W. Johnson. 2001. Allometric determination of tree growth in a CO<sub>2</sub>-enriched sweetgum stand. *New Phytologist* **150**:477-487.
- O'Neill, B. C., E. Kriegler, K. L. Ebi, E. Kemp-Benedict, K. Riahi, D. S. Rothman, B. J. van Ruijven, D. P. van Vuuren, J. Birkmann, K. Kok, M. Levy, and W. Solecki. *in press*. The roads ahead: Narratives for shared socioeconomic pathways describing world futures in the 21st century. *Global Environmental Change*.
- Olsson, L. 1993. On the Causes of Famine Drought, Desertification and Market Failure in the Sudan. *Ambio* **22**:395-403.
- Prentice I.C., A. B., W. Cramer, S.P. Harrison, T. Hickler, W. Lucht, S. Sitch, B. Smith, M.T. Sykes. 2007. Dynamic global vegetation modelling: quantifying terrestrial ecosystem responses to large-scale environmental change. Pages 175-192 *in* P. E. Canadell J.D., Pitelka L.F., editor. *Terrestrial Ecosystems in a Changing World*. Springer-Verlag, Berlin.
- Ramankutty, N., A. T. Evan, C. Monfreda, and J. A. Foley. 2008. Farming the planet: 1. Geographic distribution of global agricultural lands in the year 2000. *Global Biogeochemical Cycles* **22**.
- Ratto, M., A. Castelletti, and A. Pagano. 2012. Emulation techniques for the reduction and sensitivity analysis of complex environmental models. *Environmental Modelling & Software* **34**:1-4.
- Razavi, S., B. A. Tolson, and D. H. Burn. 2012. Numerical assessment of metamodelling strategies in computationally intensive optimization. *Environmental Modelling & Software* **34**:67-86.
- Reich, P. F., and H. Eswaran. 2002. Global resources. *In*: Lal, R. (ed.). *Encyclopedia of Soil Science*, pp. 607-611. Marcel Dekker, New York.
- Rockström, J., W. Steffen, K. Noone, A. Persson, F. S. Chapin, E. F. Lambin, T. M. Lenton, M. Scheffer, C. Folke, H. J. Schellnhuber, B. Nykvist, C. A. de Wit, T. Hughes, S. van der Leeuw, H. Rodhe, S. Sorlin, P. K. Snyder, R. Costanza, U. Svedin, M. Falkenmark, L. Karlberg, R. W. Corell, V. J. Fabry, J. Hansen, B. Walker, D. Liverman, K. Richardson, P. Crutzen, and J. A. Foley. 2009. A safe operating space for humanity. *Nature* **461**:472-475.

- Running, S. W. 2012. Ecology. A measurable planetary boundary for the biosphere. *Science* **337**:1458-1459.
- Running, S. W. 2014. A regional look at HANPP: human consumption is increasing, NPP is not. *Environmental Research Letters* **9**:111003.
- Running, S. W., R. R. Nemani, F. A. Heinsch, M. S. Zhao, M. Reeves, and H. Hashimoto. 2004. A continuous satellite-derived measure of global terrestrial primary production. *Bioscience* **54**:547-560.
- Schwarz, G. 1978. Estimating the Dimension of a Model. 461-464.
- Seaquist, J. W., L. Olsson, and J. Ardo. 2003. A remote sensing-based primary production model for grassland biomes. *Ecological Modelling* **169**:131-155.
- Shoo, L. P., and V. Valdez Ramirez. 2010. Global potential net primary production predicted from vegetation class, precipitation, and temperature: comment. *Ecology* **91**:921-923; discussion 923-925.
- Sitch, S., C. Huntingford, N. Gedney, P. E. Levy, M. Lomas, S. L. Piao, R. Betts, P. Ciais, P. Cox, P. Friedlingstein, C. D. Jones, I. C. Prentice, and F. I. Woodward. 2008. Evaluation of the terrestrial carbon cycle, future plant geography and climate-carbon cycle feedbacks using five Dynamic Global Vegetation Models (DGVMs). *Global Change Biology* **14**:2015-2039.
- Sitch, S., B. Smith, I. C. Prentice, A. Arneth, A. Bondeau, W. Cramer, J. O. Kaplan, S. Levis, W. Lucht, M. T. Sykes, K. Thonicke, and S. Venevsky. 2003. Evaluation of ecosystem dynamics, plant geography and terrestrial carbon cycling in the LPJ dynamic global vegetation model. *Global Change Biology* **9**:161-185.
- Smith, A. R., M. Lukac, R. Hood, J. R. Healey, F. Miglietta, and D. L. Godbold. 2013. Elevated CO<sub>2</sub> enrichment induces a differential biomass response in a mixed species temperate forest plantation. *New Phytologist* **198**:156-168.
- Smith, B., I. C. Prentice, and M. T. Sykes. 2001. Representation of vegetation dynamics in the modelling of terrestrial ecosystems: comparing two contrasting approaches within European climate space. *Global Ecology and Biogeography* **10**:621-637.
- Smith, B., D. Warlind, A. Arneth, T. Hickler, P. Leadley, J. Siltberg, and S. Zaehle. 2014. Implications of incorporating N cycling and N limitations on primary production in an individual-based dynamic vegetation model. *Biogeosciences* **11**:2027-2054.
- Smith, J. U., and P. Smith. 2007. *Introduction to environmental modelling*. Oxford University Press, Oxford ; New York.
- Smith, P., J. U. Smith, D. S. Powlson, W. B. McGill, J. R. M. Arah, O. G. Chertov, K. Coleman, U. Franko, S. Frohling, D. S. Jenkinson, L. S. Jensen, R. H. Kelly, H. Klein-Gunnewiek, A. S. Komarov, C. Li, J. A. E. Molina, T. Mueller, W. J. Parton, J. H. M. Thornley, and A. P. Whitmore. 1997. A comparison of the performance of nine soil organic matter models using datasets from seven long-term experiments. *Geoderma* **81**:153-225.
- Tang, G. P., B. Beckage, B. Smith, and P. A. Miller. 2010. Estimating potential forest NPP, biomass and their climatic sensitivity in New England using a dynamic ecosystem model. *Ecosphere* **1**:art18.
- Tao, F., M. Yokozawa, Z. Zhang, Y. Xu, and Y. Hayashi. 2005. Remote sensing of crop production in China by production efficiency models: models comparisons, estimates and uncertainties. *Ecological Modelling* **183**:385-396.

- van Vuuren, D. P., J. Edmonds, M. Kainuma, K. Riahi, A. Thomson, K. Hibbard, G. C. Hurtt, T. Kram, V. Krey, J.-F. Lamarque, T. Masui, M. Meinshausen, N. Nakicenovic, S. J. Smith, and S. K. Rose. 2011. The representative concentration pathways: an overview. *Climatic Change* **109**:5-31.
- van Vuuren, D. P., E. Kriegler, B. C. O'Neill, K. L. Ebi, K. Riahi, T. R. Carter, J. Edmonds, S. Hallegatte, T. Kram, R. Mathur, and H. Winkler. 2013. A new scenario framework for Climate Change Research: scenario matrix architecture. *Climatic Change* **122**:373-386.
- Villa-Vialaneix, N., M. Follador, M. Ratto, and A. Leip. 2012. A comparison of eight metamodeling techniques for the simulation of N<sub>2</sub>O fluxes and N leaching from corn crops. *Environmental Modelling & Software* **34**:51-66.
- Zak, D. R., K. S. Pregitzer, M. E. Kubiske, and A. J. Burton. 2011. Forest productivity under elevated CO<sub>2</sub> and O<sub>3</sub>: positive feedbacks to soil N cycling sustain decade-long net primary productivity enhancement by CO<sub>2</sub>. *Ecology Letters* **14**:1220-1226.
- Zaks, D. P. M., N. Ramankutty, C. C. Barford, and J. A. Foley. 2007. From Miami to Madison: Investigating the relationship between climate and terrestrial net primary production. *Global Biogeochemical Cycles* **21**:GB3004.

# Paper I





## A rapid NPP meta-model for current and future climate and CO<sub>2</sub> scenarios in Europe



Florian Sallaba\*, Dörte Lehsten, Jonathan Seaquist, Martin T. Sykes

Department of Physical Geography and Ecosystem Science, Lund University, Sölvegatan 12, 22362 Lund, Sweden

### ARTICLE INFO

#### Article history:

Received 10 July 2014  
Received in revised form  
13 December 2014  
Accepted 31 January 2015

#### Keywords:

NPP  
Ecosystem model  
Meta-modeling  
LPJ-GUESS  
Climate change  
Potential natural vegetation in Europe

### ABSTRACT

Net primary production (NPP) is the difference in gross photosynthetic assimilation of carbon and carbon loss due to autotrophic respiration, and is an important ecosystem variable that facilitates understanding of climate change impacts on terrestrial ecosystem productivity and ecosystem services. The aim of this study is to rapidly estimate the NPP of European potential natural vegetation for current and future climate and carbon-dioxide scenarios (CO<sub>2</sub>).

A NPP meta-model was developed and evaluated based on the dynamic global vegetation model LPJ-GUESS. LPJ-GUESS was used to simulate NPP under current and future climate change as well as CO<sub>2</sub> scenarios. The NPP dataset produced from these simulations was used to determine the empirical relationships between NPP and driving climate variables (maximum temperature, minimum temperature, summer precipitation, winter precipitation) along with CO<sub>2</sub> concentration. The climate variables' relationships were combined in a synergistic function including CO<sub>2</sub> relationships to estimate NPP. The meta-model was compared with randomly chosen NPP data originated from LPJ-GUESS. Furthermore, the meta-model's performance was evaluated on the European level with LPJ-GUESS simulations.

The meta-model performed reasonably well with regard to estimating total NPP while performances for species-specific NPP were poor. For total NPP, the meta-model generated an agreement of  $R^2 = 0.68$  and RMSE = 0.06 at CO<sub>2</sub> = 350 ppm in comparison to LPJ-GUESS simulations. The consideration of all CO<sub>2</sub> concentration scenarios yielded  $R^2 = 0.62$  and RMSE = 0.08.

A rapid synergistic approach is suggested that enables interactions between climate variables and their intra-annual variability to estimate NPP. This is a useful alternative to traditional empirical models that control NPP with the most limiting climate variable. The meta-model performed reasonably well for estimating total NPP for future climate change and CO<sub>2</sub> scenarios. However, species-specific NPP estimates were unsatisfactory, implying that the synergistic approach cannot account for species specific dynamics. Comparison between the meta-model and LPJ-GUESS at the European scale showed that additional environmental variables (e.g. solar radiation) would be necessary to improve the meta-model.

© 2015 Elsevier B.V. All rights reserved.

### 1. Introduction

Increasing atmospheric carbon-dioxide concentrations (CO<sub>2</sub>) and climate change are altering terrestrial ecosystem processes. This has impacts on services that are provided from ecosystems. It is therefore vital to assess these changes and provide measures of their magnitudes. Vegetation growth integrates various ecosystem processes and plays a key role expressing how productive an ecosystem is in terms of food resources, timber and biofuel production (Li et al., 2011). Net primary production (NPP) is the difference

in gross photosynthetic assimilation of carbon and carbon loss due to autotrophic respiration per area per unit time (Foley, 1994). A positive NPP illustrates an increase of structural biomass in plants (Van Oijen et al., 2010). It is a fundamental property of the biosphere, providing usable energy for all life on Earth (Zaks et al., 2007). NPP is also an important indicator for biodiversity, species composition and ecosystem services. It facilitates understanding of the global carbon cycle by providing information about CO<sub>2</sub> sinks and sources (King et al., 1995; Schuur, 2003).

Understanding the changes in NPP at the global and regional scale usually requires a modeling approach. The MIAMI model (Lieth and Whittaker, 1975) is the original global NPP model, and was formulated on basis of empirical relationship between climate variables and in situ measured NPP values. The MIAMI model

\* Corresponding author. Tel.: +46 462223659.  
E-mail address: [Florian.Sallaba@nateko.lu.se](mailto:Florian.Sallaba@nateko.lu.se) (F. Sallaba).



applies the Minimum Law, which assumes that plant productivity is limited by only a single climate variable (Lieth and Whittaker, 1975). The Minimum Law only considers the climate variable yielding the lowest NPP. However, new techniques and hypotheses about the climatic controls on NPP call for reanalysis of the problem since empirical models based on the Minimum Law hypothesis cannot always provide ecologically explainable estimates of NPP (Zaks et al., 2007).

The Miami model has been widely employed to predict NPP under current climate conditions because it is simple and often applied as a reference approach in empirical model development (Adams et al., 2004; Del Grosso et al., 2008). Extensions of the Miami model have been developed to account for CO<sub>2</sub> enrichment and other climate variables (King et al., 1997). Empirical NPP models give crucial measures of terrestrial ecosystem productivity and are major achievements in understanding global patterns of productivity (Zaks et al., 2007). But they should be treated with caution for future climate scenarios since they have been developed under current climate conditions and can lead to unreliable predictions (Adams et al., 2004).

The lack of extensive calibration and validation data limits empirical models to plot-level field measurements, and thus they may not be applicable for large scale studies (Adams et al., 2004; Clark et al., 2001; Schuur, 2003). Field measurements combined with tower-based energy flux estimations provide accurate determination of plant growth of a forest ecosystem over a time period (Fahey and Knapp, 2007). Tower-based measurements offer high temporal resolution estimations of CO<sub>2</sub> uptake or variations in CO<sub>2</sub> concentration flux during the growing season. However, they represent site-specific measurements and are therefore of limited use in the spatial domain.

At broader spatial scales remote sensing based vegetation indices have been employed to derive NPP and biomass (Ito, 2011). These methods incorporate uncertainties, because they are also location-specific, particularly in the case of purely empirical approaches. Though the integration of vegetation indices into light use efficiency models enhances their capacity to predict NPP and biomass across biomes, local calibration of these models (e.g. assignment of vegetation-specific physiological parameters such as maximum light use efficiency) is still required (Seaquist et al., 2003). The utility of satellite derived NPP estimates includes their ability to capture fine-scale detail in actual vegetation distribution, mapping vegetation change in ecosystems, as well as for calibration and validation of mechanistic ecosystem models (Smith et al., 2008; Tang et al., 2010).

Empirical or semi-empirical models have been criticized for the application of pre-processed climatologies as regards their calibration and development. Calculations of mean annual temperature and precipitation over a predefined time period do not capture patterns that are important for driving processes at shorter time scales thereby introducing spatial and temporal uncertainties. Therefore, impacts of ongoing climate change may be averaged out and the actual response of ecosystem production to climate may not be fully represented. Assumptions of an equilibrium ecosystem state are not satisfied under conditions of climate change and thus modeled NPP can be exaggerated (Del Grosso and Parton, 2010; Shoo and Valdez Ramirez, 2010). Finally, empirical NPP models are incapable of elucidating physiological and biochemical processes (e.g. photosynthesis or respiration) since they are formulated implicitly (King et al., 1997).

By contrast, dynamic global vegetation models (DGVMs) are capable of simulating fundamental plant growth processes by applying biophysical laws and biogeochemistry on a diurnal basis (Stich et al., 2003; Smith et al., 2001). This gives the advantage of being able to run DGVMs with future climate change scenarios in order to predict the NPP of ecosystem resources without

extrapolation. DGVMs have been applied for comparing the response of vegetation growth on CO<sub>2</sub> enhancement experiments locally and predicted globally (Hickler et al., 2008). However, large scale applications of DGVMs are time-consuming and computationally burdensome.

One approach for alleviating the computational burden of complex models is the meta-modeling concept, which aims to emulate the performance of complex models with simplified but efficient techniques (Ratto et al., 2012; Razavi et al., 2012). Meta-modeling is therefore suitable for overcoming time-consuming DGVM simulations. A useful technique is the development of an empirical model derived from results of DGVM simulations under various climate change scenarios. The DGVM simulation results and their driving climate variables are analyzed for empirical relationships in order to describe NPP as a function of the corresponding climatologies. This DGVM-based empirical model, referred to as a *meta-model*, can be applied for climate change scenarios, though it lacks the implementation of physical and biogeochemical processes in favor of computational speed. Such a method can therefore overcome the dependence of empirical NPP modeling applied to actual climate conditions and the limited number of available NPP field measurements, while minimizing extrapolation errors.

The development of a NPP meta-model is necessary since time-consuming simulations undermine the ability of DGVMs to be integrated in rapid and holistic assessment models. The CLIMSAVE (climate change integrated methodology for cross-sectoral adaptation and vulnerability in Europe) project is a unique example of an integrated assessment modeling framework that applies different sectoral models (e.g. urban growth, economic and coastal fluvial flood models) to holistically address impacts of climate change and increasing CO<sub>2</sub> concentrations on the environment (Harrison et al., 2012). Combining a wide range of sectoral models provides not only an assessment of the consequences of climate change on the different sectors but also allows a better understanding of their cross-sectoral feedbacks. On CLIMSAVE's web-based integrated assessment platform (IAP—[www.climsave.eu](http://www.climsave.eu)), the models have to interact rapidly on demand in order to provide reliable information about the risks of climate change to stakeholders and interested European citizens (Harrison et al., 2012). A DGVM-based meta-model is useful because it can be implemented in an IAP (e.g. CLIMSAVE IAP) in order to contribute with valuable cross-sectoral information about plant growth under climate change.

The overall aim of the study is to develop and test a rapid NPP meta-model based on DGVM simulations where the objective is to predict NPP of European potential natural vegetation (PNV) for current and future climate as well as CO<sub>2</sub> scenarios. This study hypothesizes that the meta-model is able to emulate species-specific and total NPP estimates generated by DGVM simulations. Furthermore, it is hypothesized that NPP can be described by a synergistic function of seasonal temperatures, seasonal precipitation and atmospheric CO<sub>2</sub> concentration. NPP can be therefore controlled synergistically by all climate variables instead of the most limiting one.

## 2. Materials and methods

### 2.1. Dynamic global vegetation model

In the current study, European PNV is described by NPP (kg C m<sup>-2</sup> year<sup>-1</sup>), which was simulated with the dynamic global vegetation model LPJ-GUESS (Smith et al., 2001). LPJ-GUESS combines mechanistic representations of plant physiological and biogeochemical processes and is driven by various climate variables, atmospheric CO<sub>2</sub> concentration, and soil characteristics

(Sitch et al., 2003; Smith et al., 2001). It simulates the atmosphere-vegetation carbon cycles and water fluxes, establishment of vegetation, fire impacts, random disturbance, and mortality rate of different age cohorts of vegetation (Lehsten et al., 2009, 2010; Smith et al., 2001). Additionally, successional vegetation dynamics can be simulated on different temporal and spatial scales (Schurgers et al., 2009a,b; Wania et al., 2009). Various species and their interactions can be simulated in LPJ-GUESS. They are described by their specific traits separately for each age cohort, e.g. establishment, mortality and growth rates, competition ability and canopy structure (Hickler et al., 2012). LPJ-GUESS simulates vegetation dynamics in several replicated patches within each grid cell. Wildfires and disturbance events are applied stochastically. Individuals (or a fraction of individuals) in a patch can be killed by wildfires (Sitch et al., 2003) while stochastic disturbance events remove all vegetation in a patch based on a user-defined probability. A detailed description of LPJ-GUESS can be found in (Sitch et al., 2003; Smith et al., 2001). The updated version used in this study is summarized by Hickler et al. (2012) and Smith et al. (2008).

## 2.2. Modeling protocol

European PNV was described using 16 common European trees, 3 shrubs and 2 generalized grass functional types (Hickler et al., 2012). The cohort mode was applied in LPJ-GUESS, which represents individual plant species in age-classes while accounting for vertical canopy structure within a patch. Replicate patches (here 25) were used in order to account for stochastic disturbance within a reasonable computational time frame. Disturbance was specified with an annual probability of 0.005 that corresponds, for example, with insect attacks or storms (Smith et al., 2008; Tang et al., 2010). All simulations were initiated with a de-trended 1000 years 'spin-up' phase in order to run the model from bare ground to a vegetation equilibrium state associated with a particular climate and CO<sub>2</sub> scenario. Each simulation was equipped with its unique 'spin-up' phase according to the scenario settings. The LPJ-GUESS simulations were conducted at the Lund University Numeric Intensive Computation Application Research Center (LUNARC).

## 2.3. Input data

A subset of European grid cells was selected for the meta-model development. The subset aimed to capture all the major European environmental zones as stratified by Metzger et al. (2005). The subset contained two cross European transects, consisting of 63 grid cells with a 0.5°×0.5° spatial resolution. The selection includes the main European climate conditions including cold & dry, cold & wet and warm & dry and their transition zones (Fig. 1). The 63 cells were overlaid with CRU TS 3.0 climate data (Harris et al., 2014; Mitchell and Jones, 2005), which have the same spatial resolution. CRU TS 3.0 data span from 1901 to 2006 and contain temperature, precipitation and cloudiness with a monthly temporal resolution. Soil texture characteristics of each grid cell fall into one of eight categories, and are based on the FAO global soil dataset (FAO, 1991), as described by Sitch et al. (2003) (see their Table 4). The annual atmospheric CO<sub>2</sub> concentrations for the baseline simulation were taken from records at Mauna Loa Observatory ([www.esrl.noaa.gov/gmd/ccgg/trends/](http://www.esrl.noaa.gov/gmd/ccgg/trends/)).

## 2.4. Climate change and CO<sub>2</sub> concentration scenarios of input data

The climate change scenarios are based on increasing monthly temperature and atmospheric CO<sub>2</sub> concentration, as well as changing summer (April–September) and winter precipitation

(October–March). In line with the CLIMSAVE project, maximum changes for each climate variable were defined in order to embrace the A1, A2, B1 and B2 IPCC climate change scenario families (Harrison et al., 2012; Holman and Harrison, 2011; IPCC, 2007). Maximum ranges are given in Table 1. The CRU TS 3.0 climate data were taken as the baseline climate time-series. The climate change and CO<sub>2</sub> concentration scenarios were superimposed upon the baseline climatologies (Table 1). This led to 500 different scenarios (including the baseline) for each of the 63 grid cells that were applied to simulate NPP in LPJ-GUESS.

## 2.5. Post-processing of climate data and LPJ-GUESS simulations

The combination of all possible climate change and CO<sub>2</sub> scenarios led to 31,500 simulations of 105 year long time-series. For the meta-model development it was therefore necessary to post-process this extensive dataset. Furthermore, stochastic generic-disturbance and fire events may occur in the last years of the simulations and underestimate the actual vegetation growth capability. The likelihood of these events was increased due to the low number of replicate patches (i.e. 25). These stochastic effects were therefore reduced by calculating mean NPP values over the last 20 years (providing 500 replicate patches). Likewise, we calculated mean cumulative winter (October–March) and summer precipitation (April–September) and mean monthly minimum and maximum temperatures over the same time period. The atmospheric CO<sub>2</sub> concentration was kept constant during each simulation but with levels depending on the given scenario (see Table 1).

## 2.6. NPP meta-model development

The MIAMI model (Lieth and Whittaker, 1975) has been a useful basis for the development of empirical NPP models, but such a methodology cannot account for intra-annual dynamics of climate variables because it only involves annual measures of temperature and precipitation to estimate NPP. For example, plant growth in Europe exhibits a strong seasonal cycle. In contrast, the current study is based on an account of the intra-annual dynamics of temperature and precipitation and their influence on vegetation growth. Temperature was divided into minimum winter ( $T_{\min}$ ) and maximum summer ( $T_{\max}$ ) temperatures in order to reflect intra-annual dynamics instead of using annual mean values. The two temperature variables can limit plant growth due to very high temperatures (e.g. heat stress) in the summer as well as very cold temperatures (e.g. frost damages) during winter (Flexas et al., 2014; Larcher, 2000, 2003; Wang et al., 2003). Climate change increases intra-annual precipitation variability scattered in more intense rainfall events and extended periods of droughts (Christensen et al., 2007; Fay et al., 2011; Jentsch and Beierkuhnlein, 2008). Precipitation was therefore split into summer ( $P_{\text{summer}}$ ) and winter ( $P_{\text{winter}}$ ) amounts to account for intra-annual variability. The precipitation variables can limit NPP due to water stress in drought periods (e.g. wilting) (Kreuzwieser and Gessler, 2010).

Empirical NPP models based on the Minimum Law (Lieth and Whittaker, 1975) have been critiqued for only considering the most NPP limiting climate to control NPP (Zaks et al., 2007). In the current study, it is assumed that plant species are able to compensate for moderate climatic stress under sub-optimal conditions. Their NPP can be affected by several climate variables which can act synergistically at the same time. Furthermore, it is assumed that reduced plant growth or stressed vegetation in one season may influence vegetation growth in the following season. For example, if the climate variables reduce NPP during

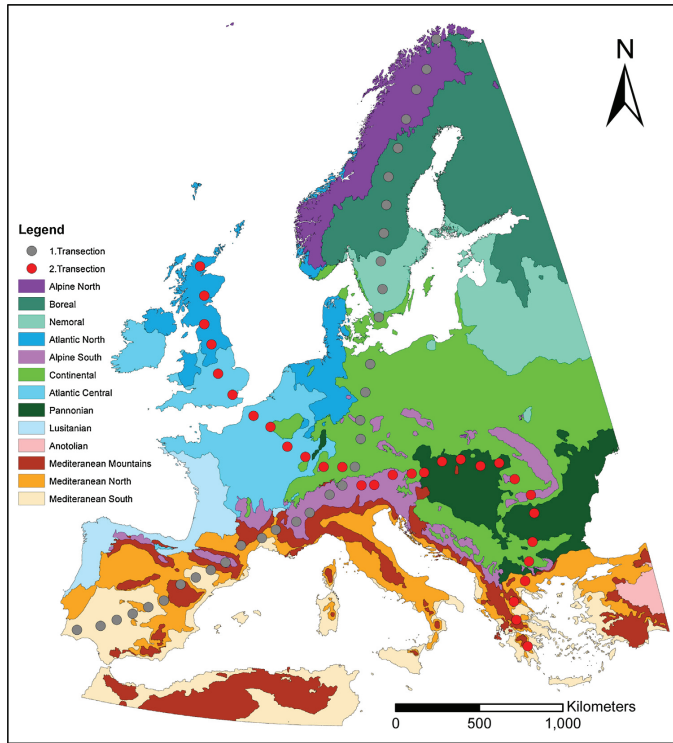


Fig. 1. A map showing European transects superimposed on the European environmental zones map from (Metzger et al., 2005).

the winter season it will also reduce NPP in the summer season. Annual NPP is therefore a combination of both seasons and not only the sum of winter and summer NPP where both are calculated independently. Seasonal NPP estimates are dependent on each other because summer NPP is also a function of winter climate and vice versa. This approach allowed an investigation of each climate variables' impact on annual NPP. These empirically developed relationships were combined to derive the NPP model.

We divided the model development in three steps: (1) NPP response to either increasing temperatures or changing precipitation at baseline CO<sub>2</sub> (350 ppm), (2) the development of a synergistic NPP function to combine changes in temperature and precipitation

estimated at CO<sub>2</sub> baseline; and (3) the analysis of CO<sub>2</sub> enhancement on NPP (Fig. 2). All steps in the development of the meta-model were applied at the species level as well as for total NPP.

#### 2.6.1. Climate variable functions

The first step focused on determining empirical relationships between the climate variables and NPP at CO<sub>2</sub> baseline concentration (Fig. 2). This analysis was based on the assumption that the maximum NPP will be only reached under optimal climate conditions. NPP decreases if one climate variable function is not at the optimum. All results of the NPP simulations at CO<sub>2</sub> baseline (i.e. 350 ppm) and their respective climate variable values were selected and merged into a new dataset. The maximum NPP

Table 1

Minimum and maximum stepwise changes in the climate variables as well as CO<sub>2</sub> concentration. The magnitudes of increases are related to how much a variable could be adjusted. Temperature was increased in four steps and the other variables in five steps leading to 500 different climate change scenarios.

Change attributes	Temperature change [°C]	Summer precipitation [% of baseline]	Winter precipitation [% of baseline]	Atmospheric CO <sub>2</sub> [ppm]
Minimum value	0	50	50	350
Maximum value	6	150	150	700
Magnitude of increase	2	25	25	87.5
No. of steps	4	5	5	5

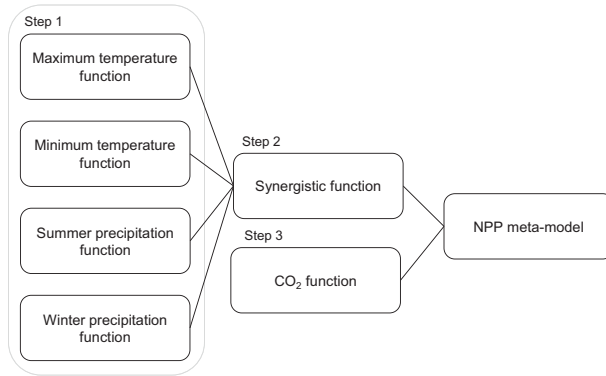


Fig. 2. Conceptual logic behind the meta-model development.

value ( $NPP_{max} = 0.7 \text{ kg C m}^{-2} \text{ year}^{-1}$ ) in the data was used to convert all values from absolute to relative NPP ranging between 0 and 1. The dataset was then duplicated four times in order to find empirical relationships between NPP and each climate variable independently. These relationships were formulated as functions describing the maximum NPP for the respective climate variables. Consequently, each dataset was sorted in ascending order with respect to the climate variable that was investigated. Each dataset consisted of the sorted climate variable values paired with their yielded NPP values derived from the LPJ-GUESS simulations.

**2.6.1.1. Temperature functions.** NPP is the difference between gross photosynthetic assimilation of carbon and carbon loss due to respiration (Foley, 1994; Ito, 2011) and is therefore strongly related to gross photosynthetic assimilation. NPP and photosynthetic response to temperature should therefore be similar. The photosynthetic response to temperature has been studied extensively and is described as a near parabolic, hump-shaped curve with a local maximum (Adams et al., 2004; Begon et al., 2006; Larcher, 2003). The photosynthetic rate starts at a local minimum and increases with increasing temperature until an optimum is reached at a maximum rate of photosynthesis. With increasing temperature, the photosynthetic rate then decreases rapidly (Adams et al., 2004; Larcher, 2003).

Seasonal changes were addressed by applying a chi-square function to summer maximum and winter minimum temperatures. Although both climate variables are correlated, their impacts on NPP differ, ranging from amplifying (optimum winter and summer temperature) to antagonistic effects (either optimum summer temperature and inhibiting winter temperatures or vice versa).

Samples describing the relationship between the climate variable value and its maximum NPP value were extracted from the sorted dataset (see above) while ignoring all NPP data reduced by the other climate variables. Each dataset was therefore processed with the following rules to detect a local maximum. (1) The first (ith) sample (i.e. NPP and its temperature value) in the sorted dataset was compared with the second sample (ith + 1). If the NPP value from the second sample was greater than the first sample (ith + 1 > ith), it was selected into list 'a', but if it was equal to or smaller than the previous sample (ith + 1 = ith), it was rejected. This procedure was repeated for the entirety of the dataset. (2) The same procedure was then executed with the dataset but starting with the last (kth) sample going backwards (k running from dataset size

to one). For example, the second-to-last (kth - 1) NPP value was compared to the last sample and if this NPP value was greater than the last sample (kth - 1 > kth), it was selected into list 'b'. If the second-to-last NPP value was equal or smaller than the last one (kth - 1 = kth), it was omitted. Both lists ('a' and 'b') were then merged to facilitate the dataset for the chi-square function fitting.

The maximum temperature function ( $f(T_{max})$ ) is given in the following equation:

$$f(T_{max}) = \frac{(T_{max}a)^{\frac{n}{2}} - 1}{2^{\frac{n}{2}} \Gamma(\frac{n}{2})} e^{-\frac{T_{max}a}{2}} b \quad (1)$$

where  $f(T_{max})$  calculates the maximum temperature NPP (relative);  $T_{max}$  is maximum summer temperature (°C) of a grid cell;  $a$  stretches the function along the abscissa;  $b$  stretches the function along the ordinate;  $n$  describes the shape of the function; and  $\Gamma$  is the gamma function. In Fig. 3a is shown how  $f(T_{max})$  bounds the maximum relative NPP -  $T_{max}$  samples. The parameter values of  $f(T_{max})$  are given in Table 2.

Minimum winter temperatures can reach sub-zero °C values (see Fig. 4b). The response function was therefore shifted along the temperature gradient to eliminate possible negative temperature values. The minimum temperature function is given in the following equation:

$$f(T_{min} - t_{min}) = \frac{((T_{min} - t_{min})a)^{\frac{n}{2}} - 1}{2^{\frac{n}{2}} \Gamma(\frac{n}{2})} e^{-\frac{(T_{min} - t_{min})a}{2}} b \quad (2)$$

where  $f(T_{min} - t_{min})$  estimates the minimum temperature NPP (relative);  $T_{min}$  is minimum winter temperature (°C) of a grid cell;  $t_{min}$  is the lowest temperature value (°C) that occurred in all grid

**Table 2**  
Parameter values of the four climate variable functions, the linear correction at CO<sub>2</sub> baseline concentration and the final model.

Eq. (1)	<i>a</i>	<i>b</i>	<i>n</i>	
Maximum temperature ( $f(T_{max})$ )	1.92	9.78	5.30	
Eq. (2)	<i>a</i>	<i>b</i>	<i>n</i>	<i>t<sub>min</sub></i>
Minimum temperature ( $f(T_{min})$ )	1.31	18.72	14.60	-40.00
Eq. (3)	<i>k</i>	<i>p</i>	<i>l</i>	
Summer precipitation ( $g(P_{summer})$ )	1.04	10.29	0.63	
Winter precipitation ( $g(P_{winter})$ )	0.92	69.21	1.34	
Eq. (4)	<i>s</i>	<i>u</i>		
Linear correction (NPP <sub>baseline</sub> )	0.96	-0.02		
Eq. (5)	<i>a</i>	<i>b</i>		
CO <sub>2</sub> relationship (NPP <sub>scenario</sub> )	-0.67	1.67		

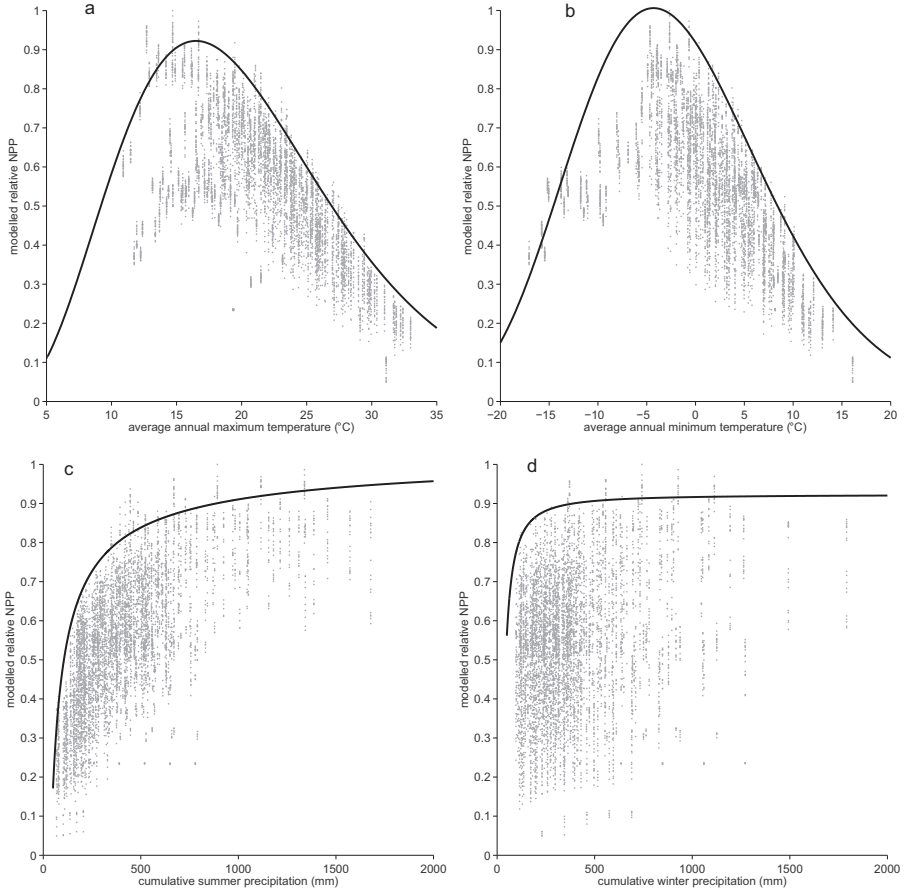


**Fig. 3.** Curves fitted to NPP-climate variable plots for (a) average annual maximum temperature vs total NPP values. (b) Average annual minimum temperature vs NPP values. (c) Summer precipitation vs total NPP (d) winter precipitation vs. total NPP.

cells and translates the function along the abscissa to the origin;  $a$  stretches the function along the abscissa;  $b$  stretches the function along the ordinate;  $n$  describes the shape of the function;  $\Gamma$  is the gamma-function. As can be seen in Fig. 3b,  $f(T_{\min} - t_{\min})$  bounds the greatest relative NPP vs  $T_{\min}$  samples. The parameter values are shown in Table 2.

**2.6.1.2. Precipitation functions.** The relationship between NPP and precipitation can be described by a saturation function (King et al., 1997; Lieth and Whittaker, 1975), starting with minimum NPP at low precipitation. NPP then increases with increasing precipitation levels until a saturation point is reached. Further increasing precipitation will not affect NPP because it is allocated as percolation or run-off. This assumption is based on the treatment of high precipitation levels in LPJ-GUESS (Gerten et al., 2004; Smith et al., 2001). The detection of local maxima in the summer and winter

precipitation data was conducted with the first rule (i.e. list 'a') applied in the temperature functions analysis.

Precipitation seasonality and its influence on NPP were captured by a saturation function for  $P_{\text{summer}}$  and  $P_{\text{winter}}$ . The function  $g(P)$  estimates relative NPP for both seasons and is given in the following equation:

$$g(P) = k - \frac{o}{p^l} \quad (3)$$

where  $p$  is the mean annual cumulative precipitation (mm) of the respective season;  $k$  is the maximum seasonal relative NPP that can be reached (derived from LPJ-GUESS simulations) and limits the growth of the function;  $o$  is a constant and  $l$  determines the slope of the function. In Fig. 3c can be seen that  $g(P_{\text{summer}})$  bounds the maximum total NPP– $P_{\text{summer}}$  samples. This also accounts for maximum total NPP– $P_{\text{winter}}$  which are limited by  $g(P_{\text{winter}})$  as can be seen in

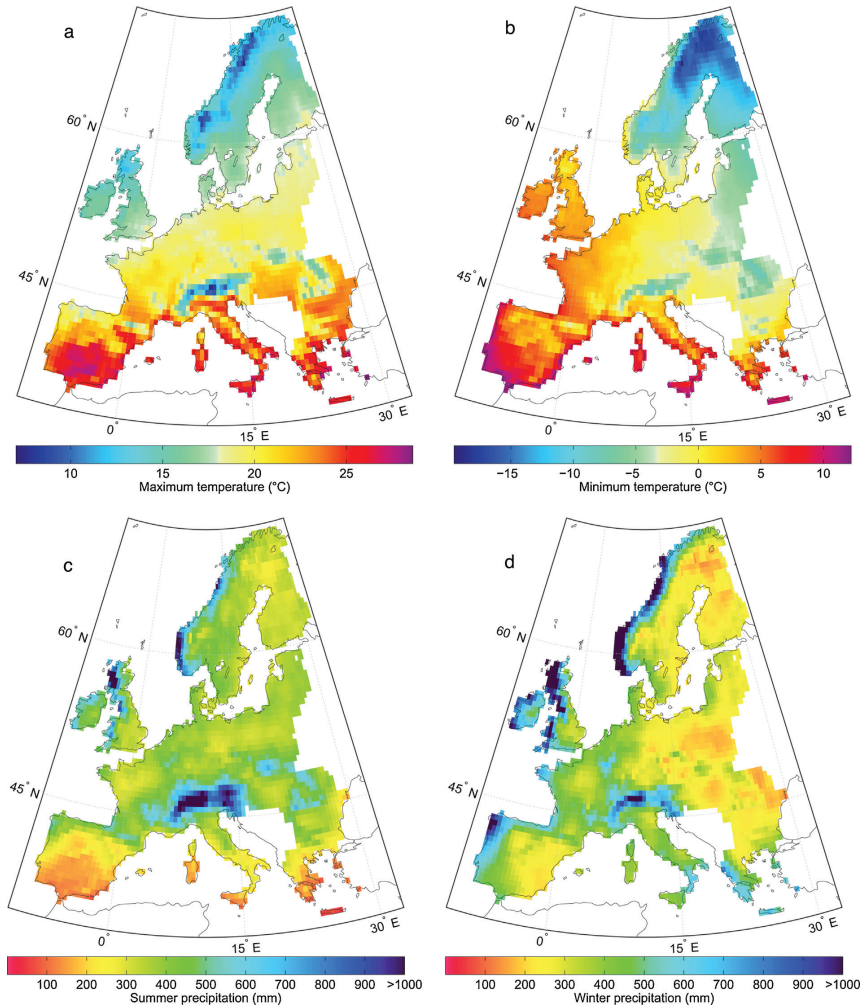


**Fig. 4.** The four climate variables on the European scale were derived from CRU TS 3.0 (Mitchell and Jones, 2005) grid cells. The climate variable values were post-processed and averaged over the last 20 years of the climate time-series from 1986 to 2006 (Section 2.5). (a) mean maximum summer temperature (b) mean minimum winter temperature, (c) mean cumulative sum of summer precipitation (d) mean cumulative sum of winter precipitation.

**Fig. 3d.** The parameter values for the precipitation functions are given in Table 2.

The parameter values of the four functions were determined with the fit command in MATLAB® (2011a), yielding a nonlinear least-squares model fit. Parameters with the lowest root mean square deviation (RMSE) were chosen for total NPP (Table 2) and the 21 species (see Appendix A), as suggested by Del Grosso et al. (2008).

#### 2.6.2. Synergistic function—Combining individual functions

In step two of the meta-model's development (Fig. 2), the four climate variables functions were combined into a synergistic function. The multiplication of seasonal temperatures and precipitation amounts yielded squared climate variable units that were therefore reduced with a square root function (e.g. mm<sup>2</sup> to mm). The function was then converted from relative to absolute NPP values as given in Eq. (4). The synergistic function was then adjusted linearly

(Eq. (4)) in order to account for maximum NPP simulations derived from LPJ-GUESS.

$$\text{NPP}_{\text{baseline}} = s \left( \sqrt{f(T_{\text{max}}) \times f(T_{\text{min}} - t_{\text{min}})} \times g(P_{\text{summer}}) \times g(P_{\text{winter}}) \right) \times \text{NPP}_{\text{max}} + u \quad (4)$$

where  $\text{NPP}_{\text{baseline}}$  is the estimated NPP ( $\text{kg C m}^{-2} \text{ year}^{-1}$ ) at baseline  $\text{CO}_2$  concentration;  $s$  is the slope;  $\text{NPP}_{\text{max}}$  is the maximum NPP ( $0.7 \text{ kg C m}^{-2} \text{ year}^{-1}$ ) of LPJ-GUESS simulations at  $\text{CO}_2$  baseline concentrations; and  $u$  is a constant. During the linear fitting procedure, the entire  $\text{CO}_2$  baseline dataset (i.e. 350 ppm) was randomly divided into an analysis subset containing the data of 30 grid cells and a validation subset containing the remaining 33 grid cells. The 'fit'-command in MATLAB® (2011a) was applied for the linear fitting procedure. The parameters with the lowest RMSE for total NPP (see Table 2) and the 21 species (see Appendix A) were selected.

### 2.6.3. $\text{CO}_2$ concentration function

Step three of the meta-model's development (Fig. 2) constituted the analysis of the effect of increasing  $\text{CO}_2$  concentration on NPP. The  $\text{CO}_2$ -dependent NPP growth is represented by a saturation function. Furthermore, as the  $\text{CO}_2$ -dependent NPP growth also depends on climate, the  $\text{CO}_2$  analysis was performed over a wide range of climate change scenarios which were kept constant for each  $\text{CO}_2$  increase (Table 1). Simulating NPP at different  $\text{CO}_2$  concentrations in LPJ-GUESS resulted in a linear relationship between NPP ratios ( $\text{NPP}_{\text{scenario}}/\text{NPP}_{\text{baseline}}$ ) and the reciprocal  $\text{CO}_2$  ratio ( $\text{CO}_{2\text{baseline}}/\text{CO}_{2\text{scenario}}$ ) (Eq. A.9 and Fig. A.3). Solving the function for  $\text{NPP}_{\text{scenario}}$  resulted in the following equation:

$$\text{NPP}_{\text{scenario}} = \text{NPP}_{\text{baseline}} \times \left( a \left( \frac{\text{CO}_{2\text{baseline}}}{\text{CO}_{2\text{scenario}}} \right) + b \right) \quad (5)$$

where  $\text{NPP}_{\text{scenario}}$  is NPP ( $\text{kg C m}^{-2} \text{ year}^{-1}$ ) of a grid cell under a scenario specific atmospheric  $\text{CO}_2$  concentration (ppm);  $\text{NPP}_{\text{baseline}}$  is the modeled NPP ( $\text{kg C m}^{-2} \text{ year}^{-1}$ ) under a  $\text{CO}_2$  concentration of 350 ppm;  $a$  is the slope of the linear relationship;  $\text{CO}_{2\text{baseline}}$  equals a concentration of 350 ppm;  $\text{CO}_{2\text{scenario}}$  is an enhanced  $\text{CO}_2$  concentration ( $>350$  ppm); and  $b$  is the constant term where the function intercepts the ordinate. The parameters  $a$  and  $b$  for total and species-specific NPP were determined with linear fitting ('fit'-command) in MATLAB® (2011a) by randomly dividing the dataset into an analysis subset (30 grid cells) and a validation subset (33 grid cells). The parameters with the lowest RMSE value for total NPP (see Table 2) and the 21 species (see Appendix A) were selected.

## 2.7. Validation of meta-model

### 2.7.1. Comparison of meta-model with LPJ-GUESS

For the assessment of meta-model performance, 100 randomly sampled CRU TS 3.0 grid cells were chosen, excluding those used previously. The same climate and  $\text{CO}_2$  adjustments were applied as in the pre-processing section (Table 1). LPJ-GUESS was forced with the data using the same modeling protocol (Section 2.2), giving a comprehensive validation dataset of 50 000 NPP simulations. The LPJ-GUESS simulations and the climate data were post-processed as in Section 2.5. Several measures were then applied in order to gauge meta-model performance against LPJ-GUESS simulations (Smith and Smith, 2007; Smith et al., 1997) (see Appendix A for details). The meta-model's agreement (i.e. precision) with LPJ-GUESS simulations was determined with the coefficient of determination ( $R^2$  value) in order to measure the strength of linear association between the models, while the root mean squared error (RMSE) gives their total difference in NPP units ( $\text{NPP kg C m}^{-2} \text{ year}^{-1}$ ). Systematic over- and underestimation (i.e. bias) of the meta-model estimates were determined with the mean

difference (MD) as suggested in inter-model comparisons (Morales et al., 2005; Smith et al., 1997) (see Appendix A):

$$\text{MD} = \sum_{i=1}^n \frac{O_i - P_i}{n} \quad (6)$$

where MD is the mean difference between the models ( $\text{kg C m}^{-2} \text{ year}^{-1}$ );  $n$  is the number of paired NPP estimates;  $O_i$  is the  $i$ th NPP simulation from LPJ-GUESS ( $\text{kg C m}^{-2} \text{ year}^{-1}$ ); and  $P_i$  is the  $i$ th meta-model NPP estimate ( $\text{kg C m}^{-2} \text{ year}^{-1}$ ); and  $i$  denotes the application of the identical climate variables in LPJ-GUESS as well as the meta-model. MD can be directly related to the Student's  $t$  and MD to be evaluated with the critical  $t$ -value for the given degrees of freedom in a paired  $t$ -test (Smith and Smith, 2007; Smith et al., 1997). In line with conservative statistical conventions a  $t$ -value greater than the critical two-tailed value for  $p < 0.001$  was chosen to determine whether the meta-model estimates show a significant bias towards over- or underestimation when compared with LPJ-GUESS NPP simulations (Morales et al., 2005; Smith et al., 1997).

### 2.7.2. Transect analysis on the European scale

Differences between total NPP from the meta-model and LPJ-GUESS were also examined across different European environmental zones. A total of 2766 CRU TS 3.0 grid cells ( $0.5^\circ \times 0.5^\circ$  spatial resolution) covering most of Europe were used. PNV was simulated in LPJ-GUESS under seven  $\text{CO}_2$  concentration scenarios. Each scenario had a different but constant  $\text{CO}_2$  concentration starting from 350 ppm up to 700 increased by 50 ppm progressively. The same LPJ-GUESS modeling protocol was followed as described in Section 2.2. The climate variables were post-processed as in Section 2.5 (Fig. 4). NPP was also estimated with the meta-model using the same climate and  $\text{CO}_2$  settings. NPP ratios between meta-model and LPJ-GUESS results were calculated in order to indicate the agreement between the models. NPP ratios  $<1$  show NPP underestimation by the meta-model while NPP ratios  $>1$  specify overestimation of the meta-model in comparison to LPJ-GUESS NPP simulations. Perfect agreement between the models is given with NPP ratio = 1. A NPP ratio range between 0.9–1.1 was defined to provide satisfactory agreement between the models since it assumes an error of  $\pm 10\%$  to be acceptable, given the inherent limitations associated with the meta-model. This provides a balance between slight over- and underestimation of meta-model NPP estimates compared to LPJ-GUESS NPP simulations.

## 3. Results

### 3.1. Comparison of meta-model with LPJ-GUESS

The meta-model estimated NPP more rapidly than LPJ-GUESS during the validation. Computational times for the meta-model and LPJ-GUESS NPP simulations were recorded for the European dataset (i.e. 2766 grid cells). The meta-model estimated total and species-wise NPP for the European dataset in less than five seconds on a standard desktop computer whereas LPJ-GUESS simulated species-specific and total NPP for all 2766 grid cells in 25:47:20 h on a powerful LUNARC mainframe.

Total NPP estimates from the meta-model and LPJ-GUESS simulations showed a sufficient agreement for all climate variable changes at baseline  $\text{CO}_2$  concentration (350 ppm). The meta-model

yielded a performance of  $R^2 = 0.68$  and a RMSE = 0.06 but overestimates total NPP with a MD =  $-0.018$  ( $t = -30.8$ ,  $df = 9999$ ,  $p < 0.001$ ) in comparison to LPJ-GUESS simulations.

Meta-model performance declined with increasing CO<sub>2</sub> concentration. The increased CO<sub>2</sub> concentrations yielded an overall agreement of  $R^2 = 0.62$  and a total difference of RMSE = 0.08. Incorporating higher CO<sub>2</sub> levels generated increased NPP overestimation by the meta-model with MD =  $-0.020$  ( $t = -56.3$ ,  $df = 49,999$ ,  $p < 0.001$ ) in comparison to LPJ-GUESS.

The species-specific NPP estimates generated by the meta-model generally show poor levels of performance with those estimates from LPJ-GUESS for all CO<sub>2</sub> concentrations. Moreover, levels of agreement for specific species vary substantially (see Appendix D). *C3 grass* (herbaceous) achieved the best association with  $R^2 = 0.33$  with a difference of RMSE = 0.04. *Populus tremula* yielded the second highest  $R^2 = 0.32$  and total difference of RMSE = 0.09. *Betula pendula* achieved the third highest  $R^2 = 0.30$  and a slightly smaller RMSE = 0.08. All other species generated  $R^2 < 0.3$ .

The sum of the individual species' NPP results was inconsistent with total NPP estimates for all climate and CO<sub>2</sub> scenarios because the meta-model overestimated species NPP. The comparison yielded a RMSE = 1.21 highlighting the poor performance of the meta-model for estimating species-specific NPP.

### 3.2. Comparison of meta-model with LPJ-GUESS—European scale

In general, favorable NPP estimates were generated by the meta-model. Nevertheless, areas with considerable under- and overestimation at baseline CO<sub>2</sub> concentration are evident. Fig. 5a shows total NPP simulations from LPJ-GUESS, Fig. 5b total NPP estimates from the meta-model, and Fig. 5c their NPP ratio at baseline CO<sub>2</sub> concentrations across Europe. Comparing Fig. 5a and b shows that the magnitudes of the meta-model's NPP estimates spatially coincide with simulations from LPJ-GUESS. The proportion of grid cells showing total NPP ratios between 0.9–1.1 (meta-model/LPG-GUESS) is 65%. Highest agreements are in central Spain, central Europe, southern Scandinavia and Eastern Europe (Fig. 5a–c).

The meta-model underestimated NPP mostly along the coasts of Western Europe at CO<sub>2</sub> baseline concentrations. Underestimations of 20–30% ( $-0.10$  to  $-0.15$  kg C m<sup>-2</sup> year<sup>-1</sup>) occur in Portugal, northern Spain and western France, Brittany, the southern coast of Ireland and UK, the Mediterranean Mountains and Southern Alps of France, including parts of the Pyrenees. Northern Sweden, Norway, Finland and Sicily also show underestimations.

Overestimations are found mostly in northern Europe (Scotland, Norwegian coast and mountains as well as western Finland) and are on the order of 20–100% (0.10–0.25 kg C m<sup>-2</sup> year<sup>-1</sup>) (Fig. 5c), where LPJ-GUESS simulations resulted in general low NPP values.

At the European scale, enhanced CO<sub>2</sub> scenarios reduced meta-model performance resulting primarily in NPP overestimation. Stepwise increase of atmospheric CO<sub>2</sub> concentration led to a progressive decline of grid cells which have a satisfactory NPP ratio (Table 3 and Fig. 5d–l).

The proportion of grid cells with an acceptable ratio declined steadily from 65% at baseline CO<sub>2</sub> concentration to 52% at CO<sub>2</sub> concentration of 700 ppm. Fig. 5 (right panels) shows that initially favorable NPP ratios in central Europe and southern Scandinavia changed to NPP ratios > 1.1 with increasing CO<sub>2</sub> concentration. In France, initial NPP ratios < 0.9 (at CO<sub>2</sub> baseline) became slightly but successively larger. Conversely, grid cells with favorable original NPP ratios in central Spain and Italy fell into NPP ratios < 0.9 (NPP underestimation) with increasing CO<sub>2</sub> concentration.

**Table 3**

Differences in total NPP from meta-model and LPJ-GUESS with enhanced CO<sub>2</sub> concentrations at the European scale (2766 grid cells).

CO <sub>2</sub> concentration (ppm)	No. of cells within NPP ratio range of 0.9–1.1	Percentage of cells in NPP ratio range of 0.9–1.1
350	1793	65
400	1753	63
450	1699	61
500	1651	60
550	1574	57
600	1529	55
650	1490	54
700	1431	52

## 4. Discussion

In the current study a meta-model was developed that estimates total and species' NPP for PNV in Europe. This meta-model is useful because it combines the simplicity and speed of empirical NPP models with the process based explanations of DGVMs. With regard to speed, the meta-model predicted total and species-wise NPP for 2766 grid cells far more rapidly than LPJ-GUESS providing a meaningful surrogate for computationally expensive LPJ-GUESS simulations. The meta-model can be easily coupled to other models because of the decrease in computational demand associated with the reduction in complexity (King et al., 1997). The meta-model has been successfully implemented into the CLIMSAVE modeling framework where it interacts rapidly with other models on a web-based IAP (Harrison et al., 2012).

Since the meta-model is derived from process-based LPJ-GUESS simulations, it has the ability to predict NPP for climate change and CO<sub>2</sub> scenarios while overcoming the extrapolation problems that beset traditional empirical models (Adams et al., 2004; Shoo and Valdez Ramirez, 2010). Despite this, the meta-models' NPP estimates are only valid as long as the input climate data does not exceed the limits of the scenarios that were applied during the meta-model development (Table 1). Outside of these climate and CO<sub>2</sub> ranges, the results need to be treated with caution.

For total NPP, the meta-model's estimates yielded reasonable agreements with LPJ-GUESS simulations. But species-specific meta-model performance was poor. Incorporating species-specific information such as competition for resources, establishment, dispersal, mortality and fire resistance into a meta-model framework provides some unique challenges because the climate variable functions cannot carry species-specific information. This information is difficult to synthesize using empirical and statistical approaches. It is therefore necessary to parameterize this information for each species but the tradeoff would be an increase in meta-model complexity.

### 4.1. Meta-model development

The Minimum Law (Lieth and Whittaker, 1975) is a standard approach applied in various empirical NPP models (Adams et al., 2004; Del Grosso et al., 2008; King et al., 1997; Schuur, 2003) but it excludes valuable information about how the ecosystem responds to all climate variables. The meta-model combines temperature and precipitation in order to describe ecosystem response to climate, as well as to capture synergistic interactions between the climate and vegetation growth. The meta-model was solely developed on LPJ-GUESS and evaluated with LPJ-GUESS NPP simulations. Prior studies have noted that LPJ-GUESS performs well in simulating the NPP of managed forest and PNV from local to global scales. Zaehle et al. (2006) demonstrate that the model is able to reproduce NPP of managed European forests with good



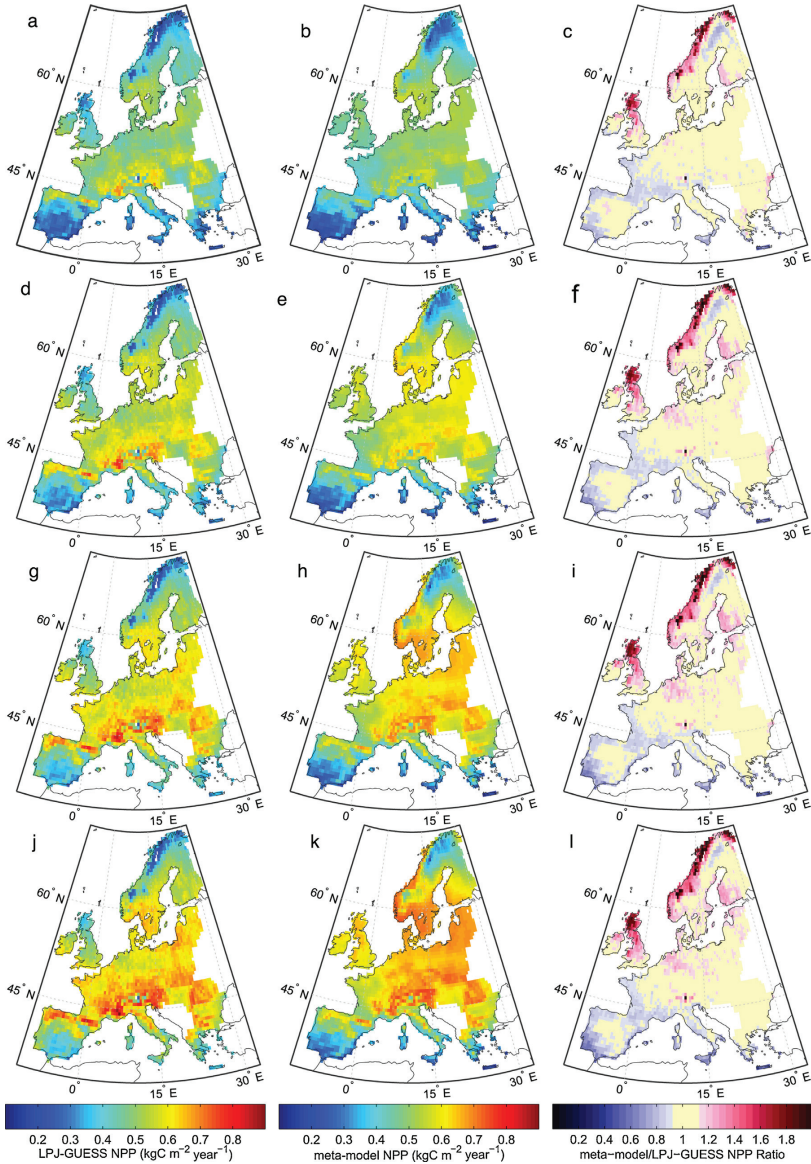


**Fig. 5.** Comparison of total NPP estimates from LPJ-GUESS and the meta-model using European baseline climate with several CO<sub>2</sub> concentrations. The selected CO<sub>2</sub> concentrations are shown row-wise in ascending order (i.e. 350 ppm (a–c), 450 ppm (d–f), 550 ppm (g–i) and 650 ppm (j–l)). Total NPP simulations from LPJ-GUESS (mean of the last 20 years of the baseline simulations) are visualized in panel (a), (d), (g) and (j). Total NPP from the meta-model forced by the preprocessed climate variables (mean of the last two decades from the baseline climate) are illustrated in panel (b), (e), (h) and (k). NPP Ratio of the meta-model's and LPJ-GUESS total NPP estimates are shown in panel (c), (f), (i) and (l). The NPP ratios between 0.9 and 1.1 are classified as satisfactory meta-model performance.

agreement compared to European forest inventory data. [Hickler et al. \(2006\)](#) compare modeled NPP of PNW with stand-scale field measurements of NPP taken from the global Ecosystem Model–Data Intercomparison (EMDI) database ([Olson et al., 2001](#)) where strong correlations between modelled NPP and observed NPP data were found. However, the model simulated on average 18.8% higher NPP values for forests compared to the observation data ([Hickler et al., 2006](#)). [Smith et al. \(2008\)](#) applied LPJ-GUESS to model NPP of boreal forests in northern Europe. The results compared well with forest inventory data (RMSE = 0.066) but indicated NPP overestimation of LPJ-GUESS. [Tang et al. \(2010\)](#) demonstrate that LPJ-GUESS NPP simulations in New England are in agreement with gridded biomass data derived from forest field-measurements. Furthermore, this study suggests that LPJ-GUESS performs better for predicting NPP compared to satellite data-derived NPP (i.e. MODIS NPP).

With regard to the approach chosen for the meta-model development, direct comparisons of the meta-model's performance with other empirical model studies based on NPP field measurements need to be treated with caution. Nevertheless, by making these comparisons, it can be shown that the representation of synergistic interactions between seasonal temperature and precipitation have good reliability for predicting NPP. [Del Grosso et al. \(2008\)](#) applied the Miami ([Lieth and Whittaker, 1975](#)), the Schuur ([Schuur, 2003](#)), and the National Center for Ecological Analysis and Synthesis (NCEAS) model on a global scale. The model's results were compared with a comprehensive NPP dataset of tree-dominated ecosystems (boreal, temperate, and tropical forests). The boreal and temperate forests are covered with the PNW definition ([Hickler et al., 2012](#)) used by the meta-model. In tree-dominated ecosystems the NCEAS model produced the best performance  $R^2 = 0.40$ , the Miami model yielded  $R^2 = 0.35$  and the Schuur model generated  $R^2 = 0.30$ . Relating these results with the meta-model's performance ( $R^2 = 0.68$ ) shows that the meta-model is a viable alternative to Minimum Law-based models for estimating NPP of complex tree-dominated systems. However, comparisons between meta-model estimates and NPP field-observation are desirable to be able to provide a better understanding of the meta-model's performance.

The meta-model exhibits a further development of synergistic interaction because it considers the seasonality of the climate variables. Most empirical models are founded on implicit formulations of ecosystem processes using annual temperature means or cumulative precipitation sums ([Adams et al., 2004](#); [Del Grosso et al., 2008](#); [Lieth and Whittaker, 1975](#); [Schuur, 2003](#)). However, valuable information on how ecosystems respond to intra-annual variability of climate cannot be captured. [Zaks et al. \(2007\)](#) results highlight the benefit of combining climate variables and their seasonality to control NPP. In this study, surrogates of seasonality (growing season photosynthetically active radiation (PAR), water stress index and growing degree-days (GDD)) were combined for estimating NPP with better performance compared to the Miami model ([Zaks et al., 2007](#)). Relating these results with the meta-model development and performance ( $R^2 = 0.68$ ) shows that incorporating synergistic interactions and climatic variability can provide satisfactory and ecologically explainable estimates of NPP.

#### 4.2. Comparison of meta-model with LPJ-GUESS—European scale

In general the meta-model NPP estimates spatially coincide with LPJ-GUESS simulations at CO<sub>2</sub> baseline concentration ([Fig. 5](#)). The meta-model performed favorably at the European scale because 65% of the grid cells were in the satisfactory NPP ratio range. Still, the meta-model considerably overestimated NPP compared to LPJ-GUESS simulations in Scotland, along the Norwegian coast and mountains ([Fig. 5c](#)). [Smith et al. \(2008\)](#) report that LPJ-GUESS overestimates NPP in Scandinavia so it is therefore assumed that the LPJ-GUESS NPP simulations that are used as validation data in the

current study also overestimate NPP in Scandinavia. This indicates that the meta-model would even more greatly overestimate NPP when compared to forest inventory data in Scandinavia. One reason for the NPP overestimation by the meta-model is that the saturation functions for precipitation cannot reflect decreasing effects of high precipitation levels on vegetation growth ([Adams et al., 2004](#); [Schuur, 2003](#)). Secondly, other explanatory variables such as solar radiation and day length are not explicitly included in the meta-model but are important drivers in LPJ-GUESS ([Stitch et al., 2003](#); [Smith et al., 2001](#)). The meta-model considerably overestimated NPP along the Norwegian coast where the warming effects of the Gulf Stream with maximum summer temperatures between 8 to 14 °C and minimum winter temperatures between –8 and 2 °C ([Fig. 4](#)) can provide positive climate conditions for plant growth. Nevertheless, this area is still limited by small amounts of solar radiation due to short day lengths and cloudiness during the winter that restrict plant growth.

Overall the magnitudes by which the meta-model underestimates NPP compared to LPJ-GUESS simulations are notably smaller (up to 30%) when compared to its NPP overestimations (up to 100%). In areas where NPP are underestimated ([Fig. 5c](#)), the climatic conditions are more diverse. Most of the areas are underrepresented or not represented at all in the dataset that was used to develop the meta-model ([Fig. 1](#)). However, LPJ-GUESS tends to overestimate NPP ([Hickler et al., 2006](#); [Ito, 2011](#); [Smith et al., 2008](#)) implying that the meta-model's NPP estimates (i.e. underestimates in comparison to LPJ-GUESS simulations) may be closer to observed data. The meta-model's NPP underestimates are therefore more justifiable than the NPP overestimates compared to LPJ-GUESS results.

The analysis with increasing CO<sub>2</sub> levels (while holding the climate variables and their bias at baseline) showed that the CO<sub>2</sub> function was the major source of imprecision and bias in the meta-model. Increasing CO<sub>2</sub> levels yielded a progressive decline of grid cells where NPP was satisfactorily estimated by the meta-model in comparison to LPJ-GUESS simulations ([Fig. 5](#) and [Table 3](#)). In northern Europe, NPP overestimations by the meta-model rose with increasing CO<sub>2</sub> levels while in central Europe the NPP ratios turned from satisfactory to overestimation (>1.1). Conversely, in southern Europe, increasing CO<sub>2</sub> concentration generated a steady increase of grid cells with NPP ratios <0.9 attributed to NPP underestimation. However, in general, the CO<sub>2</sub> function tends to overestimate the effect of CO<sub>2</sub> fertilization on NPP as implemented in LPJ-GUESS.

#### 4.3. Data

The sites used for the meta-model development cover most of the European Environmental and climate zones at baseline climate conditions. The climate change scenarios ensure that climate conditions of underrepresented environmental zones are included. However, other studies ([Zaks et al., 2007](#)) together with the European scale meta-model analysis highlight that other climate variables such as solar radiation and growing season length are also important for estimating NPP. In the climate change scenarios these other variables are disregarded. Consequently the meta-model is restricted to solar radiation and growing season length conditions of the 63 CRU TS grid cells. We suggest therefore a random stratified selection of samples using environmental stratification data for Europe as proposed by [Metzger et al. \(2005\)](#).

The development of an empirical model to predict NPP for future climate change scenarios is challenging, since the number of field-measurements is limited. This limitation is overcome by creating a meta-model that is entirely based on NPP estimates originating from LPJ-GUESS simulations but this also raises concerns about data-circularity. [Shoo and Valdez Ramirez \(2010\)](#) critiqued [Del Grosso et al. \(2008\)](#) for using modeled and interpolated NPP estimates to create an empirical NPP model. However, [Del Grosso and](#)

Parton (2010) question the independence and circularity of data used in ecological studies generally. But NPP field-measurements are also based on interpolations since NPP is difficult to measure in the field. Furthermore, NPP field-observations are usually used along with spatially interpolated climate datasets to estimate NPP leading to inconsistencies of geographical scale.

The meta-model was validated with NPP estimates from LPJ-GUESS. The meta-model was therefore compared with NPP estimates that are not independent since they were created by the same model. But the availability of NPP measurements that could be used as independent validation data is limited (Hickler et al., 2008). It requires time consuming and costly field-experiments where temperature, precipitation and CO<sub>2</sub> concentrations need to be changed experimentally. As a result, the meta-model inherited limitations of LPJ-GUESS such as NPP overestimation (Ito, 2011; Smith et al., 2008) and the lack of nutrient cycle representation (Hickler et al., 2008). However, prior studies provided evidence that LPJ-GUESS exhibits accurate skills in simulating NPP for various biomes. LPJ-GUESS has been benchmarked extensively with good results from the local to the global scale with forest inventory data, NPP field observations and remote sensing derived data (Hickler et al., 2006; Smith et al., 2008; Tang et al., 2010, 2012; Zaehle et al., 2006).

## 5. Conclusions

The current study describes a meta-model that estimates NPP rapidly with satisfactory performance for PNV in Europe. The primary advantage of the meta-model over traditional empirical models is the ability to predict NPP under projected climate change and CO<sub>2</sub> scenarios. Extrapolation was addressed during the meta-model development phase because it is based on LPJ-GUESS NPP simulations that were conducted under future climate change and CO<sub>2</sub> scenarios. However, beyond the chosen climate and CO<sub>2</sub> ranges, the meta-model NPP estimates need to be treated with caution.

The meta-model's performance was evaluated by comparing it to different NPP predictions generated by LPJ-GUESS. The meta-model estimates of total NPP are reasonably good, considering its simplicity and rapidity, thus confirming the hypothesis that the meta-model is able to emulate total NPP estimates from LPJ-GUESS. The assumption that maximum NPP can only be reached at optimal climate conditions is reasonable for total NPP, but the meta-model failed to predict species-specific NPP. Therefore the hypothesis that species-specific NPP from LPJ-GUESS can be reproduced by the meta-model is rejected.

In the current study it was demonstrated that NPP can be described by a synergistic function of seasonal temperatures, seasonal precipitation and CO<sub>2</sub> functions thereby confirming that a synergistic approach contributes to the understanding of how NPP is controlled by changes in climate and CO<sub>2</sub> concentration. In addition, results from different empirical models reported in the literature are comparable to meta-model NPP estimates reported here, thus further supporting the ability of the meta-model approach.

The meta-model evaluation revealed that the CO<sub>2</sub> and the precipitation functions led to model imprecision and bias. One way of circumventing this problem is to employ a stratified selection of sites for the meta-development in order to ensure that all European climate characteristics are represented. Moreover, additional explanatory variables are necessary to describe regional differences in vegetation growth requirements. An explicit formulation of solar radiation and growing season length would improve the estimation of vegetation NPP. The climate variables applied in this study cannot entirely carry information about these explanatory variables.

The meta-model provides a reasonable trade-off between model complexity and rapid computation time in comparison to DGVM simulations. The meta-model yielded reasonable NPP estimates for most parts of Europe, and can therefore be applied in computationally demanding projections involving both climate change and increased CO<sub>2</sub> concentrations. However, increases in CO<sub>2</sub> concentrations incrementally reduced the meta-model's performance. In northern Europe, it is suggested that the meta-model be used as an exploratory tool for illustrating the impact of very high CO<sub>2</sub> concentrations on NPP, since it still captures the positive impact of CO<sub>2</sub> fertilization on NPP (as implemented in LPJ-GUESS). The meta-model is a useful tool because it also enables easy coupling to other models which has been successfully completed in the CLIMSAVE project. In CLIMSAVE the meta-model adds valuable information about climate change impacts on plant growth and allows the assessment of its cross-sectoral feedbacks.

The meta-model may contribute to an improved understanding of how NPP, as a key environmental resource, is controlled by changes in climate and CO<sub>2</sub> concentration. The incorporation of the climate variables' seasonality in the synergistic function extends the ability of empirical models to provide improved ecologically explainable estimates of NPP.

## Key points

- 1 Development of a rapid net primary production model for current and future climate and CO<sub>2</sub> scenarios.
- 2 The model is a meta-model based on European potential natural vegetation net primary production estimates generated from dynamic global vegetation model simulations.
- 3 Temperature and precipitation and their intra-annual variability were combined synergistically to estimate net primary production.
- 4 The meta-model gives satisfactory agreement with dynamic global vegetation model net primary production simulations.

## Acknowledgements

The authors would like to thank two anonymous reviewers for thoughtful comments, which improved the manuscript. This study was supported by the CLIMSAVE Project (Climate change integrated assessment methodology for cross-sectoral adaptation and vulnerability in Europe; [www.climsave.eu](http://www.climsave.eu)) funded under the Seventh Framework Programme of the European Commission (Contract No. 2444031). CLIMSAVE is an endorsed project of the Global Land Project of the IGBP. The authors would like to thank Paula A. Harrison for the valuable comments on the meta-model development.

## Appendix A. Supplementary data

Supplementary data associated with this article can be found, in the online version, at <http://dx.doi.org/10.1016/j.ecolmodel.2015.01.026>.

## References

- Adams, B., White, A., Lenton, T.M., 2004. An analysis of some diverse approaches to modelling terrestrial net primary productivity. *Ecol. Modell.* 177, 353–391.
- Begon, M., Townsend, C.R., Harper, J.L., 2006. *Ecology: From Individuals to Ecosystems*, fourth ed. Blackwell Pub, Malden, MA (xii, 738 pp).
- Christensen, J.H., Hewitson, B., Busuioc, A., Chen, A., Gao, X., Held, I., Jones, R., Kolli, R.K., Kwon, W.T., Laprise, R., Magaña Rueda, V., Mearns, L., Menéndez, C.G., Räisänen, J., Rinke, A., Sarr, A., Whetton, P., 2007. Regional climate projections. In: Solomon, S., Qin, D., Manning, M., Chen, Z., Marquis, M., Averyt, K.B., Tignor, M., Miller, H.L. (Eds.), *Climate Change 2007: The Physical Science Basis*. Contribution of Working Group I to the Fourth Assessment Report of the Intergovernmental Panel on Climate Change. Cambridge University Press, Cambridge.

- Clark, D.A., Brown, S., Kicklighter, D.W., Chambers, J.Q., Thomlinson, J.R., Ni, J., 2001. Measuring net primary production in forests: concepts and field methods. *Ecol. Appl.* 11, 356–370.
- Del Grosso, S., Parton, W., 2010. Global potential net primary production predicted from vegetation class, precipitation, and temperature: reply. *Ecology* 91, 923–925.
- Del Grosso, S., Parton, W., Stohlgren, T., Zheng, D., Bachelet, D., Prince, S., Hibbard, K., Olson, R., 2008. Global potential net primary production predicted from vegetation class, precipitation, and temperature. *Ecology* 89, 2117–2126.
- Fahey, T.J., Knapp, A.K., 2007. Principles and Standards for Measuring Primary Production. Oxford University Press, Oxford, UK, pp. 268 (xii).
- FAO, 1991. The digitized soil map of the world (release 1.0). in: World Soil Resources Report 67/1. Food and Agriculture Organization of the United Nations, Rome.
- Fay, P.A., Blair, J.M., Smith, M.D., Nippert, J.B., Carlisle, J.D., Knapp, A.K., 2011. Relative effects of precipitation variability and warming on tallgrass prairie ecosystem function. *Biogeosciences* 8, 3053–3068.
- Flexas, J., Diaz-Espejo, A., Gago, J., Gallé, A., Galmés, J., Gulías, J., Medrano, H., 2014. Photosynthetic limitations in Mediterranean plants: a review. *Environ. Exp. Bot.* 103, 12–23.
- Foley, J.A., 1994. Net primary productivity in the terrestrial biosphere—the application of a global-model. *J. Geophys. Res.: Atmos.* 99, 20773–20783.
- Gerden, D., Schaphoff, S., Haberlandt, U., Lucht, W., Sitch, S., 2004. Terrestrial vegetation and water balance—hydrological evaluation of a dynamic global vegetation model. *J. Hydrol.* 286, 249–270.
- Harris, I., Jones, P.D., Osborn, T.J., Lister, D.H., 2014. Updated high-resolution grids of monthly climatic observations—the CRU TS3.10 dataset. *Int. J. Climatol.* 34, 623–642.
- Harrison, P.A., Holman, I.P., Cojocaru, G., Kok, K., Kontogianni, A., Metzger, M.J., Gramberger, M., 2012. Combining qualitative and quantitative understanding for exploring cross-sectoral climate change impacts, adaptation and vulnerability in Europe. *Reg. Environ. Change* 13, 761–780.
- Hickler, T., Prentice, I.C., Smith, B., Sykes, M.T., Zaehle, S., 2006. Implementing plant hydraulic architecture within the LPJ dynamic global vegetation model. *Global Ecol. Biogeogr.* 15, 567–577.
- Hickler, T., Smith, B., Prentice, I.C., Mjöfors, K., Miller, P., Arneft, A., Sykes, M.T., 2008. CO<sub>2</sub> fertilization in boreal FACE experiments not representative of temperate and tropical forests. *Global Change Biol.* 14, 1531–1542.
- Hickler, T., Vohland, K., Feehan, J., Miller, P.A., Smith, B., Costa, L., Giesecke, T., Fromtek, S., Carter, T.R., Cramer, W., Kuhn, I., Sykes, M.T., 2012. Projecting the future distribution of European potential natural vegetation zones with a generalized, tree species-based dynamic vegetation model. *Global Ecol. Biogeogr.* 21, 50–63.
- Holman, I., Harrison, P.A. (Eds.), 2011. Report Describing the Development and Validation of the Sectoral Meta-Models for Integration Into the IA Platform. CLIMSAVE Deliverable 2.2. (<http://www.climsave.eu/climsave/doc/Report-on-the-Meta-models.updated.pdf>).
- IPCC (Ed.), 2007. Climate Change 2007: Impacts, Adaptation and Vulnerability. Contribution of Working Group II to the Fourth Assessment Report of the Intergovernmental Panel on Climate Change. Cambridge University Press, Cambridge, UK.
- Ito, A., 2011. A historical meta-analysis of global terrestrial net primary productivity: are estimates converging? *Global Change Biol.* 17, 3161–3175.
- Jentsch, A., Beierkuhnlein, C., 2008. Research frontiers in climate change: effects of extreme meteorological events on ecosystems. *Comptes Rendus Geosci.* 340, 621–628.
- King, A.W., Emanuel, W.R., Wullschlegler, S.D., Post, W.M., 1995. In search of the missing carbon sink—a model of terrestrial biospheric response to land-use change and atmospheric CO<sub>2</sub>. *Tellus Ser. B—Chem. Phys. Meteorol.* 47, 501–519.
- King, A.W., Post, W.M., Wullschlegler, S.D., 1997. The potential response of terrestrial carbon storage to changes in climate and atmospheric CO<sub>2</sub>. *Clim. Change* 35, 199–227.
- Kreuzwieser, J., Gessler, A., 2010. Global climate change and tree nutrition: influence of water availability. *Tree Physiol.* 30, 1221–1234.
- Larcher, W., 2000. Temperature stress and survival ability of Mediterranean sclerophyllous plants. *Plant Biosyst.* 134, 279–295.
- Larcher, W., 2003. Physiological Plant Ecology: Ecophysiology and Stress Physiology of Functional Groups, fourth ed. Springer, Berlin, New York, pp. 513 (xx).
- Lehsten, V., Harmand, P., Palumbo, L., Arneft, A., 2010. Modelling burned area in Africa. *Biogeosciences* 7, 3199–3214.
- Lehsten, V., Tansley, K., Balzter, H., Thonicke, K., Spessa, A., Weber, U., Smith, B., Arneft, A., 2009. Estimating carbon emissions from African wildfires. *Biogeosciences* 6, 349–360.
- Li, Z.S., Liu, G.H., Fu, B.J., Zhang, J.L., 2011. The potential influence of seasonal climate variables on the net primary production of forests in eastern China. *Environ. Manage.* 48, 1173–1181.
- Lieth, H., Whittaker, R.H., 1975. Primary Productivity of the Biosphere. Springer-Verlag, New York, NY, pp. 339 p (pp. vi).
- Metzger, M.J., Bunce, R.G.H., Jongman, R.H.G., Mucher, C.A., Watkins, J.W., 2005. A climatic stratification of the environment of Europe. *Global Ecol. Biogeogr.* 14, 549–563.
- Mitchell, T.D., Jones, P.D., 2005. An improved method of constructing a database of monthly climate observations and associated high-resolution grids. *Int. J. Climatol.* 25, 693–712.
- Morales, P., Sykes, M.T., Prentice, I.C., Smith, P., Smith, B., Bugmann, H., Zierl, B., Friedlingstein, P., Viovy, N., Sabate, S., Sanchez, A., Pla, E., Gracia, C.A., Sitch, S., Arneft, A., Ogee, J., 2005. Comparing and evaluating process-based ecosystem model predictions of carbon and water fluxes in major European forest biomes. *Global Change Biol.* 11, 2211–2233.
- Olson, R.J., Scurlock, J.M.O., Prince, S.D., Zheng, D.L., Johnson, K.R., 2001. NPP Multi-Biome: NPP and Driver Data for Ecosystem Model-data Intercomparison. Data Set. Oak Ridge National Laboratory, Distributed Active Archive Center, Oak Ridge, TN. Available on-line (<http://www.daac.ornl.gov>).
- Ratto, M., Castelletti, A., Pagano, A., 2012. Emulation techniques for the reduction and sensitivity analysis of complex environmental models. *Environ. Model. Softw.* 34, 1–4.
- Razavi, S., Tolson, B.A., Burn, D.H., 2012. Numerical assessment of metamodeling strategies in computationally intensive optimization. *Environ. Model. Softw.* 34, 67–86.
- Schurgers, G., Hickler, T., Miller, P.A., Arneft, A., 2009a. European emissions of isoprene and monoterpenes from the Last Glacial Maximum to present. *Biogeosciences* 6, 2779–2797.
- Schurgers, G., Hickler, T., Miller, P.A., Arneft, A., 2009b. European emissions of isoprene and monoterpenes from the Last Glacial Maximum to present. *Biogeosciences* 6, 2779–2797.
- Schuur, E.A.G., 2003. Productivity and global climate revisited: the sensitivity of tropical forest growth to precipitation. *Ecology* 84, 1165–1170.
- Seauist, J.W., Olson, L., Ardo, J., 2003. A remote sensing-based primary production model for grassland biomes. *Ecol. Modell.* 169, 131–155.
- Shoo, L.P., Valdez Ramirez, V., 2010. Global potential net primary production predicted from vegetation class, precipitation, and temperature: comment. *Ecology* 91, 923–925 (921–923; discussion).
- Sitch, S., Smith, B., Prentice, I.C., Arneft, A., Bondeau, A., Cramer, W., Kaplan, J.O., Levis, S., Lucht, W., Sykes, M.T., Thonicke, K., Venesky, S., 2003. Evaluation of ecosystem dynamics, plant geography and terrestrial carbon cycling in the LPJ dynamic global vegetation model. *Global Change Biol.* 9, 161–185.
- Smith, B., Knorr, W., Widowski, J.L., Pinty, B., Gobron, N., 2008. Combining remote sensing data with process modelling to monitor boreal conifer forest carbon balances. *For. Ecol. Manage.* 255, 3985–3994.
- Smith, B., Prentice, I.C., Sykes, M.T., 2001. Representation of vegetation dynamics in the modelling of terrestrial ecosystems: comparing two contrasting approaches within European climate space. *Global Ecol. Biogeogr.* 10, 621–637.
- Smith, J.U., Smith, P., 2007. Introduction to Environmental Modelling. Oxford University Press, Oxford, New York (ix 180 p. pp).
- Smith, P., Smith, J.U., Powlson, D.S., McGill, W.B., Arah, J.R.M., Chertov, O.G., Coleman, K., Franko, U., Frolking, S., Jenkinson, D.S., Jensen, L.S., Kelly, R.H., Klein-Gunnewiek, H., Komarov, A.S., Li, C., Molina, J.A.E., Mueller, T., Parton, W.J., Thornley, J.H.M., Whitmore, A.P., 1997. A comparison of the performance of nine soil organic matter models using datasets from seven long-term experiments. *Geoderma* 81, 153–225.
- Tang, C., Beckage, B., Smith, B., 2012. The potential transient dynamics of forests in New England under historical and projected future climate change. *Clim. Change* 357 (114), 377.
- Tang, G.P., Beckage, B., Smith, B., Miller, P.A., 2010. Estimating potential forest NPP, biomass and their climatic sensitivity in New England using a dynamic ecosystem model. *Ecosphere* 1, art18.
- Van Oijen, M., Schapendonk, A., Hogland, M., 2010. On the relative magnitudes of photosynthesis, respiration, growth and carbon storage in vegetation. *Ann. Bot.* 105, 793–797.
- Wang, W., Vinocur, B., Altman, A., 2003. Plant responses to drought, salinity and extreme temperatures: towards genetic engineering for stress tolerance. *Planta* 218, 1–14.
- Wania, R., Ross, I., Prentice, I.C., 2009. Integrating peatlands and permafrost into a dynamic global vegetation model: evaluation and sensitivity of physical land surface processes. *Global Biogeochem. Cycle*, 23.
- Zaehle, S., Sitch, S., Prentice, I.C., Liski, J., Cramer, W., Erhard, M., Hickler, T., Smith, B., 2006. The importance of age-related decline in forest NPP for modeling regional carbon balances. *Ecol. Appl.* 16, 1555–1574.
- Zaks, D.P.M., Ramankutty, N., Barford, C.C., Foley, J.A., 2007. From Miami to Madison: investigating the relationship between climate and terrestrial net primary production. *Global Biogeochem. Cycle* 21, GB3004.



## Appendix A – equations and parameter values

### 1. Meta-model Development

During the determination of the empirical relationships between the climate variables and NPP simulations at CO<sub>2</sub> baseline (i.e. 350 ppm), it was necessary to convert the dataset from absolute to relative NPP values ranging between 0 – 1 using the maximum NPP value ( $NPP_{max}=0.7$  kgC m<sup>-2</sup> year<sup>-1</sup>) of the dataset.

#### 1.1. Temperature

In this study we applied a chi-square function to describe the temperature response of NPP due to the strong linear correlation between NPP and photosynthesis. The chi-square distribution function (see Equation A.1) was chosen since its shape can be adjusted adequately to fit the near parabolic relationship between NPP and temperature.

$$f_n(x) = \begin{cases} \frac{n}{x^2} e^{-\frac{x}{2}} & x > 0 \\ \frac{n}{2^{\frac{n}{2}} \Gamma(\frac{n}{2})} & x \leq 0 \end{cases} \quad (\text{A.1})$$

where  $x$  is a temperature value,  $n$  is an element of the natural numbers that describes the shape of the function and  $\Gamma$  is the gamma function. If  $x > 0$  then  $f_n(x)$  is applied for the estimation. If  $x \leq 0$  then it is set zero.

For the maximum temperature function ( $f(T_{max})$ ) it was necessary to include additional parameters into Equation A.1 to further improve the fit of the chi-square distribution function to the maximum temperature vs NPP data which is written in the maximum temperature function (Equation A.2).

$$f(T_{max}) = \frac{(T_{max}a)^{\frac{n}{2}-1} e^{-\frac{T_{max}a}{2}}}{2^{\frac{n}{2}} \Gamma(\frac{n}{2})} b \quad (\text{A.2})$$

where  $f(T_{max})$  estimates the maximum temperature relative NPP;  $T_{max}$  is maximum summer temperature ( $^{\circ}\text{C}$ ) of a grid cell;  $a$  stretches the function along the abscissa;  $b$  stretches the function along the ordinate;  $n$  describes the shape of the distribution; and  $\Gamma$  is the gamma function. The parameters values for the total and species'  $f(T_{max})$  were determined with the fit command in MATLAB<sup>®</sup> (2011a), yielding a nonlinear least-squares model fit. Parameter values with the lowest RMSE (Del Grosso et al., 2008) were chosen and are given in Table A.1.

**Table A.1** Parameter values of  $f(T_{max})$  (Equation A.2) for each species and total NPP (relative).

<i>Parameter</i>	<i>a</i>	<i>b</i>	<i>n</i>
Total NPP	1.92	9.78	5.30
Abies alba	0.21	28.17	47.70
BES (Vaccinium)	1.88	7.75	5.30
Betula pendula	0.77	16.13	13.70
Betula pubescens	0.84	16.12	12.20
Carpinus betulus	0.53	21.03	19.30
Corylus avellana	0.61	18.13	17.50
Fagus sylvatica	0.40	23.61	26.40
Fraxinus excelsior	0.81	16.61	12.90
Juniperus oxycedrus	0.24	21.57	48.70
MRS (Rosmarinus)	0.24	24.96	50.00
Picea abies	0.75	15.90	13.00
Pinus sylvestris	0.90	13.33	9.90
Pinus halepensis	0.25	18.23	50.00
Populus tremula	0.80	16.63	12.80
Quercus coccifera	0.25	30.02	50.00
Quercus ilex	0.41	20.14	27.30
Quercus pubescens	0.30	29.61	36.10
Quercus robur	0.76	16.68	13.50
Tilia cordata	0.70	17.31	14.50
Ulmus glabra	0.66	18.62	15.70
C3 herbaceous	1.62	7.88	5.80

Minimum winter temperatures ( $T_{min}$ ) can violate  $x>0$  (Equation A.1) because  $T_{min}$  can reach sub-zero °C temperatures. It was therefore required to introduce a parameter into the equation that moves the function along the temperature gradient to eliminate possible negative  $T_{min}$  values. The minimum temperature function is given in Equation A.3;

$$f(T_{min} - t_{min}) = \frac{((T_{min} - t_{min})a)^{\frac{n}{2}-1} e^{-\frac{(T_{min} - t_{min})a}{2}}}{2^{\frac{n}{2}} \Gamma(\frac{n}{2})} b \quad (\text{A.3})$$



where  $f(T_{min}-t_{min})$  estimates the minimum temperature relative NPP;  $T_{min}$  is minimum winter temperature ( $^{\circ}\text{C}$ ) of a grid cell;  $t_{min}$  is the lowest temperature value ( $^{\circ}\text{C}$ ) that occurred in all grid cells and translates the function along the abscissa to the origin (0);  $a$  stretches the function along the abscissa;  $b$  stretches the function along the ordinate;  $n$  describes the shape of the function;  $\Gamma$  is the gamma-function. The parameter values for total and species'  $f(T_{min}-t_{min})$  were determined with the fit command in MATLAB<sup>®</sup> (2011a), yielding a nonlinear least-squares model fit (see Table A.2). Parameter values with the lowest RMSE (Del Grosso et al., 2008) were taken into account.

**Table A.2** Parameter values of  $f(T_{min})$  (Equation A.3) for each species and total NPP (relative)

<i>Parameter</i>	<i>a</i>	<i>b</i>	<i>N</i>	<i>t<sub>min</sub></i>
Total NPP	1.31	18.72	14.60	40.00
<i>Abies alba</i>	20.00	0.21	30.68	50.00
BES ( <i>Vaccinium</i> )	36.22	0.32	25.74	49.70
<i>Betula pendula</i>	40.00	0.52	30.88	37.80
<i>Betula pubescens</i>	38.27	0.38	38.61	50.00
<i>Carpinus betulus</i>	31.14	0.31	37.70	50.00
<i>Corylus avellana</i>	23.46	0.64	20.20	18.70
<i>Fagus sylvatica</i>	20.00	0.28	28.08	37.90
<i>Fraxinus excelsior</i>	36.21	0.36	37.96	50.00
<i>Juniperus oxycedrus</i>	20.00	0.24	20.94	50.00
MRS ( <i>Rosmarinus</i> )	20.00	0.24	23.71	50.00
<i>Picea abies</i>	39.95	1.71	12.95	11.10
<i>Pinus sylvestris</i>	39.99	0.86	19.43	21.60
<i>Pinus halepensis</i>	20.00	0.26	17.40	50.00
<i>Populus tremula</i>	40.00	0.40	35.50	48.30
<i>Quercus coccifera</i>	20.00	0.26	27.42	50.00
<i>Quercus ilex</i>	20.00	0.24	22.75	50.00
<i>Quercus pubescens</i>	26.24	0.27	35.93	50.00
<i>Quercus robur</i>	20.00	0.43	26.25	23.20
<i>Tilia cordata</i>	40.00	0.39	35.38	50.00
<i>Ulmus glabra</i>	38.10	0.37	37.18	50.00
C3 herbaceous	40.00	0.65	18.53	29.40

## 1.2. Precipitation

A saturation function was used to describe the response of NPP to annual cumulative summer ( $P_{summer}$ ) and winter ( $P_{winter}$ ) precipitation. The precipitation function ( $g(P)$ ) estimates relative NPP for both summer ( $g(P_{summer})$ ) and winter ( $g(P_{winter})$ ) precipitation. The function is given in Equation A.4;

$$g(P) = k - \frac{o}{P^l} \quad (\text{A.4})$$

where  $P$  is the annual cumulative precipitation (mm) of  $P_{winter}$  or  $P_{summer}$ ,  $k$  is the maximum seasonal relative NPP that can be reached (derived from LPJ-GUESS simulations) and limits the growth of the function;  $o$  is a constant and  $l$  determines the slope of the distribution.

The parameters values for  $g(P_{summer})$  and  $g(P_{winter})$  were determined with the fit command in MATLAB® (2011a) that generates a nonlinear least-squares model fit. Parameters values for total and species' NPP with the lowest RMSE were selected. Parameters of  $g(P_{summer})$  are given in Table A.3 and parameters of  $g(P_{winter})$  are shown in Table A.4.

**Table A. 3** Parameter values of  $g(P_{summer})$  (Equation A.4) for each species and total NPP.

<i>Parameter</i>	<i>k</i>	<i>o</i>	<i>l</i>
Total NPP	1.04	10.29	0.63
<i>Abies alba</i>	0.89	823.84	1.52
BES ( <i>Vaccinium</i> )	0.76	27927953.57	3.61
<i>Betula pendula</i>	1.03	93.89	1.05
<i>Betula pubescens</i>	1.08	249.40	1.21
<i>Carpinus betulus</i>	1.05	15.86	0.71
<i>Corylus avellana</i>	1.05	10.70	0.62
<i>Fagus sylvatica</i>	1.07	16.90	0.71
<i>Fraxinus excelsior</i>	1.14	10.45	0.59
<i>Juniperus oxycedrus</i>	0.71	3.45	0.50
MRS ( <i>Rosmarinus</i> )	0.89	5.72	0.50
<i>Picea abies</i>	0.92	71957409.91	3.68
<i>Pinus sylvestris</i>	0.85	10027014.18	3.44
<i>Pinus halepensis</i>	0.73	3.53	0.50
<i>Populus tremula</i>	1.19	10.31	0.57
<i>Quercus coccifera</i>	1.10	5.86	0.50
<i>Quercus ilex</i>	1.05	6.58	0.50
<i>Quercus pubescens</i>	1.24	8.02	0.50
<i>Quercus robur</i>	1.12	11.27	0.61
<i>Tilia cordata</i>	1.01	23.83	0.80
<i>Ulmus glabra</i>	1.15	10.53	0.59
C3 herbaceous	0.76	4.76	0.54

**Table A.4** Parameter values of  $g(P_{winter})$  (Equation A.4) for each species and total NPP.

<i>Parameter</i>	<i>k</i>	<i>o</i>	<i>l</i>
Total NPP	0.92	69.21	1.34
Abies alba	0.89	4892146.98	3.53
BES (Vaccinium)	0.78	1655.75	1.92
Betula pendula	1.03	2.51	0.52
Betula pubescens	1.00	2633.03	2.05
Carpinus betulus	0.92	1718.12	2.03
Corylus avellana	0.85	198.55	1.52
Fagus sylvatica	0.91	38.37	1.53
Fraxinus excelsior	0.94	52.99	1.23
Juniperus oxycedrus	0.58	13044269.10	3.84
MRS (Rosmarinus)	0.67	9.33	1.00
Picea abies	0.94	29.69	1.07
Pinus sylvestris	0.85	16615.65	2.55
Pinus halepensis	0.62	1.92	0.50
Populus tremula	0.97	146.85	1.45
Quercus coccifera	0.91	9463790.26	3.67
Quercus ilex	0.80	7878568.58	3.55
Quercus pubescens	0.96	8719.00	2.29
Quercus robur	0.90	38.37	1.24
Tilia cordata	0.92	464.35	1.77
Ulmus glabra	0.93	79.68	1.33
C3 herbaceous	0.64	11418.64	2.47

### 1.3. Synergistic function

The synergistic function ( $NPP_{baseline}$ ) represents the combination of the four climate variables functions. It was assumed that each climate variable controls maximum reachable annual NPP. The multiplication of seasonal temperatures and precipitation amounts yielded squared climate variable units that were therefore reduced with a square root function (e.g.  $\text{mm}^2$  to  $\text{mm}$  and  $^{\circ}\text{C}^2$  to  $^{\circ}\text{C}$ ). The function was then converted from relative to absolute values to provide NPP estimates in  $\text{kgC m}^{-2} \text{ year}^{-1}$  as given in Equation A5. It was then necessary to adjust linearly the synergistic function in order to account for maximum NPP (derived from LPJ-GUESS simulations).

$$NPP_{baseline} = s(\sqrt{f(T_{max}) * f(T_{min} - t_{min}) * g(P_{summer}) * g(P_{winter})} * NPP_{max}) + u \quad (\text{A.5})$$

where  $NPP_{baseline}$  is the estimate NPP ( $\text{kgC m}^{-2} \text{ year}^{-1}$ ) at baseline  $\text{CO}_2$  concentration;  $s$  is the slope;  $NPP_{max}$  is the maximum NPP ( $0.7 \text{ kgC m}^{-2} \text{ year}^{-1}$ ) of LPJ-GUESS simulations at  $\text{CO}_2$  baseline concentrations; and  $u$  is the constant term. The entire  $\text{CO}_2$  baseline dataset was randomly split into an analysis subset containing the data of 30 grid cells and a validation subset containing the remaining 33 grid cells. The 'fit'-command in MATLAB® (2011a) was utilized for the linear fitting procedure. The parameters with the lowest RMSE value for species and total NPP were selected and are shown in Table A.5. The validation of the applied parameter values in the linearly-corrected synergistic function for total NPP values is shown in Fig. A.1.

**Table A.5** Parameter values of the linear fitting (Equation A.5) in the synergistic function for each species and total NPP are shown here.

<i>Parameter</i>	<i>s</i>	<i>u</i>
Total NPP	0.96	-0.02
<i>Abies alba</i>	0.48	0.17
BES ( <i>Vaccinium</i> )	0.64	0.11
<i>Betula pendula</i>	0.62	0.13
<i>Betula pubescens</i>	0.44	0.19
<i>Carpinus betulus</i>	0.41	0.25
<i>Corylus avellana</i>	0.65	0.11
<i>Fagus sylvatica</i>	0.50	0.22
<i>Fraxinus excelsior</i>	0.44	0.23
<i>Juniperus oxycedrus</i>	0.68	0.16
MRS ( <i>Rosmarinus</i> )	0.73	0.14
<i>Picea abies</i>	0.65	0.15
<i>Pinus sylvestris</i>	0.68	0.14
<i>Pinus halepensis</i>	1.11	0.10
<i>Populus tremula</i>	0.59	0.13
<i>Quercus coccifera</i>	0.65	0.17
<i>Quercus ilex</i>	0.77	0.11
<i>Quercus pubescens</i>	0.48	0.20
<i>Quercus robur</i>	0.39	0.26
<i>Tilia cordata</i>	0.55	0.18
<i>Ulmus glabra</i>	0.56	0.16
C3 herbaceous	0.60	0.17

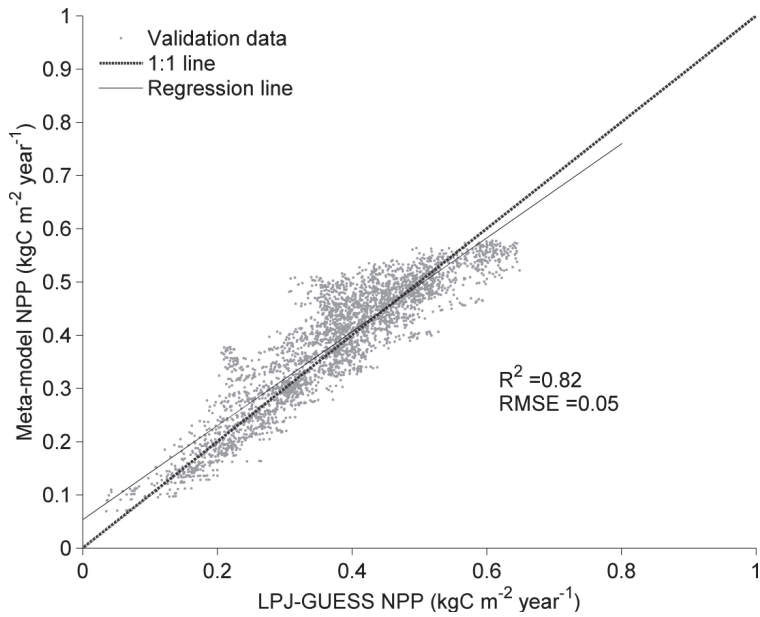


**Fig. A.1** Comparison of the meta-model total NPP estimates (synergistic-function) and LPJ-GUESS simulations. The linear correction provided a good agreement ( $R^2=0.82$ ) and total difference of  $RMSE=0.05 \text{ kgC m}^{-2} \text{ year}^{-1}$  between both models. The parameters of the function were determined with linear fitting ('fit'-command) in MATLAB® (2011a) using the analysis dataset.



## 1.4. CO<sub>2</sub> concentrations

The CO<sub>2</sub>-dependent NPP growth is assumed to be a saturation function. Furthermore, as the CO<sub>2</sub>-dependent NPP growth also depends on climate, the CO<sub>2</sub> analysis was performed over a wide range of climate change scenarios which were kept constant for each CO<sub>2</sub> increase (Table 1). In the current study is therefore assumed that a linear correlation exist between the reciprocal CO<sub>2</sub> ratio (i.e. ratio between baseline and increased CO<sub>2</sub> concentrations) and the difference between LPJ-GUESS NPP simulations at increased CO<sub>2</sub> (>350ppm) and baseline CO<sub>2</sub> (350ppm) concentrations. The linear relationship between reciprocal CO<sub>2</sub> ratios and the NPP differences ( $NPP_{scenario} - NPP_{baseline}$ ) is visualized in Fig. A.2.

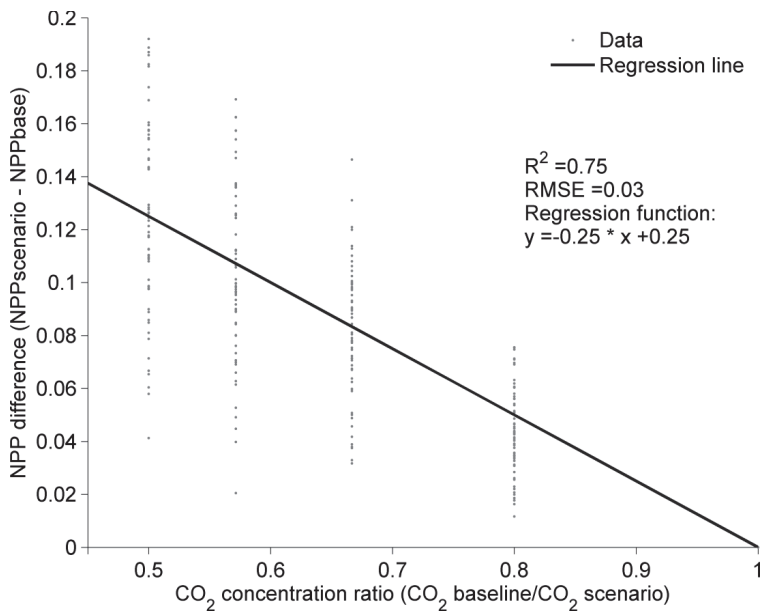


**Fig. A.2** Linear relationship between NPP differences ( $NPP_{scenario} - NPP_{baseline}$ ) and reciprocal CO<sub>2</sub> concentration ratios ( $CO_{2baseline} / CO_{2scenario}$ ); the slope of the linear function was determined with linear fitting based on the total NPP analysis subset. The parameters of the function were determined with linear fitting ('fit'-command) in MATLAB® (2011a) using the analysis dataset.

The linear relationship between NPP differences and reciprocal CO<sub>2</sub> concentration ratios can be described as follows;

$$\Delta NPP = d \left( \frac{CO_2 \text{ baseline}}{CO_2 \text{ scenario}} \right) + e \quad (\text{A.6})$$

where  $\Delta NPP$  is the difference in NPP (kgC m<sup>-2</sup> year<sup>-1</sup>) of  $NPP_{\text{scenario}}$  and  $NPP_{\text{baseline}}$ ;  $NPP_{\text{scenario}}$  is NPP (kgC m<sup>-2</sup> year<sup>-1</sup>) of a grid cell under a scenario-specific CO<sub>2</sub> concentration (ppm);  $NPP_{\text{baseline}}$  is the modeled NPP (kgC m<sup>-2</sup> year<sup>-1</sup>) under a CO<sub>2</sub> concentration of 350 ppm;  $d$  is the slope of the linear relationship;  $CO_2 \text{ baseline}$  equals a concentration of 350ppm;  $CO_2 \text{ scenario}$  is an enhanced CO<sub>2</sub> concentration (>350ppm); and  $e$  is the constant term where the function intercepts the ordinate.

By adding simulated  $NPP_{\text{baseline}}$  (kgC m<sup>-2</sup> year<sup>-1</sup>) in Equation A.6 the equation changes as follow:

$$NPP_{\text{baseline}} + \Delta NPP = NPP_{\text{baseline}} + \left( d \left( \frac{CO_2 \text{ baseline}}{CO_2 \text{ scenario}} \right) + e \right) \quad (\text{A.7})$$

and could be written as:

$$NPP_{\text{scenario}} = NPP_{\text{baseline}} + \left( d \left( \frac{CO_2 \text{ baseline}}{CO_2 \text{ scenario}} \right) + e \right) \quad (\text{A.8})$$

A division of Equation A.8 by  $NPP_{\text{baseline}}$  leads to equation A.9, which shows that the ratio between  $NPP_{\text{scenario}}$  and  $NPP_{\text{baseline}}$  is indirect proportional to the corresponding reciprocal CO<sub>2</sub> ratio.

$$\frac{NPP_{\text{scenario}}}{NPP_{\text{baseline}}} = a \left( \frac{CO_2 \text{ baseline}}{CO_2 \text{ scenario}} \right) + b \quad (\text{A.9})$$

where  $NPP_{\text{scenario}}$  is NPP (kgC m<sup>-2</sup> year<sup>-1</sup>) of a grid cell under a scenario-specific CO<sub>2</sub> concentration (>350ppm);  $NPP_{\text{baseline}}$  is the modeled NPP (kgC m<sup>-2</sup> year<sup>-1</sup>) under a CO<sub>2</sub> concentration of 350 ppm ( $CO_{2\text{baseline}}$ );  $a$  is the slope of the linear relationship and consist of the term  $d/CO_{2\text{baseline}}$ ;  $CO_2 \text{ scenario}$  is an enhanced CO<sub>2</sub> concentration; and  $b$  is the constant parameter where the function intercepts the ordinate that consists of the term  $(1+e/CO_{2\text{baseline}})$ . This relationship is shown in Fig. A.3.

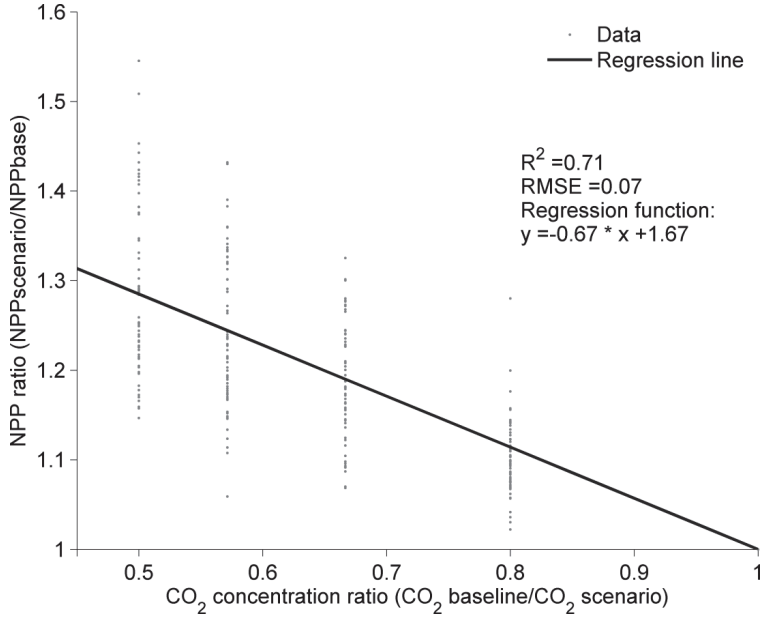


**Fig. A.3** Plot of reciprocal CO<sub>2</sub> ratios ( $CO_{2baseline}/CO_{2scenario}$ ) and indirect proportional NPP ratio ( $NPP_{scenario}/NPP_{baseline}$ ). The trend line shows a linear correlation ( $R^2=0.71$ ). The parameters of the trend line were determined with linear fitting ('fit'-command) in MATLAB® (2011a) using the analysis dataset.

Hence,  $NPP_{scenario}$  can be described by equation A.10;

$$NPP_{scenario} = NPP_{baseline} * \left( a \left( \frac{CO_{2baseline}}{CO_{2scenario}} \right) + b \right) \quad (\text{A.10})$$

The parameters  $a$  and  $b$  were determined for total and species' NPP by randomly dividing the entire dataset into an analysis subset containing data of 30 grid cells and a validation subset containing the remaining 33 grid cells. The 'fit'-command in MATLAB® (2011a) was utilized for the linear fitting procedure. The parameters with the lowest RMSE value for species' and total NPP were selected and are shown in Table A.6. The validation of the applied parameter values in the CO<sub>2</sub> function for total NPP is shown in Fig. A.4.

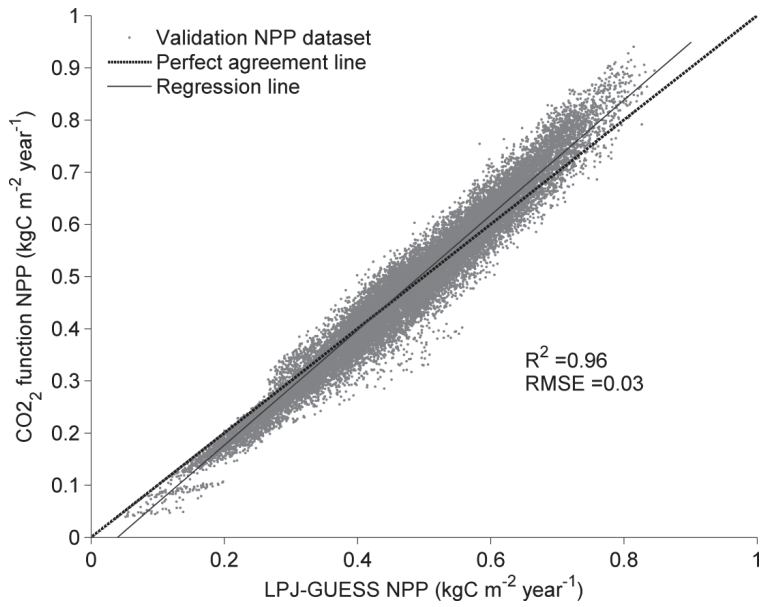


**Fig. A.4** Validation of the CO<sub>2</sub> function formulated in Equation A.10 based on the validation subset containing 33 randomly chosen grid cells.

**Table A.6** Parameter values of the CO<sub>2</sub> function in Equation A.10 for each species and total NPP.

<i>Parameter</i>	<i>a</i>	<i>b</i>
Total NPP	-0.67	1.67
Abies alba	-0.58	1.58
BES (Vaccinium)	-0.63	1.63
Betula pendula	-0.54	1.54
Betula pubescens	-0.51	1.51
Carpinus betulus	-0.51	1.51
Corylus avellana	-0.60	1.60
Fagus sylvatica	-0.51	1.51
Fraxinus excelsior	-0.48	1.48
Juniperus oxycedrus	-0.77	1.77
MRS (Rosmarinus)	-1.29	2.29
Picea abies	-0.46	1.46
Pinus sylvestris	-0.43	1.43
Pinus halepensis	-0.91	1.91
Populus tremula	-0.56	1.56
Quercus coccifera	-0.82	1.82
Quercus ilex	-0.73	1.73
Quercus pubescens	-0.55	1.55
Quercus robur	-0.50	1.50
Tilia cordata	-0.52	1.52
Ulmus glabra	-0.49	1.49
C3 herbaceous	-0.42	1.41

## 2. Evaluating methods for model comparison

The meta-model NPP estimates were compared to LPJ-GUESS simulations using similar climate conditions and CO<sub>2</sub> concentrations (section 2.4). Several objective measures were selected from a range of tests (Smith and Smith, 2007; Smith et al., 1997). The chosen methods for the comparison and their equations are described below:

The coefficient of determination ( $R^2$ ) was chosen because it provides a measure of the strength of the linear association between the meta-models NPP estimates and LPJ-GUESS simulations. The closer  $R^2$  is to 1, the better the agreements between both models.  $R^2$  is calculated as follows;

$$R^2 = \left( \frac{\sum_{i=1}^n (O_i - \bar{O})(P_i - \bar{P})}{\sqrt{\sum_{i=1}^n (O_i - \bar{O})^2} \sqrt{\sum_{i=1}^n (P_i - \bar{P})^2}} \right)^2 \quad (\text{A.11})$$

where:  $n$  is the total number of all paired NPP values in the dataset,  $O_i$  is the  $i$ th NPP simulation from LPJ-GUESS (kgC m<sup>-2</sup> year<sup>-1</sup>),  $\bar{O}$  is the average NPP value of all LPJ-GUESS simulations (kgC m<sup>-2</sup> year<sup>-1</sup>),  $P_i$  is the  $i$ th meta-model NPP estimate (kgC m<sup>-2</sup> year<sup>-1</sup>) and  $\bar{P}$  is the average of all NPP estimates (kgC m<sup>-2</sup> year<sup>-1</sup>).

Root mean squared error (RMSE) is the total difference between the results of both models. RMSE provides an accurate comparison of the size of the difference in the entire comparison dataset. RMSE provides the total difference of NPP (kgC m<sup>-2</sup> year<sup>-1</sup>) and is given in Equation A.12;

$$RMSE = \sqrt{\frac{\sum_{i=1}^n (P_i - O_i)^2}{n}} \quad (\text{A.12})$$

The bias (over- and underestimation) of the meta-model NPP estimates was quantified with mean difference in kgC m<sup>-2</sup> year<sup>-1</sup> (MD) which is given Equation A.13. MD can be used to calculate the

value of the Student's  $t$  by using variation across the different NPP estimates (Smith and Smith, 2007).

$$MD = \sum_{i=1}^n \frac{(O_i - P_i)}{n} \quad (\text{A.13})$$

MD can be directly related to Student's  $t$  by using Equation A.14 (Smith and Smith, 2007);

$$Student's\ t = \frac{MD\sqrt{n}}{\sqrt{\frac{\sum_{i=1}^n \left( O_i - P_i - \left( \frac{\sum_{i=1}^n (P_i - O_i)}{n} \right) \right)^2}{n-1}}} \quad (\text{A.14})$$

Then, MD can be compared with the critical  $t$ -value for the given degrees of freedom in a paired  $t$ -test. In line with conservative statistical conventions a  $t$ -value greater than the critical two-tailed value for  $P < 0.001$  was chosen to determine whether the meta-model estimates show a significant bias towards over- or underestimation when compared with LPJ-GUESS NPP simulations (Morales et al., 2005; Smith and Smith, 2007; Smith et al., 1997).

## Appendix B Comparison of meta-model with LPJ-GUESS

Total NPP estimates from the meta-model and LPJ-GUESS simulations show a sufficient agreement for all climate variable changes at baseline CO<sub>2</sub> concentration (350ppm). The meta-model yielded a performance of  $R^2=0.68$  and a RMSE= $0.06 \text{ kgC m}^{-2} \text{ year}^{-1}$  but overestimates total NPP with a MD= $-0.018$  ( $t=-3083$ ,  $df=9999$ ,  $p < 0.001$ ) in comparison to LPJ-GUESS simulations (Fig. B.1 a). In Fig. B.1 a, the regression line (solid gray line) shows the linear association between the results of the models. Interpretation of Fig. B.1 a shows that the meta-model overestimates NPP where LPJ-GUESS NPP  $\leq 0.5 \text{ kgC m}^{-2} \text{ year}^{-1}$  (along the abscissa). Additionally, the meta-model underestimates NPP where LPJ-GUESS NPP  $> 0.5 \text{ kgC m}^{-2} \text{ year}^{-1}$ . Furthermore, there is considerable variation in the meta-models' NPP estimates (max.  $\sim 0.25 \text{ kgC m}^{-2} \text{ year}^{-1}$ ) for LPJ-GUESS NPP simulations between  $0.3\text{-}0.45 \text{ kgC m}^{-2} \text{ year}^{-1}$ . However, the meta-models' NPP estimates that are within a standard deviation (68%) show smaller variation (max.  $\sim 0.15 \text{ kgC m}^{-2} \text{ year}^{-1}$ ) as can be seen in Fig. B.1 a (dashed black lines).

Meta-model performance declines with increasing CO<sub>2</sub> concentration. The increased CO<sub>2</sub> concentrations yielded an agreement of  $R^2=0.62$  and a total difference of RMSE= $0.08 \text{ kgC m}^{-2} \text{ year}^{-1}$ . Incorporating higher CO<sub>2</sub> levels generated significant NPP underestimation by the meta-model with MD= $-0.020$  ( $t=-56.3$ ,  $df=49999$ ,  $p < 0.001$ ) in comparison to LPJ-GUESS. Fig. B.1 b presents total NPP estimates from both models for all climate change and CO<sub>2</sub> scenarios. Furthermore, Fig. B.1 b shows that the meta-model overestimates NPP where LPJ-GUESS NPP  $\leq 0.7 \text{ kgC m}^{-2} \text{ year}^{-1}$  but it underestimates NPP where LPJ-GUESS NPP  $> 0.7 \text{ kgC m}^{-2} \text{ year}^{-1}$ . The NPP underestimation sets on significantly later than in Fig. B.1 a (NPP  $> 0.5 \text{ kgC m}^{-2} \text{ year}^{-1}$ ). Furthermore, the variations of the meta-models' NPP estimates are remarkably high (max.



$\sim 0.35 \text{ kgC m}^{-2} \text{ year}^{-1}$ ) in areas where LPJ-GUESS simulated NPP between  $0.3\text{-}0.55 \text{ kgC m}^{-2} \text{ year}^{-1}$  (A.Fig 3 b). However, A.Fig 3 b (dashed black lines) shows that the majority of meta-model's NPP estimates (within a standard deviation) have smaller variation (max.  $\sim 0.15 \text{ kgC m}^{-2} \text{ year}^{-1}$ ).

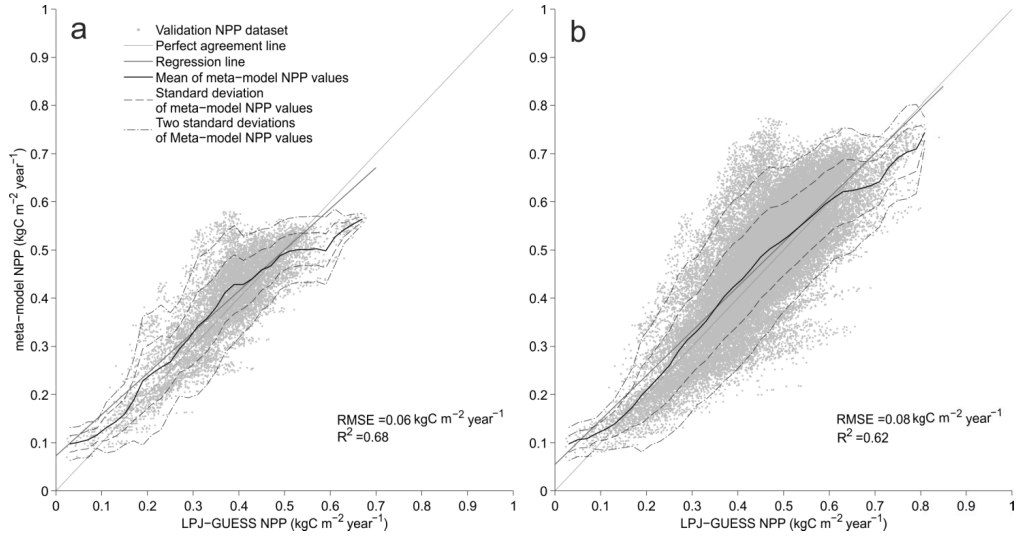


**Fig. B. 1** Validation of the meta-model at different  $\text{CO}_2$  levels; total NPP estimated by the meta-model versus total NPP from LPJ-GUESS (a) for all climate change scenarios at a  $\text{CO}_2$  concentration of 350 ppm. In the right panel (b) climate change scenarios with all  $\text{CO}_2$  concentrations are shown. The solid light gray 1:1 line shows the perfect agreement between the meta-model estimates and LPJ-GUESS NPP simulations. The solid gray line is the regression line that represents the linear association between both model NPP results. The dispersion of the meta-model predictions along the ordinate in comparison to the LPJ-GUESS simulations on the abscissa are quantified with the mean (solid black line), standard deviation (dashed black lines) and two standards deviations (dash-dot black lines) of the meta-model NPP estimates.

## Appendix C Sensitivity Analysis

### 1. Methods

The results of the meta-model sensitivity were assessed for each climate variable. This was accomplished with a local-factorial approach where only one climate variable value was changed according to Table 1 (Smith and Smith, 2007). The other variables were kept at baseline values. We changed the climate variable values as in section 2.4 (Table 1). Then,  $R^2$  value and RMSE (NPP in  $\text{kgC m}^{-2} \text{ year}^{-1}$ ) were estimated in comparison to LPJ-GUESS total NPP simulations for each change in the value of the climate. Additionally, the mean  $R^2$  and RMSE of the changes and their ranges were calculated. Hence, a measure of dispersion for each respective climate variable was achieved, which is an indicator of how much a climate variable influences the meta-model's performance.

### 2. Results

During the sensitivity analysis, enhanced  $\text{CO}_2$  concentrations led to the poorest meta-model performance. By increasing the  $\text{CO}_2$  levels in a stepwise manner the correlation decreases steadily between the meta-model estimates and LPJ-GUESS simulations while the RMSE increases.  $\text{CO}_2$  level changes yielded the largest range of  $\text{RMSE}=0.037$  and a range of  $R^2=0.20$  (Table C.1). The  $\text{CO}_2$  concentration changes generated the lowest mean  $R^2=0.58$  and the highest mean RMSE 0.081. A further investigation of the meta-model performance at different  $\text{CO}_2$  concentrations showed that the best NPP estimates with greatest association ( $R^2=0.68$ ) and lowest total difference ( $\text{RMSE}=0.061$ ) with LPJ-GUESS simulations were generated at baseline  $\text{CO}_2$  concentration. Table C.2 shows that an increase of  $\text{CO}_2$  levels in a stepwise manner decreases

steadily the correlation between the meta-model estimates and LPJ-GUESS simulations. This results in the lowest  $R^2=0.48$  and the largest RMSE=0.091 at  $CO_2$  concentration of 700ppm. This goes in hand with the observed decrease in  $R^2$  and a deterioration of RMSE in Fig. B1.

The summer precipitation function is the second most important contributor to reduced meta-model performance, especially at high summer precipitation levels. Changes in summer precipitation values generated the second largest range in  $R^2=0.13$  with a mean  $R^2=0.67$  between the meta-model NPP estimates and LPJ-GUESS simulations. The range in RMSE=0.010 is the second smallest with a mean RMSE=0.061 (Table C.1). At a 75% reduction of summer baseline precipitation, the meta-model yielded the greatest association ( $R^2=0.72$ ) and smallest total difference (RMSE=0.053) with LPJ-GUESS simulations. However, an increase of precipitation progressively undermines the statistical association and the total differences between the meta-model and LPJ-GUESS. Changing the baseline precipitation by 150% yielded the lowest  $R^2=0.59$  and greatest RMSE=0.067 between the models. However, it was observed that high precipitation levels in combination with high temperature values yielded satisfactory performance.

The other climate variables contribute positively to the meta-model performance. The temperature changes yielded the second smallest range in  $R^2=0.08$  with a mean  $R^2=0.64$  comparing the meta-models' NPP estimates and LPJ-GUESS simulations (Table C.1). The agreement between the models increases with rising temperatures (Table C.2) but a slight correlation dip ( $R=0.62$ ) appears at a baseline temperature increase of  $4^\circ C$ . However, the total difference between the models generated a range of RMSE=0.015 with a mean RMSE=0.063 because RMSE inflated steadily with increasing temperatures. The meta-models' NPP estimates yielded RMSE=0.056 compared to LPJ-GUESS results while a baseline temperature increase of  $6^\circ C$  generated a RMSE=0.069.

**Table C.1** Results of the sensitivity analysis. The individual performance of each climate variable is summarized with the mean  $R^2$  and the range of  $R^2$  values.

Parameter	Range of $R^2$	Mean $R^2$ for all steps of change $\pm$ standard deviation	Range of RMSE	Mean RMSE for all steps of change $\pm$ standard deviation
CO <sub>2</sub> Concentration	0.20	0.58 $\pm$ 0.08	0.037	0.081 $\pm$ 0.015
Summer Precipitation	0.13	0.67 $\pm$ 0.06	0.010	0.061 $\pm$ 0.004
Temperature	0.08	0.64 $\pm$ 0.04	0.015	0.061 $\pm$ 0.007
Winter Precipitation	0.03	0.68 $\pm$ 0.01	0.001	0.061 $\pm$ 0.000

Winter precipitation changes resulted in the best mean  $R^2=0.68$  and the smallest range of  $R^2=0.03$  between the meta-models' NPP estimates and LPJ-GUESS simulations. A slightly better performance is given at reduced precipitation than for increased precipitation levels (Table C.2). The total difference is almost stable around a mean RMSE=0.061 with a range of RMSE=0.01.

**Table C.2** The coefficient of determination results of the local-factorial sensitivity analysis for total NPP. For each local-factorial change of a variable is shows the resulting coefficient of determination between the meta-model NPP estimates and LPJ-GUESS simulation.

CO <sub>2</sub> concentration		Summer Precipitation		Temperature		Winter Precipitation	
Change [ppm]	$R^2$ -value	Change [% of baseline]	$R^2$ -value	Change [°C]	$R^2$ -value	Change [% of baseline]	$R^2$ -value
350	0.68	0.5	0.72	0	0.60	0.5	0.69
437.5	0.63	0.75	0.72	2	0.65	0.75	0.68
525	0.58	1	0.68	4	0.62	1	0.68
612.5	0.53	1.25	0.63	6	0.69	1.25	0.67
700	0.48	1.5	0.59	-	-	1.5	0.67

### **3. Discussion**

#### **3.1. CO<sub>2</sub> function**

The meta-model sensitivity analysis revealed that the CO<sub>2</sub> function is the largest source of uncertainty among the functions. The total difference of the meta-model worsened steadily with increasing CO<sub>2</sub> concentrations. This can be explained by the fact that the CO<sub>2</sub> function is built upon the synergistic function and thus inherits uncertainties originating from the climate variable functions but this conceptual logic has also been applied successfully in other studies (King et al., 1997; Post et al., 1997). Another reason is the small dataset used during the development of the function (section 2.6). For the analysis of the function 30 grid cells were used and 33 grid cells for its validation. The CO<sub>2</sub> function is therefore tailored to the local conditions of the chosen samples. We suggest an increase of the dataset size and a random stratified selection of samples in order to increase the general applicability of the CO<sub>2</sub> function.

Furthermore, the sensitivity analysis showed that the CO<sub>2</sub> function can capture the fertilization effect of enhanced CO<sub>2</sub> concentrations on plant growth but yielding an overall overestimation of NPP by the meta-model compared to LPJ-GUESS. This finding is further discussed in section 4.

#### **3.2. Precipitation functions**

In general the summer precipitation function generated acceptable outcomes at low to moderate (0-700mm) precipitation levels. This can be explained with the good fit of the function that frames the maximum samples of total NPP vs. summer precipitation in the precipitation range between 0-700mm, where the majority of samples are also located (Fig 3 c). But at high precipitation levels (>700mm) the function cannot accurately capture the samples with a

saturation function. As can be seen in Fig 3 c only a small number of samples with decreased NPP are available at precipitation levels above 700mm. Therefore the saturation function yielded a poor fit to these samples with a decline in performance especially with increasing summer precipitation. This is also highlighted by the results of the sensitivity analysis where the summer precipitation function contributes primarily to uncertainties in the synergistic function as can be seen in Table C.1 & Table C.2.

This finding underscores the difficulties of using a saturation function to describe the response of NPP to higher summer precipitation levels. Kreuzwieser and Gessler (2010) described the negative impacts of strong rainfall (e.g. waterlogging) on plant growth. Furthermore, high precipitation levels decrease NPP in tropical ecosystems (Schuur, 2003). This is explained with a decrease in decomposition rates of biomass because of a slow diffusion of oxygen through water filled soil pores. Therefore the aerobic demand of roots and microbes cannot be satisfied (e.g. oxygen deprivation). Adams et al. (2004) analyzed the water stress on NPP among different models and found that NPP decreases when an optimum level of water availability is exceeded. A parabolic relationship between NPP and precipitation may eliminate these concerns as applied in (Svirezhev and von Bloh, 1998).

The winter precipitation function performed slightly better than the summer precipitation function in the sensitivity analysis yielding the lowest dispersion of RMSE (see Table C.1). However, it suffers from the same limitations discussed in the summer precipitation case. As shown in Fig 3 d the winter precipitation function fits well to the maximum NPP-winter precipitation samples for the range 0-700mm, where most of the samples are located, whereas the samples above 700mm have lower NPP values and cannot be represented well with a saturation function. A parabolic function would capture the relationship between NPP and winter

precipitation more accurately due to decreasing NPP at higher precipitation levels. Further investigations of the meta-models' sensitivity show that high precipitation levels can be buffered by increased evaporation due high temperatures and vice versa due to the cooling effect of evaporation (Table C.2).

### **3.3. Temperature functions**

The temperature functions yielded a reasonable performance and captured the relationship between temperature and NPP. The four temperature changes in the sensitivity analysis yielded an acceptable RMSE and statistical association with LPJ-GUESS simulations (Table C.1 & Table C.2). On the other hand, the results of the temperature sensitivity analysis are difficult to interpret, since it was not possible to differentiate between the maximum and minimum temperature functions. For example, an increase of temperature by 2°C will always affect both temperature climate variables. This made the analysis unidirectional because in a simulation it was impossible to individually change maximum and minimum temperatures with different magnitudes (e.g. increase of minimum temperatures by 2°C and maximum temperature by 6°C at the same time). Furthermore, this approach cannot quantify the extent to which the minimum and maximum temperature functions contribute to the meta-model's uncertainties. This analysis represents the summed uncertainties from the minimum and maximum temperature functions.

In general, (Adams et al., 2004) reviewed the NPP-temperature relationship in empirical models and suggested a near-parabolic function because NPP decreases when an optimum temperature has been exceeded. We chose therefore a chi-square distribution function (Fig 3 **a** and **b**) to describe the relationships of NPP to maximum and minimum temperature. The equations are constrained indirectly by the dataset used to develop the meta-model, i.e. bioclimatic limits of the

chosen species in the LPJ-GUESS modeling protocol. As seen in Fig 3 **a** and **b** the total NPP maximum and minimum temperature functions give NPP predictions at lower maximum and minimum temperature ranges where in reality no growth takes place which could yield NPP overestimation. We therefore suggest an explicit constraint to the bioclimatic limits in the species' temperature functions as well as for total NPP.



## Appendix D Species NPP

Species NPP estimations by the meta-model in comparison to LPJ-GUESS simulations

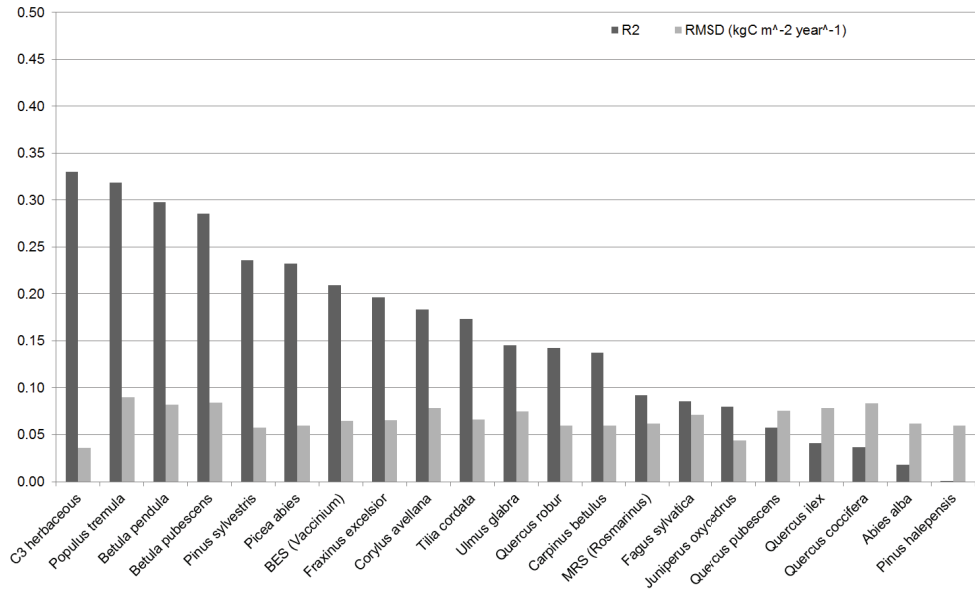


**Fig. D.1** Comparison of the species NPP meta-model estimates with LPJ-GUESS estimates for all climate change and CO<sub>2</sub> concentration scenarios. The light gray bars represent the linear correlation association (R<sup>2</sup>) between the models while the dark gray bars display the RMSE in NPP kgC<sup>-2</sup> year<sup>-1</sup>. The species are ordered according to their R<sup>2</sup> values.

## References

- Adams, B., White, A., Lenton, T.M., 2004. An analysis of some diverse approaches to modelling terrestrial net primary productivity. *Ecological Modelling* 177, 353-391.
- Del Grosso, S., Parton, W., Stohlgren, T., Zheng, D., Bachelet, D., Prince, S., Hibbard, K., Olson, R., 2008. Global potential net primary production predicted from vegetation class, precipitation, and temperature. *Ecology* 89, 2117-2126.
- King, A.W., Post, W.M., Wullschleger, S.D., 1997. The potential response of terrestrial carbon storage to changes in climate and atmospheric CO<sub>2</sub>. *Climatic Change* 35, 199-227.
- Kreuzwieser, J., Gessler, A., 2010. Global climate change and tree nutrition: influence of water availability. *Tree Physiology* 30, 1221-1234.
- Morales, P., Sykes, M.T., Prentice, I.C., Smith, P., Smith, B., Bugmann, H., Zierl, B., Friedlingstein, P., Viovy, N., Sabate, S., Sanchez, A., Pla, E., Gracia, C.A., Sitch, S., Arneeth, A., Ogee, J., 2005. Comparing and evaluating process-based ecosystem model predictions of carbon and water fluxes in major European forest biomes. *Global Change Biology* 11, 2211-2233.
- Post, W.M., King, A.W., Wullschleger, S.D., 1997. Historical variations in terrestrial biospheric carbon storage. *Global Biogeochem Cy* 11, 99-109.
- Schuur, E.A.G., 2003. Productivity and global climate revisited: The sensitivity of tropical forest growth to precipitation. *Ecology* 84, 1165-1170.
- Smith, J.U., Smith, P., 2007. *Introduction to environmental modelling*. Oxford University Press, Oxford ; New York ix, 180 p. pp.
- Smith, P., Smith, J.U., Powlson, D.S., McGill, W.B., Arah, J.R.M., Chertov, O.G., Coleman, K., Franko, U., Frolking, S., Jenkinson, D.S., Jensen, L.S., Kelly, R.H., Klein-Gunnewiek, H.,

- Komarov, A.S., Li, C., Molina, J.A.E., Mueller, T., Parton, W.J., Thornley, J.H.M., Whitmore, A.P., 1997. A comparison of the performance of nine soil organic matter models using datasets from seven long-term experiments. *Geoderma* 81, 153-225.
- Svirezhev, Y.M., von Bloh, W., 1998. A zero-dimensional climate-vegetation model containing global carbon and hydrological cycle. *Ecological Modelling* 106, 119-127.

# Paper II



# Direct and indirect impacts of climate and socio-economic change in Europe: a sensitivity analysis for key land- and water-based sectors

A. S. Kebede · R. Dunford · M. Mokrech · E. Audsley · P. A. Harrison ·  
I. P. Holman · R. J. Nicholls · S. Rickebusch · M. D. A. Rounsevell ·  
S. Sabaté · F. Sallaba · A. Sanchez · C. Savin · M. Trnka · F. Wimmer

Received: 22 January 2014 / Accepted: 18 December 2014  
© Springer Science+Business Media Dordrecht 2015

**Abstract** Integrated cross-sectoral impact assessments facilitate a comprehensive understanding of interdependencies and potential synergies, conflicts, and trade-offs between sectors under changing conditions. This paper presents a sensitivity analysis of a European integrated assessment model, the CLIMSAVE integrated assessment platform (IAP). The IAP incorporates important cross-sectoral linkages between six key European land- and water-based sectors: agriculture, biodiversity, flooding, forests, urban, and water. Using the IAP, we investigate the direct and indirect implications of a wide range of climatic and socio-economic drivers to identify: (1) those sectors and regions most sensitive to future changes,

---

This article is part of a Special Issue on “Regional Integrated Assessment of Cross-sectoral Climate Change Impacts, Adaptation, and Vulnerability” with Guest Editors Paula A. Harrison and Pam M. Berry.

**Electronic supplementary material** The online version of this article (doi:10.1007/s10584-014-1313-y) contains supplementary material, which is available to authorized users.

---

A. S. Kebede (✉) · R. J. Nicholls  
Faculty of Engineering and the Environment, Tyndall Centre for Climate Change Research, University of Southampton, Highfield, Southampton SO17 1BJ, UK  
e-mail: ask2g08@soton.ac.uk

R. Dunford · P. A. Harrison  
Environmental Change Institute, University of Oxford, South Parks Road, Oxford OX1 3QY, UK

M. Mokrech  
School of Science and Computer Engineering, University of Houston-Clear Lake, 2700 Bay Area Blvd.,  
Box 540, Houston, USA

E. Audsley · I. P. Holman  
Cranfield Water Sciences Institute, Cranfield University, Cranfield, Bedford MK43 0AL, UK

S. Rickebusch  
Environmental Systems Analysis Group, Wageningen University, P.O. Box 47, 6700 AA Wageningen,  
The Netherlands

S. Rickebusch · M. D. A. Rounsevell  
School of GeoSciences, University of Edinburgh, Drummond Street, Edinburgh EH8 9XP, UK

(2) the mechanisms and directions of sensitivity (direct/indirect and positive/negative), (3) the form and magnitudes of sensitivity (linear/non-linear and strong/weak/insignificant), and (4) the relative importance of the key drivers across sectors and regions. The results are complex. Most sectors are either directly or indirectly sensitive to a large number of drivers (more than 18 out of 24 drivers considered). Over twelve of these drivers have indirect impacts on biodiversity, forests, land use diversity, and water, while only four drivers have indirect effects on flooding. In contrast, for the urban sector all the drivers are direct. Moreover, most of the driver–indicator relationships are non-linear, and hence there is the potential for ‘surprises’. This highlights the importance of considering cross-sectoral interactions in future impact assessments. Such systematic analysis provides improved information for decision-makers to formulate appropriate adaptation policies to maximise benefits and minimise unintended consequences.

## 1 Introduction

Climate change is projected to impact human and natural systems worldwide. Some examples of potential impacts in Europe include: declining agricultural productivity in some regions that threatens food security (Audsley et al. 2006; Aydinalp and Cresser 2008); shifts in species distribution and composition of habitats/ecosystems that characterise landscapes (Green et al. 2003; Berry et al. 2006); increasing risk of flooding for people and properties and associated economic damages (Mokrech et al. 2008; Hinkel et al. 2010); adverse effects of prolonged drought on forest growth and wood production (Ciais et al. 2005; Lindner et al. 2008); and altered hydrological processes/regimes and associated effects on the availability, quality and use of water resources (EEA 2007; Bates et al. 2008). These climate impacts are in addition to the continuing pressures from changing demographics, economies, technologies, lifestyles, and policies (Moss et al. 2010). The extent and magnitude of impacts varies: over time; across regions, ecosystems, and sectors; and with the ability of these regions, ecosystems and sectors to adapt to, or cope with, these impacts.

---

S. Sabaté · A. Sanchez

Centre for Ecological Research and Forestry Applications (CREAF), Universitat autonoma de Barcelona, Edifici C, Bellaterra 08193, Spain

S. Sabaté

Ecology Department, University of Barcelona, Diagonal 643, 08028 Barcelona, Spain

F. Sallaba

Department of Physical Geography and Ecosystem Science, Lund University, Sölvegatan 12, Lund 22362, Sweden

C. Savin

TIAMASG Foundation, Sfintii Voievozi 6, 010963 Bucharest, Romania

M. Trnka

Institute of Agrosystems and Bioclimatology, Mendel University in Brno, Zemědělská 1, Brno 61300, Czech Republic

M. Trnka

Global Change Research Centre AS CR v.v.i, Bělidla 986/4a, 603 00 Brno, Czech Republic

F. Wimmer

Center for Environmental Systems Research, University of Kassel, Kassel 34109, Germany

Furthermore, impacts occurring in one sector or region are not likely to be confined to that particular sector or region, with a potential for cascading indirect effects with far reaching repercussions across different sectors or regions (Toth et al. 2003; Nicholls and Kebede 2012). However, such interdependencies are currently poorly understood (Frieler and the ISI-MIP Team 2013). Most impact assessment studies to date have focused on sector-based analysis and often with a particular emphasis on the implications of climate drivers only (Holman et al. 2008a, b). Other drivers such as socio-economic changes have often been given little attention and when considered they are treated either independently or rigidly combined with climate scenarios. While there might be a pragmatic interest behind such approaches, they can potentially under- or over-estimate future impacts (Carter et al. 2007), and hence adaptation needs. However, policy-relevant impact assessments require a comprehensive understanding and a systematic integrated assessment of future impacts which takes account of both cross-sectoral effects and climate and socio-economic drivers (Holman et al. 2005; Harrison et al. 2013). Integrated assessment (IA) models provide such a holistic and consistent framework that can complement existing sector-specific assessments and methods. They bring together wide ranges of relevant disciplines and methods and provide a better understanding of important system inter-linkages and feedbacks to organise and deliver policy-relevant information suitable for robust decision-making (Harremoes and Turner 2001). Despite the limitations in terms of their quantitative applications, the use of IA models has grown rapidly in the past decade across a range of disciplines, scales and complexities (e.g., Kenny et al. 2001; Matsuoka et al. 2001; Holman et al. 2008a).

This paper presents a sensitivity analysis of the European IA model developed within the CLIMSAVE<sup>1</sup> project. It investigates the effects of wide ranges of climatic and socio-economic change drivers on model outputs related to key land- and water-based sectors in Europe. Such analysis provides better quantification and increased understanding of the complex relationships between input and output variables in a system or integrated model. The paper is structured as follows: Section 2 introduces the CLIMSAVE approach, including its innovation and application. Section 3 describes the materials and methodology used. The results are then presented and discussed in Section 4. Finally, key messages are summarised and conclusions are drawn in Section 5.

## 2 The CLIMSAVE approach: cross-sectoral focus

CLIMSAVE is a pan-European project that has developed an IA model, the CLIMSAVE integrated assessment platform (IAP). The IAP allows stakeholders to investigate cross-sectoral impacts of both climatic and socio-economic drivers and explore the potential for adaptation to offset or reduce any associated vulnerability in Europe. It is a unique interactive, exploratory, web-based tool that provides broad sectoral and cross-sectoral insights and helps build the capacity of decision-makers to address the complex multi-sectoral issues surrounding climate change impacts and associated cross-sectoral benefits and conflicts of different adaptation options under uncertain futures (Harrison et al. 2013; Harrison et al. 2014a).

The key aspects of the IAP, in terms of advancing current knowledge in IA model applications, lies in its holistic methodological framework which improves on previous studies

---

<sup>1</sup> Climate change Integrated assessment Methodology for cross-Sectoral Adaptation and Vulnerability in Europe ([www.climsave.eu](http://www.climsave.eu))



in three important ways: (i) greater consideration of cross-sectoral linkages and interactions by integrating six key sectors (agriculture, biodiversity, flooding, forests, urban, and water), (ii) consideration of both climatic and socio-economic factors, and (iii) multi-scale application (continental scale: Europe and regional scale: Scotland. Here, only the European scale results are considered). The development of the IAP uses meta-modelling approaches which allow integration of various sectoral models to provide stakeholders with an interactive assessment tool with reasonably fast run-times (Holman et al. 2008a; Holman and Harrison 2012). Meta-models (also termed ‘reduced-form models’) are computationally simple(r), but efficient, modelling techniques that emulate the performance of more complex models (Ratto et al. 2012). Examples of meta-model techniques used in the IAP include look-up tables, artificial neural networks, and soil/climate clustering. Hence, the IAP contains a series of inter-linked sectoral meta-models, a database, wide ranges of climate and socio-economic scenarios, and a GIS-based user interface, which capture the complex interactions between sectors (Fig. 1).

The sensitivity analysis of the IAP aims to define and quantify the interactions among the various sectoral models integrated within the IAP in order to help better understand the potential impacts of future changing conditions, which cross sectoral and regional boundaries. The analysis enables an assessment and better interpretation of the effects of uncertainty in future changes in climate as well as social, economic, technological, environmental, and policy governance scenario settings. This provides broad insights into how different assumptions affect decision choices and which parameters or assumptions are most important in planning future cross-sectoral adaptation priorities in Europe. See the Electronic Supplementary Material (ESM 1) for a more detailed description of the conceptual framework of CLIMSAVE’s integrated methodology and its application.

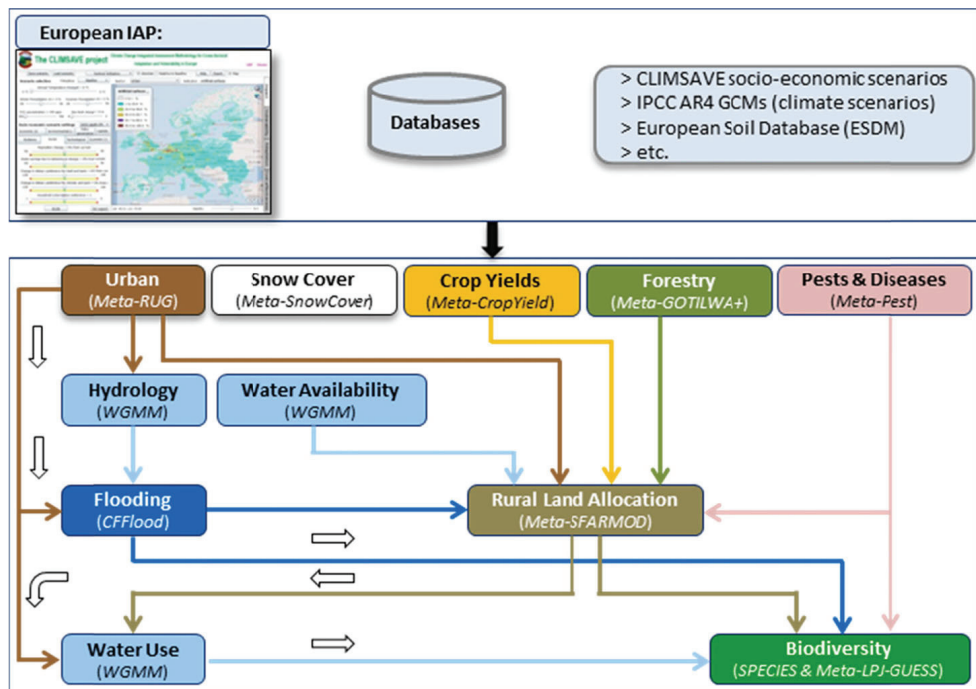


**Fig. 1** Simplified schematic diagram of the various sectoral meta-model linkages and associated data flows integrated within the European CLIMSAVE IAP (Adapted from Harrison et al. 2013)

### 3 Materials and methods

#### 3.1 Scale of analysis

The European CLIMSAVE IAP operates at a  $10\times 10$  arc-minutes grid resolution, which produces outputs for a total of 23,871 grid cells in Europe. Examination of the outputs indicated that differential effects between regions could be captured by dividing Europe into four regions (eastern, northern, southern, and western Europe). Hence, focussing on a cross-sectoral and regional comparison of impacts in Europe, this paper analyses the grid-based outputs aggregated into five spatial extents: Europe-wide and the four regions. The regional divisions are based on river basins classification (see [ESM 2](#)), selected to have a consistent scale of analysis across all sectors. This is necessary, as the water sector model uses ‘river basins’ as its modelling spatial unit. These are made up either of a single large river catchment or clusters of several smaller, neighbouring catchments with similar hydro-geographic properties (Wimmer et al. 2014).

#### 3.2 Selected impact indicators

The CLIMSAVE IAP outputs a large number of sectoral indicators, which were identified and prioritised based on their relevance for stakeholders and adaptation (Harrison et al. 2013). This analysis focuses on six key indicators (one per sector): (1) Artificial surfaces; (2) People flooded in a 1 in 100 year flood event; (3) Timber production; (4) Land use diversity; (5) Water exploitation index; and (6) Biodiversity vulnerability index (see [ESM 3](#)). The indicators were selected by sectoral experts after considering: (i) representativeness for the sector; (ii) reliability of the IAP in reproducing observed values of the indicators; and (iii) their relevance to stakeholders.

#### 3.3 Climate and socio-economic change drivers

A driver is defined as ‘any natural or human-induced factor that directly or indirectly causes a change in an ecosystem’ (MEA 2005). CLIMSAVE considers two classes of underlying environmental change drivers, reflecting climatic (Dubrovsky et al. 2014) and socio-economic (Kok et al. 2014) change factors. Various definitions of drivers can be found in the literature (e.g., Nelson et al. 2005). In this paper, the mechanisms by which a driver affects a sectoral indicator are classified as: (a) *direct* if it affects the indicator as a direct IAP input to the meta-model from which the indicator was output, (b) *indirect* if it affects the indicator by a cascading effect on another sector via the interconnected meta-model chain, and (c) *combined* if it affects the indicator both as a direct and indirect driver (see [ESM 4](#) for a schematic illustration of these sectoral interdependencies). For example, sea-level rise is a direct input variable into the flood meta-model that directly affects the number of people flooded. Conversely, food imports has an indirect effect on biodiversity through its impacts on land use patterns, which in turn affect habitat availability and thereby the biodiversity vulnerability index. Precipitation change, in contrast, has a combined effect on biodiversity, affecting the suitability of climate space for species (direct effect) as well as influencing the suitability of land use for different crop types, which in turn influences available habitat (indirect effect).

In this paper, wide ranges of future climatic and socio-economic drivers are explored in order to understand the complex relationships between the drivers (represented by the IAP input variables) and sectoral responses (represented by the selected indicators), and the

potential interactions between the different sectors. Table 1 presents the full list of the 24 IAP input variables representing the various climatic and socio-economic drivers and the ranges of values selected from each driver for this analysis.

### 3.4 Sensitivity analysis

Sensitivity analysis is the study of how the uncertainty or variation in model outputs can be (qualitatively/quantitatively) apportioned among the various model inputs (Saltelli et al. 2000). The CLIMSAVE IAP facilitates a comprehensive sensitivity analysis to investigate the response of indicators to changes in driver settings. In this paper, a “One-Driver-at-a-Time” (ODAT) approach is implemented to assess sensitivities of key European sectors to cross-sectoral impacts of both climatic and socio-economic drivers. This single-factor approach is selected to define the IAP input/output variable relationships and track if, and how, the effects of individual drivers on a sector/region is transferred and felt by other sectors/regions. This helps to identify the key drivers, and plays a crucial role in better understanding and interpreting outputs from complex IA methods, such as scenario (Harrison et al. 2014b) and uncertainty (Brown et al. 2014) analysis with changes in multiple drivers. The key steps of the analysis are:

#### Step 1: IAP sensitivity runs

- The sensitivity runs are undertaken by modifying one input variable across the range defined in Table 1 while keeping all remaining inputs at their baseline values.
- Outputs for each driver–indicator combination are aggregated for Europe and the four regions.

#### Step 2: Sensitivity plots and summary statistics

- Those driver–indicator combinations with no sensitivity (zero variance) are identified and excluded from further analysis.
- The results for those drivers that affect each indicator are summarised as xy-plots for each driver–indicator combination to estimate the general trends/directions of change in the indicator with changes in the driver.
- The mechanisms by which each indicator is sensitive to each driver are identified based on the CLIMSAVE variable-to-variable network (Dunford et al. 2014) and in consultation with the sectoral modellers.
- Key sensitivity statistics (mean, range and standard deviation) are computed for each driver–indicator combination per region. The statistics are estimated across the number of runs used to cover each driver range (Table 1).

#### Step 3: Regression analysis and sensitivity thresholds

- A standardised curve fitting analysis (using  $I = \mathbf{a} * \mathbf{D}^n$  relationship for drivers represented in the IAP as continuous variables and  $I = \mathbf{a} * \mathbf{D}$  for drivers represented as discrete variables) is implemented using an iterative non-linear least squares regression (e.g., Brown 2001).  $\mathbf{D}$  (Driver) and  $\mathbf{I}$  (Indicator) represent normalised values of the independent and dependent variables, respectively;  $\mathbf{a}$  (Strength of sensitivity) and  $\mathbf{n}$  (Nature of sensitivity) represent the magnitude (rate of change as percentage) and linearity/non-linearity of sensitivity, respectively. The iteration is performed using the

**Table 1** List of the IAP climate and socio-economic change driver variables and associated input values selected for the sensitivity analysis

IAP driver		Selected sensitivity values and range			
Group/Sub-group	Input variables (units)	Short name	Baseline	Minimum	Maximum
<b>Climate change drivers:</b>					
<b>Climate:</b>					
1	Annual temperature change (°C)	Temp	0	0	6
2	Winter precipitation change (%)	WPre	0	-50	50
3	Summer precipitation change (%)	SPre	0	-50	50
4	CO <sub>2</sub> concentration (ppm)	CO <sub>2</sub>	350	350	700
5	Sea level change (m)	SLR	0	0	2
<b>Socio-economic change drivers:</b>					
<b>Social:</b>					
6	Population change (%)	Population	0	-50	50
7	Water savings due to behavioural change (%)	StrucChange	0	-50	50
8	Change in dietary preference for beef and lamb (%)	Ruminant	0	-60	100
9	Change in dietary preference for chicken and pork (%)	NonRuminant	0	-100	100
10	Household externalities preference (#)	GreenRed	3	1	5
11	GDP change (%)	GDP	0	-20	200
12	Change in oil price (%)	OilPrice	0	0	400
13	Change in food imports (%)	FoodImports	0	-20	60
14	Set aside (%)	SetAside	3	0	8
15	Reducing diffuse source of pollution from irrigation (-)	ReduceDiffuse	1	0.5	2
16	Forest management (-)	ForestMgmt	Optimum	Options <sup>a</sup>	
17	Change in agricultural mechanisation (%)	TechFactor	0	0	100
18	Water savings due to technological change (%)	TechChange	0	-75	75
19	Change in agricultural yields (%)	YieldFactor	0	-50	100
20	Change in irrigation efficiency (%)	IrrigEfficiency	0	-50	100
21	Compact vs sprawled development (-)	DevCompaction	Medium	Options <sup>b</sup>	
22	Attractiveness of coast (-)	CoastAttract	Medium	Options <sup>b</sup>	
23	Water demand prioritization (-)	WaterDistribRule	Baseline	Options <sup>c</sup>	
24	Level of flood protection (-)	FloodProtection	Minimum	Options <sup>d</sup>	
<b>Options</b>					

<sup>a</sup> Forest management: [1] Optimum, [2] Un-evenaged, [3] Even-aged (considering 5 Tree species: (1) Pinus sylvestris, (2) Pinus halepensis, (3) Pinus pinaster, (4) Quercus ilex, and (5) Fagus sylvatica)

<sup>b</sup> Compact vs sprawled development /Attractiveness of coast: [1] Low, [2] Medium, [3] High

<sup>c</sup> Water demand prioritization: [1] Baseline, [2] Prioritizing food production, [3] Prioritizing environmental needs, [4] Prioritizing domestic/industrial needs

<sup>d</sup> Level of flood protection: [1] No protection, [2] Minimum, [3] Maximum

SOLVER macro function in Microsoft Excel<sup>®</sup>, which uses the robust and efficient Generalised Reduced Gradient (GRG) algorithm (Lasdon et al. 1978).

- Based on the strength of sensitivity for each driver–indicator combination, the drivers are ranked into five classes: strong increase, weak increase, insignificant change, weak decrease, and strong decrease. Insignificant change is defined as ‘ $-5\% \leq a \leq 5\%$ ’. For the weak-strong classes, a  $\pm 35\%$  threshold is selected based on sectoral expert judgment.
- The nature of relationship is classified as linear for values ‘ $0.9 \leq n \leq 1.1$ ’, otherwise non-linear.

#### Step 4: Key impacts and cross-sectoral and regional comparison

- Those sectors and regions that are most sensitive to changes in drivers are identified.
- The mechanisms (direct/indirect/combined) by which the sectoral indicators are sensitive to each driver are compared.
- The trends/directions of sensitivity (positive/negative) are examined.
- The form of sensitivity (linearity/non-linearity) is analysed.
- The relative importance of drivers, based on the qualitative ranking using the strength of sensitivity, is examined.
- Finally, which sectors gain/win and which lose under which drivers are identified.

## 4 Results and discussion

The results are summarised by focussing on five key aspects of sensitivity: (i) sectoral interdependence: the extent to which a sector is sensitive to changes in other sectors; (ii) the direction of influence of each driver: whether an increase in the driver contributes to an increase or decrease in the indicator; (iii) the nature of sensitivity: linearity/non-linearity of the relationship for each driver–indicator combination, (iv) the level of contribution that each driver has to the sensitivity of each sectoral indicator; and (v) the key drivers to which an indicator is sensitive. Figure 2 shows a summary of the sensitivity analysis highlighting these key aspects. Table 2 then presents the Europe-wide<sup>2</sup> sensitivity statistics: mean, range, and standard deviation. The results show significant differences in impacts across the sectors and regions, as discussed in detail in the following sections.

### 4.1 Europe-wide sectoral sensitivity

#### 4.1.1 Artificial surfaces

Future urban growth (change in artificial surfaces, AS) is driven by five of the 21 socio-economic drivers only, and all the climatic drivers have no effect (Fig. 2). This is due to the urban model set-up (the variables included, Holman and Harrison 2012) and the fact that it is at the start of the meta-model chain (Fig. 1), so the drivers can only have a direct effect. AS shows the highest sensitivity to GDP growth, with a Europe-wide sensitivity range greater than 3% (Table 2), followed by population growth with a range greater than 0.2%. These two variables are therefore the two principal drivers of urban growth.

<sup>2</sup> See ESM 5 for the regional sensitivity statistics.

DRIVER	SECTOR: Indicator																	
	Urban: AS			Flooding: PF100			Forest: TP			Land use: LUD			Water: WEI			Biodiversity: BVI		
	Model	Form	Chain	Model	Form	Chain	Model	Form	Chain	Model	Form	Chain	Model	Form	Chain	Model	Form	Chain
Climate	Temp																	
	WPrec																	
	SPrec																	
	CO2																	
Socio-economic	SLR																	
	Population																	
	StructChange																	
	Ruminant																	
	NonRuminant																	
	GreenRed																	
	GDP																	
	OilPrice																	
	ImportFactor																	
	SetAside																	
Total Drivers	ReducedDiffuse																	
	ForestMgmt																	
	TechFactor																	
	TechChange																	
	YieldFactor																	
	IrrigEfficiency																	
	DevCompaction																	
	CoastAttract																	
	WaterDistribRule																	
	FloodProtection																	
5	5	5	5	5	5	5	5	5	5	5	5	5	5	5	5	5	5	5
(5/0/0)																		
6	6	6	6	6	6	6	6	6	6	6	6	6	6	6	6	6	6	6
(2/3/1)																		
6	6	6	6	6	6	6	6	6	6	6	6	6	6	6	6	6	6	6
(1/16/4)																		
21	21	21	21	21	21	21	21	21	21	21	21	21	21	21	21	21	21	21
(1/7/6)																		
21	21	21	21	21	21	21	21	21	21	21	21	21	21	21	21	21	21	21
(2/16/6)																		
24	24	24	24	24	24	24	24	24	24	24	24	24	24	24	24	24	24	24
(0/2/15)																		
18	18	18	18	18	18	18	18	18	18	18	18	18	18	18	18	18	18	18

**Fig. 2** Summary of the sensitivity analysis for each driver–indicator combination highlighting: (i) the trends/directions and strength of sensitivity (strong/weak increase (positive change), strong/weak decrease (negative change), or insignificant change); (ii) the form/nature of sensitivity (linear or non-linear); and (iii) the mechanisms of sensitivity (direct/indirect/combined). Note: EU (whole of Europe), WE (Western Europe), SE (Southern Europe), EE (Eastern Europe), and NE (Northern Europe) represent the five spatial extents considered (see also *ESM 2*)

**Table 2** A Europe-wide statistical summary of the sensitivity of the sectoral indicators to changes in the climate and socio-economic drivers affecting each sector. Similar tables for the four regions are provided in *ESM 5*

Drivers	Urban			Flooding			Forest			Land use			Water			Biodiversity		
	Baseline=3.67 %			Baseline=17.40 million			Baseline=262.28 Gt			Baseline=0.857			Baseline=0.145			Baseline=0		
	Mean	Range	SD	Mean	Range	SD	Mean	Range	SD	Mean	Range	SD	Mean	Range	SD	Mean	Range	SD
Climate drivers:																		
1 Temp				16.95	0.71	0.29	158.26	159.03	58.02	0.806	0.073	0.030	0.192	0.081	0.027	0.110	0.268	0.097
2 WPrece				17.41	2.57	1.10	229.91	160.88	64.73	0.842	0.080	0.031	0.172	0.203	0.076	0.007	0.155	0.057
3 SPrec				17.41	2.57	1.10	176.32	257.77	109.63	0.796	0.125	0.049	0.174	0.144	0.057	0.026	0.304	0.111
4 CO <sub>2</sub>							278.06	32.81	8.92	0.776	0.145	0.052	0.142	0.012	0.004	0.043	0.090	0.031
5 SLR				26.82	17.21	5.94	260.15	3.16	1.11	0.852	0.011	0.004	0.145	0.001	0.000	0.002	0.003	0.001
Socio-economic drivers:																		
6 Population	3.74	0.23	0.09	17.37	17.27	6.47	147.43	248.73	92.38	0.761	0.856	0.093	0.160	0.024	0.009	0.053	0.163	0.059
7 StructChange													0.145	0.033	0.012			
8 Ruminant							237.70	76.43	34.72	0.849	0.105	0.041	0.149	0.006	0.003	0.005	0.010	0.005
9 NonRuminant							245.66	95.26	38.54	0.830	0.079	0.036	0.150	0.011	0.005	0.010	0.042	0.017
10 GreenRed	3.69	0.03	0.01				262.23	0.09	0.04	0.858	0.001	0.000	0.145	0.000	0.000			
11 GDP	5.03	3.05	1.09				236.40	45.56	12.93	0.840	0.034	0.014	0.200	0.101	0.036	0.010	0.016	0.005
12 OilPrice							224.68	72.48	29.09	0.861	0.031	0.012	0.153	0.013	0.005	0.000	0.005	0.002
13 ImportFactor							236.90	131.76	58.57	0.748	0.286	0.121	0.146	0.021	0.008	0.060	0.165	0.069
14 Set/Aside													0.145	0.002	0.001			
15 ReduceDiffuse							202.67	101.00	43.63	0.850	0.003	0.001	0.156	0.012	0.005	0.001	0.015	0.005
16 ForestMgmt							216.14	99.93	50.41	0.860	0.005	0.002	0.147	0.006	0.004	0.001	0.002	0.001
17 TechFactor							231.78	47.75	16.40	0.835	0.045	0.017	0.147	0.004	0.002	0.006	0.013	0.005
18 TechChange													0.154	0.134	0.051			
19 YieldFactor							197.34	262.28	107.08	0.779	0.135	0.048	0.184	0.142	0.048	0.046	0.083	0.031
20 IrrigEfficiency							256.40	16.66	5.89	0.857	0.009	0.003	0.161	0.053	0.022	0.004	0.011	0.004
21 DevCompaction	3.68	0.04	0.02				262.24	0.11	0.07	0.858	0.001	0.000	0.145	0.000	0.000			
22 CoastAttract	3.67	0.00	0.00				262.28	0.01	0.01	0.857	0.000	0.000	0.145	0.000	0.000			
23 WaterDistriRule							262.24	0.17	0.08	0.857	0.000	0.000	0.145	0.002	0.001	0.000	0.000	0.000
24 FloodProtection				15.49	27.58	13.89	261.29	8.21	4.19	0.853	0.010	0.005	0.145	0.001	0.001	0.004	0.013	0.008

The sensitivity range for the three remaining socio-economic drivers (attractiveness of coast, compact vs sprawled development and household externalities preference) is less than 0.05 % (Table 2). However, it is worth noting that although these drivers have less effect on the amount of AS, they play an important role in determining the spatial distribution of changes in AS. These changes (both in magnitude and spatial distribution) have important indirect implications on other sectors, as discussed below.

#### 4.1.2 People flooded in a 1 in 100 year event

Flooding (PF100) is sensitive to six of the 24 drivers (Fig. 2). Temperature and precipitation changes have indirect effects (via the water sector) on fluvial flooding through changes in river flood flows with a Europe-wide sensitivity range around 0.7 million people (temperature) and 2.6 million people (precipitation) (Table 2). Increasing temperature or decreasing precipitation results in a drier Europe (compared to the current climate) causing decreases in river flood flows, which lead to smaller fluvial floodplains, and hence fewer people affected. In contrast, flood protection has a direct effect on PF100, with higher defences reducing impacts significantly; it shows the highest sensitivity range of 27.6 million people (the Europe-wide total being reduced from 28.3 million people under no protection to 0.7 million people under the maximum protection). This highlights the key importance of defences and more generally adaptation, which is also consistent with other studies (e.g., Hinkel et al. 2013). PF100 also shows high sensitivity to changes in sea level and population; both with a range greater than 17 million people.

The direct effect of sea-level change is always negative; PF100 increases with sea-level rise due to the increase in areas at risk of coastal flooding. Under the extreme 2 m sea-level rise, the Europe-wide total PF100 is projected to double from the baseline estimate, reaching up to 35 million people. On the other hand, the effect of population change is rather complex with a combined (direct/indirect) sensitivity. It affects both coastal and fluvial flood impacts through changes in the number of people living within floodplains and via the change in urban growth influencing the distribution of AS (residential/non-residential) that affects where people live, including floodplains. These sensitivities and the illustrated model behaviour help to interpret more complex scenarios with change in multiple drivers (Mokrech et al. 2014).

#### 4.1.3 Timber production and land use diversity

Both timber production (TP) and land use diversity (LUD) are sensitive to 21 of the 24 drivers (Fig. 2). Fifteen of these have a Europe-wide sensitivity range greater than 15Gt (for timber), while 12 have a range greater than 0.03 units (for diversity) (Table 2). The sensitivity of forestry is complex as it is intimately connected with the distribution of intensive agriculture (Audsley et al. 2014). The land use allocation model prioritises food provision. Therefore, those drivers that affect the distribution of intensive agriculture tend to have a large influence on all indicators associated with land use patterns, including TP and LUD. Hence, TP is most sensitive to indirect socio-economic factors (e.g., agricultural yields, population, and food imports), along with the climatic drivers (temperature and precipitation) with a range greater than 130Gt. For example, an extreme decrease in crop yields results in areas which are currently forest becoming intensive agriculture to meet food provision demand, leading to a decline in TP. Similarly, an increasing population requires increased food production, which means that more land is used for agriculture leading to a decline in forest area, and hence less TP. Moreover, the climatic factors that influence timber yields often also improve crop yields leading to complex interactions in terms of overall land profitability. Greater timber yield



potential also leads to less forest area being needed to produce the same levels of timber, and as such allows losses in total forest area to more profitable land uses. Hence, temperature increase reduces Europe-wide forest productivity, whilst increasing precipitation leads to increased (winter) and decreased (summer) productivity. Other important indirect drivers for TP include reducing diffuse sources of pollution from agriculture, forest management, and changes in oil price and dietary preferences (ruminant/non-ruminant) with a range greater than 75Gt.

LUD (representing landscape multifunctionality based on Shannon Index of diversity) is also driven by complex changes in different land uses including urban, intensive arable, intensive/extensive grassland, forest, and unmanaged. As diversity is greatest in areas where there is a broad mix of land use, it is positively influenced by drivers that lead to new land uses becoming present in a grid cell, provided that the changes are not at the expense of a total removal of another land use. Hence, the sensitivity of LUD is influenced positively by drivers that encourage agriculture to spread more widely into new areas (e.g., change in population and dietary preferences). However, it is influenced negatively by factors that: make it easier to produce more food in less area (improvements in agricultural technology or crop yields); decrease the need for crop production (increases in food imports); make it harder for agriculture to spread (hotter climates); and make other land uses more competitive (increases in CO<sub>2</sub> leading to increased timber yield).

#### 4.1.4 Water exploitation index

The water exploitation index (WEI: dimensionless ratio of total water withdrawal to water availability) is sensitive to all of the 24 drivers, which directly and/or indirectly influence the amount of water use and/or availability (Fig. 2). Five of these have a Europe-wide sensitivity range greater than 0.1 units (Table 2). Precipitation and temperature directly affect long-term annual water availability. WEI shows the highest sensitivity to precipitation change: increasing precipitation leads to increasing water availability, thereby decreasing WEI. In contrast, WEI increases with rising temperature due to decreasing water availability. On the water demand side, rising temperatures lead to increasing irrigation water demand (indirect effect), and hence increasing WEI. In addition to the climatic factors, socio-economic drivers also directly/indirectly influence water use by affecting water demand in the domestic, manufacturing, and energy (cooling) sectors, as well as irrigation water withdrawals (driven mainly by the demand for crop production and change in prices for agricultural inputs). These include crop yields, water savings due to technological change, GDP, and irrigation efficiency, all of which have a range greater than 0.05 units. The effect of changes in agricultural yields is always negative; both increasing and decreasing yields lead to increasing irrigation water use, and hence increasing WEI. This is due to the fact that when yields increase the least productive agricultural areas become no longer profitable as the most productive areas are able to produce a greater proportion of the total food demand. This has the effect of increasing the marginal value of irrigation leading to higher WEI. Similarly, a decrease in yield means that more land is used for agriculture (including in northern Europe) to meet existing food demand resulting in increasing irrigation water demand, thereby increasing WEI. GDP growth also leads to increasing WEI due to increasing domestic water use as more water-intensive appliances are used when people have higher incomes. On the other hand, technological improvements have a direct effect in reducing WEI through water savings due to increasing water efficiency in the domestic, manufacturing and energy sectors. Other drivers that also have some impact on WEI include: water savings due to behavioural change lowering domestic water use (↓WEI), population growth leading to higher domestic water use (↑WEI), and increasing food imports leading to declining irrigation water demand (↓WEI).

The sensitivities observed are consistent with the model structure which applies a water allocation scheme to derive actual water withdrawals in non-agricultural sectors as well as the maximum volume of water available for irrigation based on water availability and demand (Wimmer et al. 2014).

#### 4.1.5 Biodiversity vulnerability index

Out of the 24 drivers, 18 have some impact on the biodiversity vulnerability index (BVI) (Fig. 2). Eight of these have a Europe-wide impact with a range greater than 0.02 units (Table 2). BVI shows the highest sensitivity to climatic drivers, particularly summer precipitation and annual temperature. Increasing temperature leads to increasing BVI due to decreases in the climate suitability for species, except in northern Europe where a warmer climate means the area becomes suitable for species from further south, leading to an increase in the number of species present. However, changes in precipitation have an inverse relationship with BVI, where increasing precipitation leads to a reduction in species' vulnerability and vice versa. Also, changes at very low levels of precipitation show more pronounced effects than those at very high levels, i.e., changes from drought to dry conditions are more beneficial for most of the species than wet conditions becoming very wet. In addition to these climatic drivers, socio-economic factors that influence land use distribution (e.g., food imports, population growth, agricultural yields, and dietary preferences) also have indirect impacts on BVI. Spatial analysis of the impacts of these factors reveal that land use changes often include the full removal of arable farming from grid cells which removes habitat for arable-related species such as the Linnet (*Carduelis cannabina*). Under some drivers (e.g., agricultural yields), vulnerability increases with both increases and decreases in the driver. Increases in agricultural yields leads to productive agricultural areas producing more and those with lower productivity become less profitable and are prioritised for other uses, e.g., southern Sweden losing its arable croplands. Conversely, when agricultural yields decrease, the extent of farming in northern Europe increases to meet demand, but declines in areas such as Lithuania where the profitability of arable land is not as great.

This combined climate and socio-economic influence on BVI is expected and reflects the SPECIES bio-climatic envelope model that underpins the index (Holman and Harrison 2012). Climate determines the boundary conditions for the species and land use determines whether or not habitats are available within the climatically suitable areas. BVI is therefore sensitive to factors that influence either of these factors.

#### 4.2 Nature of sensitivity and ranking of drivers: cross-sectoral and regional comparison

The standardised regression analysis was used to identify the form of sensitivity (linear/non-linear) and the relative importance (the 5-class ranking) of the climatic and socio-economic drivers affecting each indicator. This allowed a cross-sectoral and regional comparison of impacts and identification of which sectors lose and which gain under which key drivers (Fig. 2). The results show that 18 of the 24 drivers have a non-linear effect on one or more of the sectors at the European level. Most of the non-linearities observed are related to drivers that have some indirect effect on indicators. The urban sector is the exception, as all its drivers are direct. The indirect/combined drivers represent 54 of the 65 non-linear driver-indicator relationships. Only 19 % (18 out of the total 95) of the relationships are direct (excluding the direct effect of the combined drivers), of which 11 also have non-linear effect. These results highlight the complexity and highly non-linear nature of the cross-sectoral interactions due to the cascading impacts of most climatic and socio-economic drivers across sectors. Either

ignoring or having a limited understanding of these interactions could therefore lead to potential under- or over-estimation of impacts, including the possible non-linear amplifications of such interactions on the impacts (e.g., Ludwig et al. 2013).

The qualitative ranking of the drivers also highlighted the varied level of contribution of each driver to the sensitivity of each sectoral indicator in different regions (Fig. 2). It also illustrated the sectoral winners (reduced impacts) and losers (increased impacts) as discussed below.

#### 4.2.1 Cross-sectoral comparison of Europe-wide impacts

At the European level, 12 of the 24 drivers have strong implications on one or more of the sectors (Fig. 2). A warmer future climate generally has strong negative impacts on most sectors; biodiversity, water, and forests being the most affected, followed by land use diversity. However, increases in precipitation are positive for biodiversity and water leading to strong decreases in water stress and biodiversity vulnerability. Conversely, land use diversity decreases with higher summer precipitation. Flooding also significantly increases with sea-level rise. Forestry gains strongly with increasing CO<sub>2</sub>, which has a knock-on effect on other sectors; increasing timber yield leading to productive areas producing more of the total timber and large areas becoming abandoned, negatively affecting biodiversity and land use diversity. The implications of climate drivers on other sectors are relatively small.

When considering socio-economic drivers, while a wealthier Europe (higher GDP) is expected to experience strong urban growth, it will lead to significant stresses on water resources due to the associated additional pressures on water demand. Forests, land use diversity and biodiversity are also negatively affected (albeit relatively weak in magnitude) with increasing GDP, via its influence on land use distribution such as increased labour costs leading to increased crop prices, thereby increasing irrigation profitability in some areas (e.g., the new EU countries). Similarly, increasing population has a negative effect on most sectors; flooding, forests, land use diversity and biodiversity being the most affected, followed by water. Other key socio-economic drivers include agricultural yields, food imports, and dietary preferences, which have varied indirect implications across all sectors. For example, increasing food imports reduces the need for agriculture, which has a knock-on effect on other sectors, with biodiversity and land use diversity being the most affected. In contrast, the forest and water sectors gain in this situation due to more land being available for forestry and declining irrigation water demand reducing water stress. Flooding also reduces with increased flood protection.

#### 4.2.2 Cross-sectoral comparison of regional impacts

Figure 2 shows that between 5 and 12 of the 24 drivers have strong regional implications on one or more of the sectors. A warmer climate has significant regional negative impacts on forests and biodiversity: forestry losing in all regions (particularly strongly in western Europe) and biodiversity losing significantly in all regions except northern Europe. This is followed by the water sector, also losing in western and eastern Europe due to declining water availability and increasing demand for irrigation. Higher temperatures also have varied regional effects on land use diversity; declining in southern and northern Europe and increasing in western and eastern Europe (but with a weak magnitude). Increasing CO<sub>2</sub>, however, results in strong gains for forestry in eastern and northern Europe due to relatively higher profitability when compared with western and southern Europe. In contrast, biodiversity loses in all regions (except northern Europe) with higher CO<sub>2</sub>. In terms of precipitation, both biodiversity and water are the winners. For water, increasing winter precipitation leads to a strong decrease in WEI, particularly in southern and eastern Europe, followed by western Europe. For biodiversity, increasing summer precipitation leads to a strong

decrease in BVI, particularly in southern, eastern, and northern Europe. In contrast, forestry shows significant regional variation with precipitation change, which most, if not all, of the time is due to associated indirect implications on agricultural land use change. For example, forestry strongly gains with increasing winter precipitation, but strongly loses with increasing summer precipitation in western Europe. This is due to lower relative profitability in western than northern and eastern Europe, in particular, where increase in precipitation leads to increasing timber production. Flooding also increases with increased precipitation, particularly in western and eastern Europe (although this trend is relatively weak in strength).

In terms of the socio-economic drivers, those identified with Europe-wide relevance also have important regional implications for each sector. These include population, GDP, agricultural yields, food imports and dietary preferences. In addition, forest management, reducing diffuse sources of pollution from irrigation and irrigation efficiency have notable implications. For example, forestry consistently loses in all regions with changes in agricultural yields due to changes in the relative profitability of forestry and agricultural land use. Similarly, biodiversity (in all regions) and water (in southern and eastern Europe) also lose, again related to changes in irrigation water demand (stress on water) and changes in arable farming (effect on biodiversity). Conversely, increasing food imports has positive implications on forests (increasing TP in all regions, especially in western Europe), water (especially in southern Europe) and biodiversity (in all regions).

## 5 Conclusion

The paper analysed a Europe-wide integrated assessment model (the CLIMSAVE IAP) using an extensive and systematic sensitivity analysis of a wide range of climatic and socio-economic drivers. The focus was on investigating how changes in individual drivers affect European landscape change dynamics. It considered the implications of important cross-sectoral interactions and identified the mechanisms and directions (direct/indirect and positive/negative) and the form and magnitudes (linear/non-linear and insignificant/weak/strong) of sensitivities of sectoral indicators to cross-sectoral impacts. The study allowed a better understanding of the complex relationships between the input driver variables and output sectoral indicator parameters within the IAP. It tracks if, and how, the effects of one driver on a sector/region are transferred and felt by other sectors/regions and identifies those sectors and regions most sensitive to future changes and the relative importance of the drivers across sectors and regions. This is crucial for providing a better understanding of future impacts in a world where climate and socio-economic conditions are changing together.

The analysis includes holistic insights into the complex interactions and potential synergies, conflicts and trade-offs between sectors and appropriate adaptation priorities. This demonstrated the importance of considering the implications of cross-sectoral linkages in impact assessments. However, it is worth noting that these results do not account for sensitivities (e.g., indirect effects and non-linearities) associated with changes in multiple drivers, as some scenario combinations could have much higher impacts than those presented here. This is being investigated in a future paper. Nonetheless, it provides important sectoral and cross-sectoral insights on the effects of individual drivers/stresses. Building on this analysis, Harrison et al. (2014b) also investigated the cross-sectoral implications of selected ranges of climatic and socio-economic scenario futures, which accounts for a combination of multiple drivers of change. As such, these analyses provide important information to understand the potential benefits and conflicts of different adaptation measures across sectors (e.g., Berry et al. 2014).

**Acknowledgments** The research leading to these results has received funding from the European Commission Seventh Framework Programme under Grant Agreement No. 244031 (The CLIMSAVE Project; Climate change integrated assessment methodology for cross-sectoral adaptation and vulnerability in Europe; [www.climsave.eu](http://www.climsave.eu)). CLIMSAVE is an endorsed project of the Global Land Project of the IGBP. MT was in addition supported through project: 'Building Up a Multidisciplinary Scientific Team Focussed on Drought', no. CZ.1.07/2.3.00/20.0248.

## References

- Audsley E, Pearn KR, Simota C et al (2006) What can scenario modelling tell us about future European scale agricultural land use, and what not? *Environ Sci Pol* 9:148–162
- Audsley E, Trnka M, Sabaté S et al (2014) Interactively modelling land profitability to estimate European agricultural and forest land use under future scenarios of climate, socio-economics and adaptation. *Climatic Change*. doi:10.1007/s10584-014-1164-6
- Aydinalp C, Cresser MS (2008) The effects of global climate change on agriculture. *Am Eurasian J Agric Environ Sci* 3(5):672–676
- Bates BC, Kundzewicz ZW, Wu S, Palutikof JP (eds) (2008) *Climate Change and Water*. Technical Paper of the Intergovernmental Panel for Climate Change. IPCC Secretariat, Geneva, 210 pp
- Berry PM, Rounsevell MDA, Harrison PA, Audsley E (2006) Assessing the vulnerability of agricultural land use and species climate change and the role of policy in facilitating adaptation. *Environ Sci Pol* 9(2):189–204
- Berry PM, Brown S, Chen M et al. (2014) Cross-sectoral interactions of adaptation and mitigation measures. *Clim Chang*. doi:10.1007/s10584-014-1214-0
- Brown AM (2001) A step-by-step guide to non-linear regression analysis of experimental data using a Microsoft Excel spreadsheet. *Comput Methods Prog Biomed* 65:191–200
- Brown C, Brown E, Murray-Rust D et al (2014) Analysing uncertainties in climate change impact assessment across sectors and scenarios. *Clim Chang*. doi:10.1007/s10584-014-1133-0
- Carter TR, Jones RN, Lu X et al (2007) New assessment methods and the characterisation of future conditions. In: Parry ML et al (eds) *Climate change 2007: Impacts, adaptation and vulnerability*. Cambridge University Press, Cambridge, pp 133–171
- Ciais P, Reichstein M, Viovy N et al (2005) Europe-wide reduction in primary productivity caused by the heat and drought in 2003. *Nature* 437:529–533
- Dubrovsky M, Trnka M, Holman IP et al (2014) Developing a reduced-form ensemble of climate change scenarios for Europe and its application to selected impact indicators. *Clim Chang*. doi:10.1007/s10584-014-1297-7
- Dunford R, Harrison PA, Rounsevell MDA (2014) Exploring scenario and model uncertainty in cross-sectoral integrated assessment approaches to climate change impacts. *Clim Chang*. doi:10.1007/s10584-014-1211-3
- EEA (2007) *Climate change and water adaptation issues*. European Environment Agency, EEA Technical Report, No. 2/2007, 110pp
- Frieler K and the ISI-MIP Team (2013) Accounting for cross-sectoral linkages of climate change impacts based on multi-model projections. *Geophysical Research Abstracts*, EGU General Assembly 2013, 15:EGU2013–12601
- Green RE, Harley M, Miles L et al (eds.) (2003) *Global climate change and biodiversity*. Summary of papers and discussion, Norwich, UK
- Harremoes P, Turner RK (2001) Methods for integrated assessment. *Reg Environ Chang* 2:57–65
- Harrison PA, Holman IP, Cojocaru G et al (2013) Combining qualitative and quantitative understanding for exploring cross-sectoral climate change impacts, adaptation and vulnerability in Europe. *Reg Environ Chang* 13:761–780
- Harrison PA, Holman IP, Berry PM (2014a) Assessing cross-sectoral climate change impacts, vulnerability and adaptation: An Introduction to the CLIMSAVE project. *Climatic Change* (Editorial)
- Harrison PA, Dunford R, Savin C et al (2014b) Cross-sectoral impacts of climate change and socio-economic change for multiple, European land- and water-based sectors. *Clim Chang*. doi:10.1007/s10584-014-1239-4
- Hinkel J, Nicholls RJ, Vafeidis AT et al (2010) Assessing risk of and adaptation to sea-level rise in the European Union: an application of DIVA. *Mitig Adapt Strateg Glob Change* 15:703–719
- Hinkel J, Lincke D, Vafeidis AT et al (2013) Coastal flood damage and adaptation costs under 21st century sea-level rise. *PNAS* 111(9):3292–3297
- Holman IP, Harrison PA (eds.) (2012) Report describing the development and validation of the sectoral meta-models for integration into the IA Platform. CLIMSAVE Deliverable D2.2. [http://www.climsave.eu/climsave/doc/Report\\_on\\_the\\_Meta-models.pdf](http://www.climsave.eu/climsave/doc/Report_on_the_Meta-models.pdf). Accessed 09 Feb 2013

- Holman IP, Rounsevell MDA, Shackley S et al (2005) A regional, multi-sectoral and integrated assessment of the impacts of climate and socio-economic change in the UK, Part I: Methodology. *Clim Chang* 71:9–41
- Holman IP, Rounsevell MDA, Berry PM, Nicholls RJ (2008a) Development and application of participatory integrated assessment software to support local/regional impact and adaptation assessment. *Clim Chang* 90: 1–4
- Holman IP, Rounsevell MDA, Cojocar G et al (2008b) The concepts and development of a participatory regional integrated assessment tool. *Clim Chang* 90(1–2):5–30
- Kenny GJ, Ye W, Flux T, Warrick RA (2001) Climate variations and New Zealand agriculture: The CLIMFACTS system and issues of spatial and temporal scale. *Environ Int* 27(2–3):189–195
- Kok K, Bärlund I, Flörke M et al (2014) European participatory scenario development: strengthening the link between stories and models. *Clim Chang*. doi:10.1007/s10584-014-1143-y
- Lasdon LS, Waren AD, Jain A, Ratner M (1978) Design and testing of a generalised reduced gradient code for non-linear programming. *ACM Trans. Math Softw* 4:34–50
- Lindner M, Maroschek M, Netherer S et al (2008) Climate change impacts, adaptive capacity, and vulnerability of European forest ecosystems. *For Ecol Manag* 259(4):698–709
- Ludwig F, van Vliet MTH, Biemans H (2013) Climate change impacts on the water-food-energy nexus. IMAPCTS WORLD 2013, International Conference on Climate Change Effects, May 27–30, Potsdam, Germany
- Matsuoka Y, Morita T, Kainuma M (2001) Integrated Assessment Model of Climate Change: The AIM Approach. In: Matsuno T, Kida H (eds), *Present and Future of Modelling Global Environmental Change: Toward Integrated Modelling*, pp.339–361
- Millennium Ecosystem Assessment (2005) *Ecosystems and Human Well-being: Synthesis*. Island PRESS, Washington, DC
- Mokrech M, Nicholls RJ, Richards JA et al (2008) Regional impact assessment of flooding under future climate and socio-economic scenarios for East Anglia and North West England. *Clim Chang* 90:31–55
- Mokrech M, Kebede AS, Nicholls RJ et al (2014) An integrated approach for assessing flood impacts due to future climate and socio-economic conditions and the scope of adaptation in Europe. *Clim Chang*. doi:10.1007/s10584-014-1298-6
- Moss RH, Edmonds JA, Hibbard KA et al (2010) The next generation of scenarios for climate change research and assessment. *Nature* 463:747–756
- Nelson GC, Janetos A, Bennet E (2005) Drivers of change in ecosystem condition and services. In: Carpenter SR et al (eds) *Scenarios Assessment of the Millennium Ecosystem Assessment*. Island Press, London, UK, pp 173–222
- Nicholls RJ, Kebede AS (2012) Indirect impacts of coastal climate change and sea-level rise: the UK example. *Clim Pol* 12:S28–S52
- Ratto M, Castelletti A, Pagano A (2012) Emulation techniques for the reduction and sensitivity analysis of complex environmental models. *Environ Model Softw* 34:1–4
- Saltelli A, Chan K, Scott M (eds) (2000) *Sensitivity Analysis. Probability and Statistics Series*. Wiley, New York
- Toth FL, Bruckner T, Füssel H-M et al (2003) Integrated assessment of long-term climate policies. Part 1. Model presentation. *Clim Chang* 56:37–56
- Wimmer F, Audsley E, Malsy M et al. (2014) Modelling the effects of cross-sectoral water allocation schemes in Europe. *Clim Chang*. doi:10.1007/s10584-014-1161-9



# Direct and indirect impacts of climate and socio-economic change in Europe: a sensitivity analysis for key land- and water-based sectors

## Electronic Supplementary Material (ESM)

A.S. Kebede<sup>1\*</sup>, R. Dunford<sup>2</sup>, M. Mokrech<sup>3</sup>, E. Audsley<sup>4</sup>, P.A. Harrison<sup>2</sup>, I.P. Holman<sup>4</sup>, R.J. Nicholls<sup>1</sup>, S. Rickebusch<sup>5,6</sup>, M.D.A. Rounsevell<sup>6</sup>, S. Sabaté<sup>7,8</sup>, F. Sallaba<sup>9</sup>, A. Sanchez<sup>7</sup>, C. Savin<sup>10</sup>, M. Trnka<sup>11,12</sup> and F. Wimmer<sup>13</sup>

<sup>1</sup> Faculty of Engineering and the Environment, Tyndall Centre for Climate Change Research, University of Southampton, Highfield, Southampton SO17 1BJ UK

<sup>2</sup> Environmental Change Institute, University of Oxford, South Parks Road, Oxford OX1 3QY, United Kingdom

<sup>3</sup> School of Science and Computer Engineering, University of Houston Clear Lake, 2700 Bay Area Blvd., Box 540, Houston, United States

<sup>4</sup> Cranfield Water Sciences Institute, Cranfield University, Cranfield, Bedford, MK43 0AL UK

<sup>5</sup> Environmental Systems Analysis Group, Wageningen University, P.O. Box 47, 6700 AA Wageningen, The Netherlands

<sup>6</sup> School of GeoSciences, University of Edinburgh, Drummond Street, Edinburgh EH8 9XP, United Kingdom

<sup>7</sup> Centre for Ecological Research and Forestry Applications (CREAF), Universitat autonoma de Barcelona, Edifici C, Bellaterra 08193, Spain

<sup>8</sup> Ecology Department, University of Barcelona, Diagonal 643, 08028 Barcelona, Spain

<sup>9</sup> Department of Physical Geography and Ecosystem Science, Lund University, Sölvegatan 12, Lund 22362, Sweden

<sup>10</sup> TIAMASG Foundation, Sfintii Voievozi 6, 010963 Bucharest, Romania

<sup>11</sup> Institute of Agrosystems and Bioclimatology, Mendel University in Brno, Zemědělská 1, Brno 61300, Czech Republic

<sup>12</sup> Global Change Research Centre AS CR v.v.i, Bělidla 986/4a, 603 00 Brno, Czech Republic

<sup>13</sup> Center for Environmental Systems Research, University of Kassel, Kassel 34109, Germany

\* Corresponding author: Email: [ask2q08@soton.ac.uk](mailto:ask2q08@soton.ac.uk); Tel. +44 (0) 23 8059 2134

## ESM1: THE CLIMSAVE Approach: Cross-Sectoral Focus

### The CLIMSAVE Integrated Framework

CLIMSAVE<sup>1</sup> is a pan-European research project (conducted during 2010 to 2013) funded under the European Commission's Seventh Framework Programme. The project is coordinated by the Environmental Change Institute at the University of Oxford. The consortium involves 18 partner institutions from 13 different countries in Europe as well as from China and Australia. The overall aim of the CLIMSAVE project is to deliver a European level integrated assessment methodology that allows stakeholders to investigate the cross-sectoral impacts of, and vulnerabilities and adaptation to, a range of climatic and non-climatic drivers of change in Europe.

To achieve this, a range of sectoral impact models have been developed and integrated within a common web-based assessment platform, the CLIMSAVE integrated assessment platform (IAP). The study focuses on six key European land- and water-based sectors, including: agriculture, biodiversity, coastal environments, forestry, urban areas, and water resources. The development of the integrated assessment platform involves linking of ten disparate impact assessment models from these six different sectors to better understand the complex multi-sectoral issues such as competition for land, competition for water, and associated cross-sectoral impacts and potential synergies, conflicts, and trade-offs between different adaptation options. [Figure \(i\)](#) presents a

---

<sup>1</sup> Climate change Integrated assessment Methodology for cross-Sectoral Adaptation and Vulnerability in Europe (Project website: [www.climsave.eu](http://www.climsave.eu)). Additional details on the conceptual framework of the CLIMSAVE integrated methodology can also be found in [Harrison et al. \(2013\)](#) and [Harrison et al. \(this volume \(a\)\)](#).



schematic illustration of the interaction and feedbacks between the sectors integrated within the CLIMSAVE IAP.

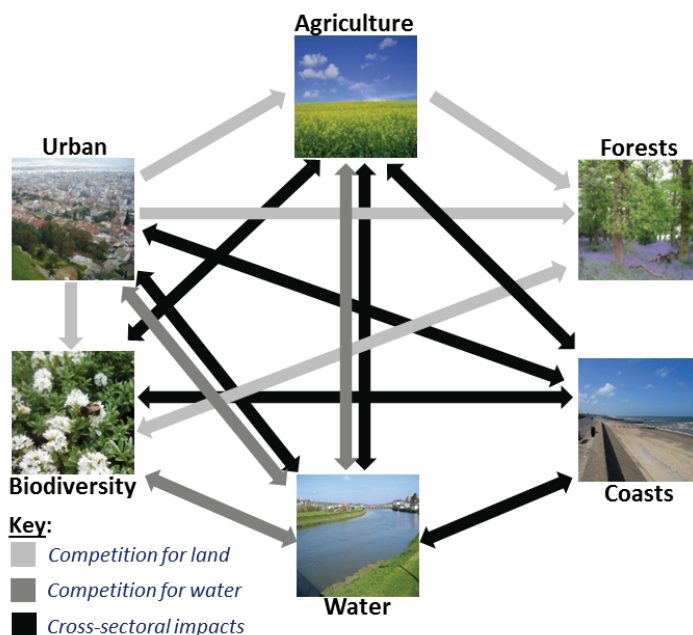


**Figure (i):** Schematic diagram of the six key sectors and associated interactions considered within the CLIMSAVE integrated assessment platform.

The tool is intended to put science in the service of stakeholders and policy-makers by providing a common platform for an improved integrated assessment of climate change impacts, vulnerabilities and related cost-effective cross-sectoral adaptation measures in Europe. The linking and integration of the different sectoral impact models will allow stakeholders (such as academic, governmental, professional, and other interested citizens) to explore and better understand how the interactions between the different sectors could affect the dynamics of future European landscape change, rather than viewing each sector and/or their own region in isolation. However, it is worth stating that the IAP is intended to complement, rather than replace, the use of more detailed sectoral tools in informing the development of robust adaptation policy responses. In doing so, it provides important sectoral and cross-sectoral insights by exploring a range of ‘what if’ scenarios under different climate change and socio-economic conditions. As such, it provides important information which contributes to the development of a well-adapted Europe by building the capacity of stakeholders and decision-makers to better understand the complex issues surrounding climate change. It allows to exploring appropriate adaption opportunities under uncertain futures for making more reliable choices and robust decision-making based on solid scientific knowledge (see Harrison et al. 2013; Harrison et al. this volume (a)).

### **The CLIMSAVE Integrated Assessment Platform**

The CLIMSAVE integrated assessment platform (IAP) is a unique user-friendly, interactive and exploratory web-based tool<sup>2</sup>. It provides an integrated methodology intended to assist stakeholders and decision-makers in improving their understanding about the complex challenges surrounding cross-sectoral impacts, vulnerability and adaptation responses due to future climate and socio-

<sup>2</sup> The IAP is freely accessible online through the CLIMSAVE project website: [www.climsave.eu](http://www.climsave.eu)

economic change under uncertain futures. It also allows stakeholders and researchers to explore how climate change will interact with changing social, economic and political conditions in the future and that all these factors need to be considered to assess the robustness of cross-sectoral adaptation responses (e.g., [Berry et al. this volume](#)). [Figure \(ii\)](#) (also available in the main paper) shows a simplified schematic diagram of the conceptual framework of the CLIMSAVE integrated methodology illustrating the data transfers between the various sectoral meta-models integrated within the IAP.

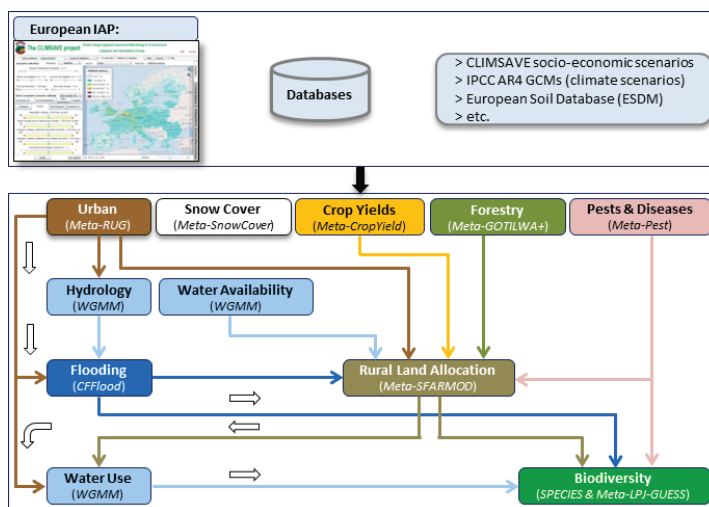


**Figure (ii):** Simplified schematic diagram of the various sectoral meta-model linkages and associated data flows as integrated within the European CLIMSAVE integrated assessment platform (Adapted from [Harrison et al. 2013](#)).

The key aspects of the CLIMSAVE IAP lies in its holistic methodology framework which improves on previous studies in various important ways, including: (i) higher integration of knowledge from stakeholders and scientists, (ii) greater consideration of important cross-sectoral linkages, interactions and feedbacks by integrating six key land- and water-based sectors (agriculture, biodiversity, coasts, forestry, urban areas, and water resources), (iii) holistic consideration of the combined effects of both climatic and socio-economic factors, and (iv) multi-scale applications (continental scale: Europe and regional scale: Scotland). The European scale IAP operates at a 10x10 arc minute grid resolution (a total of 23,871 grid cells in Europe), while the regional scale IAP developed for Scotland operates at a 5 km x 5 km grid resolution (a total of 3,472 grid cells in Scotland). In this paper, only results of the European IAP application are presented.

The development of the IAP uses *meta-modelling* approaches which allow integration of sectoral impact assessment meta-models to provide stakeholders with an interactive assessment tool with reasonably fast run-times ([Holman et al. 2008a,b](#); [Holman and Harrison 2012](#)). Meta-models (also termed as ‘reduced-form models’) are computationally simple(r) but efficient modelling techniques that emulate the performance of more complex models ([Ratto et al. 2012](#)). Examples of meta-modelling techniques used in the CLIMSAVE IAP<sup>3</sup> include *look-up tables*, *artificial neural networks (ANN)*, and *soil/climate clustering*. Hence, the integrated assessment platform contains a series of inter-linked meta-models (implemented as Dynamic-Link Libraries, DLLs), an internal database (e.g.,

<sup>3</sup> See [Harrison et al. \(2013\)](#) and [Holman and Harrison \(2012\)](#) for more details on the meta-modelling approach used for, and on the development and validation of, the various sectoral meta-models integrated within the CLIMSAVE IAP.

elevation data), a wide range of climate and socio-economic scenarios, and a GIS-based user interface that captures the complex interactions and feedbacks between different sectors. Each of the sectoral meta-models is developed using different approaches representing a good compromise between fast run-times and model accuracy. Each meta-model is designed to be modular, independent, and replaceable at any time. This allows efficient integration and development of the IAP as well as providing flexibility in future development by integrating new knowledge and data as it emerges.

### ***Systematic Sensitivity Analysis of the IAP***

In this paper, we present an application of the European integrated assessment platform (IAP) based on an extensive and systematic sensitivity analysis, using a One-Driver-at-a-Time (ODAT) approach. The ODAT approach allows assessing the complex interactions and feedbacks between the various sectoral models in order to better understand cross-sectoral impacts of a range of climate and socio-economic change drivers on six key European land- and water-based sectors. The study focuses on a set of six sectoral indicators, one for each sector (as described in [ESM3](#) below). The objective is to identify and quantify the relationships between the various climatic (e.g., changes in temperature, precipitation, sea-level rise, and CO<sub>2</sub> concentration) and non-climatic (e.g., changes in the social, economic, technological, environmental, and policy governance factors) IAP input variables (drivers) and outputs (sectoral indicators). The particular focus of the analysis is to track if, and how, the direct effect of an individual driver on a sector or region is transferred and felt by other sectors or regions in order to identify:

- Those sectors and regions most sensitive to future changes (i.e., which sector or region gain or lose most under a given change of driver),
- The mechanisms of sensitivity (i.e., whether the effect of the drivers on each sectoral indicator is direct, indirect or combined),
- The trends or directions of sensitivity in terms of the influence of each driver on the sensitivity of indicators (i.e., whether an increase in the driver contributes to an increase (positive effect) or decrease (negative effect) in the indicator),
- The forms or nature of sensitivity (i.e., linearity or non-linearity of the relationship for each driver–indicator combination),
- The magnitudes of sensitivity (strong, weak, insignificant change), and
- The relative importance of the key drivers across sectors and regions.

The results help to understand and better interpret outputs from complex integrated assessments of cross-sectoral impacts of both climate and socio-economic change drivers based on, for example, a scenario analysis ([Harrison et al. this volume \(b\)](#)) and uncertainty analysis ([Brown et al. this volume](#)) under change in multiple drivers. As such, they provide broad sectoral and cross-sectoral insights into how different assumptions or future scenarios affect decision choices and help identify which parameters or assumptions are most important in affecting future cross-sectoral impacts and adaptation priorities.



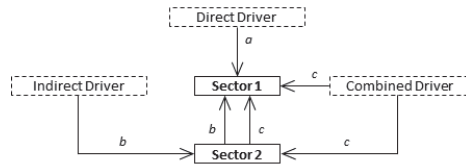
**ESM2:** European and regional domains, classified based on river basins. Eastern Europe (EE) includes: Bulgaria, Estonia, Germany (far north-east), Hungary (east), Latvia, Lithuania, Poland, Romania, and Slovakia (east); Northern Europe (NE): includes: Finland, Norway, and Sweden; Southern Europe (SE) includes: Bulgaria (south-west), Greece, France (Mediterranean coast), Italy, Portugal, Spain, and Slovenia; and Western Europe (WE) includes: Austria, Belgium, Czech Republic, Denmark, France, Germany, Hungary (west), Ireland, Luxembourg, Netherlands, Slovakia (west), Switzerland, and UK.

**ESM3:** Descriptions of the selected sectoral indicators. More details and descriptions of each of the selected indicators, as well as the rest of the IAP output variables for the six key sectors considered within the CLIMSAVE project, can be found in [Holman and Harrison \(2012\)](#).

Sector (Meta-model)	Impact Indicator (Unit)	Indicator Description
Urban (RUG)	Artificial surfaces (%)	The mean percentage change in artificial surfaces (i.e., CORINE land-cover class 1, representing residential and non-residential areas).
Flooding (CFFlood)	People flooded in a 1 in 100 year event (millions)	The number of people flooded by a 1 in 100 year (1%) event due to coastal and fluvial flooding.
Land use (SFARMOD + metaGOTILWA)	Timber production (Mt)	Total timber produced based on the modelled timber productivity of five representative species <sup>4</sup> within areas of modelled profitable managed forest.
	Land use diversity (-)	Representation of multi-functionality of the landscape based on Shannon Index (for land uses including urban, intensive arable, intensive grass, extensive grass, forest and others).
Water (WGMM)	Water exploitation index (-)	Dimensionless ratio of long-term annual water withdrawals to long-term annual renewable water resources. It is a water stress indicator reflecting the degree of pressure put on natural water resources by all water users (e.g., abstraction for agriculture, domestic or energy production).
Biodiversity (SPECIES)	Biodiversity vulnerability index (-)	An index based on changes in climate and habitat space suitability for 12 representative species <sup>5</sup> covering a range of European flora and fauna from different taxa, habitats and regions.

<sup>4</sup> The 5 representative tree species considered are: (1) *Pinus sylvestris*, (2) *Pinus halepensis*, (3) *Pinus pinaster*, (4) *Quercus ilex*, and (5) *Fagus sylvatica*).

<sup>5</sup> The 12 selected mixed representative species group in Europe are: (1) Common poppy (*Papaver rhoeas*), (2) Linnet (*Carduelis cannabina*), (3) Bilberry (*Vaccinium myrtillus*), (4) Hornbeam (*Carpinus betulus*), (5) Norway spruce (*Picea abies*), (6) Brown bear (*Ursus arctos arctos*), (7) Western dappled white butterfly (*Euchloe crameri*), (8) Common saltmarsh grass (*Puccinellia maritima*), (9) Strawberry clover (*Trifolium fragiferum*), (10) Bell heather (*Erica cinerea*), (11) Red deer (*Cervus elaphas*), & (12) Capercaillie (*Tetrao urogallus*). The above list of species group is selected to represent species associated with a cross section of types of species, habitats and European regions.



**ESM4:** Schematic diagram of sectoral interdependencies and mechanisms by which a driver affects a sector (in this case, Sector 1). Pathway 'a' represents a direct driver affecting Sector 1 as a direct input to the sectoral meta-model; 'b' represents the pathway of an indirect driver, which affects Sector 1 indirectly through its cascading effect in the IAP on Sector 2, and 'c' represents the pathways of a combined driver, which affects Sector 1 both as direct IAP inputs and indirectly through Sector 2.

ESMS: Regional (based on river basins; see ESM2) statistical summary of the sensitivity of the sectoral indicators to changes in the climate and socio-economic drivers affecting each indicator.

**Eastern Europe (EE):**

Drivers	URBAN <i>Baseline = 4.08%</i>		FLOODING <i>Baseline = 4.65 million</i>		FOREST <i>Baseline = 47.40 Gt</i>		LAND USE <i>Baseline = 1.039</i>		WATER <i>Baseline = 0.177</i>		BIODIVERSITY <i>Baseline = 0</i>				
	Mean	SD	Mean	SD	Mean	SD	Mean	SD	Mean	SD	Mean	SD			
<b>CLIMATE DRIVERS:</b>															
1 Temp			4.35	0.44	0.17		23.05	39.50	15.26	1.038	0.093	0.031	0.169	0.383	0.143
2 WPPrec			4.60	1.01	0.43		43.11	21.16	7.82	1.042	0.007	0.002	-0.009	0.250	0.095
3 SPPrec			4.60	1.01	0.43		36.33	69.89	26.87	0.993	0.155	0.054	0.041	0.416	0.152
4 CO <sub>2</sub>							81.25	52.36	20.36	1.042	0.067	0.021	0.177	0.015	0.005
5 SLR			4.91	0.46	0.15		46.98	0.56	0.19	1.033	0.008	0.003	0.176	0.001	0.000
<b>SOCIO-ECONOMIC DRIVERS:</b>															
6 Population	4.18	0.33	0.14	4.73	4.92	1.84	26.02	47.47	18.94	0.907	0.380	0.135	0.197	0.043	0.017
7 StructChange							42.06	16.94	7.75	1.046	0.019	0.008	0.178	0.002	0.001
8 Ruminant							43.13	26.13	10.58	1.024	0.066	0.026	0.180	0.008	0.004
9 NonRuminant	4.10	0.04	0.01				47.39	0.02	0.01	1.039	0.001	0.000	0.177	0.000	0.000
10 GreenRed	4.46	0.89	0.31				45.86	5.20	1.56	1.049	0.025	0.009	0.290	0.198	0.078
11 GDP							42.60	11.16	4.12	1.035	0.036	0.013	0.182	0.015	0.006
12 OilPrice							41.15	32.87	14.63	0.925	0.328	0.146	0.178	0.013	0.005
13 ImportFactor										0.177	0.002	0.001			
14 SetAside							35.06	23.55	10.39	1.031	0.039	0.015	0.187	0.025	0.010
15 ReduceDiffuse							37.81	26.35	14.57	1.057	0.068	0.038	0.178	0.002	0.001
16 ForestMgmt							33.01	23.69	8.07	0.991	0.136	0.052	0.178	0.002	0.001
17 TechFactor										0.191	0.178	0.068			
18 TechChange							35.19	47.73	21.30	0.940	0.260	0.090	0.238	0.289	0.102
19 YieldFactor							47.13	0.90	0.36	1.045	0.014	0.006	0.210	0.110	0.044
20 IrrigEfficiency							47.39	0.02	0.01	1.039	0.001	0.000	0.177	0.000	0.000
21 DevCompaction	4.09	0.03	0.02				47.40	0.00	0.00	1.039	0.000	0.000	0.177	0.000	0.000
22 CoastAttract	4.08	0.01	0.00				47.40	0.00	0.00	1.039	0.000	0.000	0.177	0.002	0.001
23 WaterDistriRule				3.24	4.44	2.53	46.83	1.73	1.00	1.033	0.016	0.009	0.177	0.001	0.001
24 FloodProtection										0.177	0.001	0.001	0.092	0.282	0.101

### Northern Europe (NE):

Drivers	URBAN <i>Baseline = 1.22%</i>		FLOODING <i>Baseline = 1.06 million</i>		FOREST <i>Baseline = 72.83 Gt</i>		LAND USE <i>Baseline = 0.583</i>		WATER <i>Baseline = 0.015</i>		BIODIVERSITY <i>Baseline = 0</i>							
	Mean	SD	Mean	SD	Mean	SD	Mean	SD	Mean	SD	Mean	SD						
<b>CLIMATE DRIVERS:</b>																		
1 Temp			1.03	0.04	0.01	56.88	28.88	10.57	0.453	0.192	0.080	0.016	0.004	0.002	-0.102	0.199	0.072	
2 WPrec			1.04	0.08	0.03	72.41	48.11	17.57	0.538	0.230	0.087	0.016	0.013	0.005	0.006	0.108	0.038	
3 SPrec			1.04	0.08	0.03	62.88	106.28	38.81	0.461	0.176	0.073	0.016	0.013	0.005	0.017	0.321	0.114	
4 CO <sub>2</sub>						99.84	40.58	14.24	0.425	0.213	0.087	0.015	0.000	0.000	0.018	0.031	0.009	
5 SLR			1.37	0.55	0.18	72.33	0.70	0.22	0.583	0.002	0.001	0.015	0.000	0.000	0.000	0.000	0.000	
<b>SOCIO-ECONOMIC DRIVERS:</b>																		
6 Population	1.23	0.04	0.02	1.00	0.89	0.33	52.73	67.26	25.55	0.486	0.334	0.152	0.014	0.005	0.002	0.031	0.073	0.033
7 StructChange													0.015	0.005	0.002			
8 Ruminant						70.80	7.38	3.20	0.565	0.265	0.107	0.015	0.000	0.000	0.003	0.009	0.004	
9 NonRuminant						71.70	6.49	2.63	0.516	0.222	0.109	0.015	0.000	0.000	0.006	0.018	0.009	
10 GreenRed	1.22	0.01	0.00	72.83	0.01	0.00	0.583	0.000	0.000	0.000	0.000	0.015	0.000	0.000				
11 GDP	1.85	1.38	0.50	68.36	6.24	2.23	0.486	0.162	0.067	0.015	0.001	0.000	0.015	0.001	0.000	0.002	0.023	0.006
12 OilPrice				72.67	0.71	0.26	0.532	0.176	0.067	0.015	0.000	0.000	0.015	0.000	0.000	0.008	0.017	0.009
13 ImportFactor				71.44	7.43	3.31	0.454	0.287	0.141	0.015	0.000	0.000	0.015	0.000	0.000	0.017	0.033	0.015
14 SetAside													0.015	0.000	0.000			
15 ReduceDiffuse				68.26	13.29	5.71	0.586	0.080	0.029	0.015	0.000	0.000	0.015	0.000	0.000	0.000	0.036	0.012
16 ForestMgmt				62.03	30.57	17.15	0.568	0.046	0.027	0.015	0.000	0.000	0.015	0.000	0.000	0.001	0.001	0.000
17 TechFactor				72.08	1.00	0.38	0.583	0.017	0.007	0.015	0.000	0.000	0.015	0.000	0.000	0.017	0.029	0.012
18 TechChange										0.015	0.018	0.007						
19 YieldFactor				59.73	72.83	27.10	0.474	0.312	0.146	0.015	0.001	0.000	0.015	0.001	0.000	0.028	0.076	0.023
20 IrrigEfficiency				72.50	0.55	0.24	0.582	0.023	0.007	0.015	0.000	0.000	0.015	0.000	0.000	0.004	0.010	0.004
21 DevCompaction	1.22	0.01	0.01	72.83	0.01	0.01	0.583	0.000	0.000	0.015	0.000	0.000	0.015	0.000	0.000			
22 CoastAttract	1.22	0.00	0.00	72.83	0.00	0.00	0.583	0.000	0.000	0.015	0.000	0.000	0.015	0.000	0.000			
23 WaterDistriRule				72.83	0.00	0.00	0.583	0.000	0.000	0.015	0.000	0.000	0.015	0.000	0.000	0.000	0.000	0.000
24 FloodProtection				0.74	1.16	0.64	0.580	0.010	0.005	0.015	0.000	0.000	0.015	0.000	0.000	0.001	0.002	0.001

### Southern Europe (SE):

Drivers	URBAN <i>Baseline = 3.03%</i>		FLOODING <i>Baseline = 3.42 million</i>		FOREST <i>Baseline = 35.58 Gt</i>		LAND USE <i>Baseline = 1.063</i>		WATER <i>Baseline = 0.268</i>		BIODIVERSITY <i>Baseline = 0</i>				
	Mean	SD	Mean	SD	Mean	SD	Mean	SD	Mean	SD	Mean	SD			
	CLIMATE DRIVERS:		CLIMATE DRIVERS:		CLIMATE DRIVERS:		CLIMATE DRIVERS:		CLIMATE DRIVERS:		CLIMATE DRIVERS:				
1 Temp	3.37	0.08	0.03	15.49	28.54	10.20	0.996	0.223	0.083	0.374	0.139	0.048	0.285	0.566	0.201
2 WPPrec	3.38	0.34	0.14	24.03	31.08	12.68	1.056	0.060	0.023	0.342	0.494	0.186	0.009	0.185	0.072
3 SPrec	3.38	0.34	0.14	16.53	31.42	10.92	1.052	0.141	0.051	0.352	0.250	0.096	-0.010	0.357	0.134
4 CO <sub>2</sub>	19.94	24.95	10.73	19.94	24.95	10.73	0.975	0.219	0.083	0.251	0.043	0.017	0.069	0.140	0.048
5 SLR	4.75	2.40	0.78	35.35	0.32	0.12	1.058	0.009	0.004	0.266	0.003	0.001	0.003	0.004	0.002
<b>SOCIO-ECONOMIC DRIVERS:</b>															
6 Population	3.08	0.13	0.06	13.46	30.23	13.26	0.961	0.238	0.092	0.326	0.073	0.031	0.037	0.181	0.072
7 StructChange										0.267	0.054	0.020			
8 Ruminant				31.82	10.42	4.63	1.040	0.080	0.033	0.285	0.031	0.016	0.005	0.041	0.016
9 NonRuminant				32.43	16.80	6.71	1.049	0.051	0.020	0.290	0.049	0.025	0.012	0.080	0.028
10 GreenRed	3.05	0.03	0.01	35.58	0.02	0.01	1.064	0.001	0.000	0.268	0.000	0.000			
11 GDP	4.23	2.76	0.98	29.63	11.07	3.47	1.070	0.013	0.004	0.425	0.306	0.101	0.007	0.016	0.005
12 OilPrice				23.13	22.71	9.80	1.113	0.115	0.050	0.302	0.054	0.019	-0.010	0.020	0.009
13 ImportFactor				31.57	20.45	9.03	0.924	0.366	0.150	0.270	0.094	0.036	0.091	0.282	0.117
14 SetAside										0.266	0.010	0.004			
15 ReduceDiffuse				24.71	16.10	7.03	1.054	0.014	0.006	0.313	0.040	0.016	-0.008	0.015	0.007
16 ForestMgmt				28.57	13.96	6.98	1.068	0.007	0.004	0.278	0.031	0.018	0.000	0.001	0.000
17 TechFactor				30.88	7.62	2.67	1.038	0.041	0.017	0.279	0.023	0.009	-0.003	0.005	0.002
18 TechChange										0.275	0.169	0.064			
19 YieldFactor				23.72	35.58	14.06	0.999	0.129	0.039	0.401	0.396	0.131	0.027	0.095	0.038
20 IrrigEfficiency				31.88	9.03	3.93	1.055	0.023	0.008	0.317	0.159	0.069	0.006	0.050	0.021
21 DevCompaction	3.04	0.03	0.02	35.58	0.02	0.01	1.064	0.001	0.000	0.268	0.000	0.000			
22 CoastAttract	3.03	0.01	0.00	35.58	0.00	0.00	1.063	0.000	0.000	0.268	0.000	0.000			
23 WaterDistriRule				35.54	0.17	0.08	1.063	0.000	0.000	0.264	0.012	0.005	0.000	0.001	0.000
24 FloodProtection	2.38	3.70	2.06	35.50	0.43	0.23	1.062	0.004	0.002	0.266	0.004	0.002	0.003	0.009	0.005



### Western Europe (WE):

Drivers	URBAN <i>Baseline = 6.48%</i>		FLOODING <i>Baseline = 8.28 million</i>		FOREST <i>Baseline = 106.47 Gt</i>		LAND USE <i>Baseline = 0.911</i>		WATER <i>Baseline = 0.189</i>		BIODIVERSITY <i>Baseline = 0</i>					
	Mean	SD	Mean	SD	Mean	SD	Mean	SD	Mean	SD	Mean	SD				
	CLIMATE DRIVERS:		CLIMATE DRIVERS:		CLIMATE DRIVERS:		CLIMATE DRIVERS:		CLIMATE DRIVERS:		CLIMATE DRIVERS:					
1 Temp	8.20	0.28	0.10		62.85	71.09	23.97	0.923	0.061	0.023	0.214	0.065	0.022	0.192	0.466	0.181
2 WPPrec	8.38	1.17	0.50		90.36	73.14	29.04	0.912	0.056	0.023	0.208	0.188	0.070	0.017	0.130	0.048
3 SPrec	8.38	1.17	0.50		60.57	108.14	43.03	0.873	0.118	0.044	0.208	0.189	0.071	0.048	0.190	0.075
4 CO <sub>2</sub>					77.03	51.97	21.71	0.866	0.117	0.037	0.190	0.002	0.001	0.065	0.126	0.047
5 SLR	15.79	13.79	4.85		105.49	1.57	0.62	0.901	0.027	0.010	0.189	0.000	0.000	0.002	0.006	0.002
<b>SOCIO-ECONOMIC DRIVERS:</b>																
6 Population	6.61	0.43	0.18		55.21	103.86	40.14	0.842	0.199	0.075	0.189	0.028	0.010	0.062	0.182	0.067
7 StructChange											0.189	0.042	0.016			
8 Ruminant					93.02	41.85	19.27	0.914	0.029	0.011	0.189	0.000	0.000	0.007	0.014	0.007
9 NonRuminant					98.39	46.10	18.64	0.912	0.087	0.031	0.189	0.000	0.000	0.008	0.029	0.011
10 GreenRed	6.51	0.05	0.02		106.44	0.05	0.02	0.911	0.001	0.000	0.189	0.000	0.000			
11 GDP	9.33	6.38	2.28		92.55	25.52	7.10	0.946	0.083	0.027	0.201	0.032	0.010	0.009	0.016	0.005
12 OilPrice					86.28	39.09	15.62	0.948	0.090	0.039	0.189	0.000	0.000	0.003	0.007	0.002
13 ImportFactor					92.74	71.01	31.61	0.845	0.290	0.114	0.189	0.001	0.000	0.071	0.202	0.082
14 SetAside											0.189	0.000	0.000			
15 ReduceDiffuse					74.63	50.04	22.47	0.894	0.049	0.021	0.190	0.002	0.001	0.005	0.005	0.002
16 ForestMgmt					87.73	35.93	18.02	0.921	0.017	0.009	0.189	0.000	0.000	0.003	0.006	0.003
17 TechFactor					95.80	15.59	5.74	0.881	0.046	0.016	0.189	0.001	0.000	0.008	0.011	0.004
18 TechChange											0.206	0.208	0.080			
19 YieldFactor					78.70	106.62	47.39	0.871	0.202	0.067	0.196	0.043	0.016	0.062	0.120	0.042
20 IrrigEfficiency					104.89	6.55	2.31	0.914	0.008	0.003	0.191	0.008	0.003	0.003	0.009	0.003
21 DevCompaction	6.50	0.07	0.04		106.45	0.07	0.04	0.911	0.001	0.001	0.189	0.000	0.000			
22 CoastAttract	6.48	0.01	0.00		106.47	0.01	0.00	0.911	0.000	0.000	0.189	0.000	0.000			
23 WaterDistriRule					106.47	0.00	0.00	0.911	0.000	0.000	0.189	0.000	0.000	0.000	0.000	0.000
24 FloodProtection					9.13	18.27	9.17	0.903	0.021	0.011	0.189	0.000	0.000	0.010	0.029	0.017

## References

- Berry PM, Brown S, Chen M *et al.* (this volume) Cross-sectoral interactions of adaptation and mitigation measures. *Climatic Change*. DOI:10.1007/s10584-014-1214-0
- Brown C, Brown E, Murray-Rust D *et al.* (this volume) Analysing uncertainties in climate change impact assessment across sectors and scenarios. *Climatic Change*. DOI:10.1007/s10584-014-1133-0
- Harrison PA, Dunford R, Savin C-M *et al.* (this volume (b)) Cross-sectoral impacts of climatic change and socio-economic change for multiple, European land- and water-based sectors. *Climatic Change*.
- Harrison PA, Holman IP, Berry PM (this volume (a)) Assessing cross-sectoral climate change impacts, vulnerability and adaptation: An Introduction to the CLIMSAVE project. *Climatic Change* (Editorial).
- Harrison PA, Holman IP, Cojocaru G *et al.* (2013) Combining qualitative and quantitative understanding for exploring cross-sectoral climate change impacts, adaptation and vulnerability in Europe. *Regional Environmental Change*, 13:761–780
- Holman IP, Harrison PA (eds.) (2012) Report describing the development and validation of the sectoral meta-models for integration into the IA Platform. CLIMSAVE Deliverable D2.2. [http://www.climsave.eu/climsave/doc/Report\\_on\\_the\\_Meta-models.pdf](http://www.climsave.eu/climsave/doc/Report_on_the_Meta-models.pdf). Accessed 09 February 2013
- Holman IP, Rounsevell MDA, Berry PM, Nicholls RJ (2008a) Development and application of participatory integrated assessment software to support local/regional impact and adaptation assessment. *Climatic Change*, 90:1–4.
- Holman IP, Rounsevell MDA, Cojocaru G *et al.* (2008b) The concepts and development of a participatory regional integrated assessment tool. *Climatic Change*, 90(1-2):5–30.
- Ratto M, Castelletti A, Pagano A (2012) Emulation techniques for the reduction and sensitivity analysis of complex environmental models. *Environmental Modelling and Software*, 34:1–4.



**Avhandlingar från Institutionen för naturgeografi och ekosystemanalys (INES),  
Lunds universitet**

----

**Dissertations from Department of Physical Geography and Ecosystem Science,  
University of Lund**

---

*Martin Sjöström, 2012:* Satellite remote sensing of primary production in semi-arid Africa.

*Zhenlin Yang, 2012:* Small-scale climate variability and its ecosystem impacts in the sub-Arctic.

*Ara Toomanian, 2012:* Methods to improve and evaluate spatial data infrastructures.

*Michal Heliasz, 2012:* Spatial and temporal dynamics of subarctic birch forest carbon exchange.

*Abdulghani Hasan, 2012:* Spatially distributed hydrological modelling : wetness derived from digital elevation models to estimate peatland carbon.

*Julia Bosiö, 2013:* A green future with thawing permafrost mires? : a study of climate-vegetation interactions in European subarctic peatlands. (Lic.)

*Anders Ahlström, 2013:* Terrestrial ecosystem interactions with global climate and socio-economics.

*Kerstin Baumanns, 2013:* Drivers of global land use change : are increasing demands for food and bioenergy offset by technological change and yield increase? (Lic.)

*Yengoh Genesis Tambang, 2013:* Explaining agricultural yield gaps in Cameroon.

*Olofsson, Jörgen, 2013:* The Earth : climate and anthropogenic interactions in a long time perspective.

*Wårilind, David, 2013:* The role of carbon-nitrogen interactions for terrestrial ecosystem dynamics under global change : a modelling perspective.

*Sundqvist, Elin, 2014:* Methane exchange in a boreal forest : the role of soils, vegetation and forest management.

*Falk, Julie Maria, 2014:* Plant-soil-herbivore interactions in a high Arctic wetland : feedbacks to the carbon cycle.

*Hedefalk, Finn, 2014:* Life histories across space and time : methods for including geographic factors on the micro-level in longitudinal demographic research. (Lic.)

*Jamali, Sadegh, 2014:* Analyzing vegetation trends with sensor data from earth observation satellites.

*Olsson, Cecilia, 2014*: Tree phenology modelling in the boreal and temperate climate zones : timing of spring and autumn events.

*Jing Tang, 2014*: Linking distributed hydrological processes with ecosystem vegetation dynamics and carbon cycling : modelling studies in a subarctic catchment of northern Sweden.

*Zhang Wenxin, 2015*: The role of biogeophysical feedbacks and their impacts in the arctic and boreal climate system.

*Lina Eklund, 2015*: “No Friends but the Mountains” : understanding population mobility and land dynamics in Iraqi Kurdistan.

*Stefan Olin, 2015*: Ecosystems in the Anthropocene : the role of cropland management for carbon and nitrogen cycle processes.

*Thomas Möckel, 2015*: Hyperspectral and multispectral remote sensing for mapping grassland vegetation.

*Hongxiao Jin, 2015*: Remote sensing phenology at European northern latitudes : from ground spectral towers to satellites.

*Bakhtiyor Pulatov, 2015*: Potential impact of climate change on European agriculture : a case study of potato and Colorado potato beetle.

*Christian Stiegler, 2016*: Surface energy exchange and land-atmosphere interactions of Arctic and subarctic tundra ecosystems under climate change.

*Per-Ola Olsson, 2016*: Monitoring insect defoliation in forests with time-series of satellite based remote sensing data : near real-time methods and impact on the carbon balance.

*Jonas Dalmayne, 2016*: Monitoring biodiversity in cultural landscapes : development of remote sensing- and GIS-based methods.

*Balathandayuthabani Panneer Selvam, 2016*: Reactive dissolved organic carbon dynamics in a changing environment : experimental evidence from soil and water.

*Kerstin Engström, 2016*: Pathways to future cropland : assessing uncertainties in socio-economic processes by applying a global land-use model.

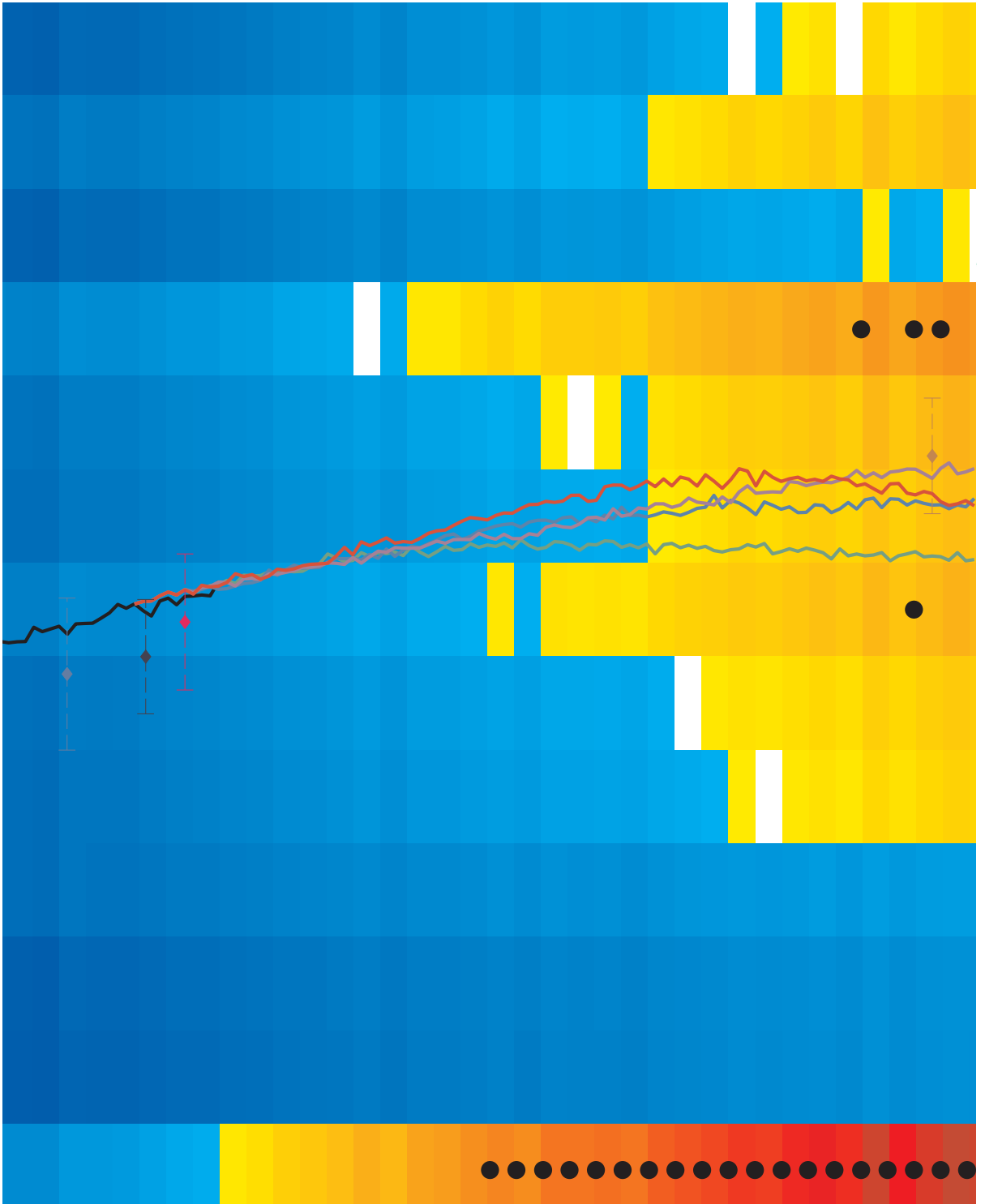
*Finn Hedefalk, 2016*: Life paths through space and time : adding the micro-level geographic context to longitudinal historical demographic research.

*Ehsan Abdolmajidi, 2016*: Modeling and improving Spatial Data Infrastructure (SDI).

*Giuliana Zanchi, 2016*: Modelling nutrient transport from forest ecosystems to surface waters.

*Florian Sallaba, 2016*: Biophysical and human controls of land productivity under global change : development and demonstration of parsimonious modelling techniques.





LUND  
UNIVERSITY

LUND UNIVERSITY  
Faculty of Science  
Department of Physical Geography and Ecosystem Science  
Centre for GeoBiosphere Science  
ISBN 978-91-85793-69-3

